Natural leakage pathways through smectite clay: a hydrological synthesis of data from the Hudson Agricultural Trial Site on the Liverpool Plains. August 2002.

Author:
Timms, W. A.; Acworth, R. I.

Publication details:
Commissioning Body: Land & Water Australia. National Program for Irrigation Research and Development.
Report No. UNSW Water Research Laboratory Report No. 209
0858240521 (ISBN)

Publication Date:
2002

DOI:
https://doi.org/10.4225/53/578841e29c9c7

THE UNIVERSITY OF NEW SOUTH WALES
GROUNDWATER CENTRE

Natural leakage pathways through smectite clay: A Hydrogeological Synthesis of data from the Hudson Agricultural Trial Site on the Liverpool Plains

WATER RESEARCH LABORATORY
RESEARCH REPORT
No. 209

Prepared by

WA Timms and RI Acworth, UNSW Groundwater Centre, Water Research Laboratory King, Street, Manly Vale 2093 NSW

RR Young, NSW Agriculture, Tamworth Centre for Crop Improvement

August 2002

Acknowledgments

We thank Robert and Edwina Duddy for the use of the research site area on 'Hudson'.

This work has benefitted by the help of many at WRL and at The Tamworth Centre for Crop Improvement. The inputs by Rolf Beck, Tim Chambers, Will Minchin and Ian Brandes from WRL, Tony Bernardi from TCCI and Stephan Hidenreich and Dawit Berhane from GRC are acknowledged.

We acknoweldge funding from Salt Action for the installation of piezometers and groundwater monitoring and from the Grains Research and Development Corporation for operation of the trial site.

Land and Water Australia provided funds through the National Program for Irrigation Research and Development for one of the authors (Wendy Timms) to compile and interpret hydrogeological datasets.

ISBN: 85 824 052 1

https://doi.org/10.4225/53/578841e29c9c7

Water Research Laboratory Research Report Number 209 is published on the web. The report can be downloaded from the Water Research Laboratory web site as a pdf document. Further printed copies can be supplied on application to the Librarian, Water Reference Library, School of Civil and Environmental Engineering, King Street, MANLY VALE 2093, Australia.

The Water Research Laboratory web site address is `http://www.wrl.unsw.edu.au/research`

EXECUTIVE SUMMARY

This report provides a synthesis of available hydrogeological data for a site at Hudson on the southern footslopes of the Liverpool Plains. Agronomic processes at the site have been the subject of detailed study since it was suspected that significant groundwater recharge in the area was caused by deep drainage beneath short rooted crops.

The assembled data strongly indicate that soils cultivated on the smectite dominated silt and clay soils do not wet up uniformly. The presence of air filled fractures at depth is deduced from the barometric efficiency of water in piezometers installed at 15 m beneath the trial site. Investigation using the electrical image method has indicated that changes in bulk resistivity occur to a depth of at least 8 m. It is deduced that these resistivity changes must be caused by changes in soil moisture. If this deduction is correct then lucerne seems to have changed the soil moisture status to as deep as 8 m. The reduction in soil moisture is believed to have promoted deep cracking in the soil column at depths greater than those normally associated with agriculture.

Bypass flow in soils of this type have been identified in other areas and there are strong indications that the cracking associated with growing lucerne is significantly adding to this type of flow. This finding requires substantiation but if correct indicates that the water balance in swelling clay soils is perturbed to greater depth than previously suspected and requires quantification. The possibility of modifying the water balance module in the APSIM package to account for bypass flow should be investigated.

At the Hudson Site, deep drainage via fractures contributes to perched, episodically saturated zones and is intercepted by caliche (Ca and Mg carbonate) horizons. Preferential flow appears to occur above at least two caliche horizons between 8 and 15 m depth. A small proportion of deep drainage slowly leaks through clay to the weathered basalt aquifer. A more effecient local recharge source appears to be leakage from the base of an erosion gully crossing the lower part of the trial site.

Non-fractured and saturated Ca-smectite clay was characterised by a low hydraulic conductivity, but was not impermeable. Leakage was transmitted to the deeper aquifer with a delay of several hundred days following recharge events. The low specific storage means that relatively small quantities of recharge have led to increases in water level of several metres beneath the trial site. Hydrogeochemical changes and incongruent isotope results indicated that water at 15 m depth was dominated by old matrix water contaminated by only a small proportion of recent recharge. The efficiency of recharge will be much greater in areas where weathered basalt is less than 10 m depth.

Conceptual models of a dual-porosity and compressible weathered basalt medium were best able to explain the field observations. The present work has been able to confirm that a small quantity of deep drainage to the saturated aquifer has occurred but is not able to quantify this. More accurate quantification will require extensive monitoring and the development of appropriate models of water movement through deformable smectite dominated silty clays.

The initial suspicion that deep drainage occurs beneath short rooted crops, based on a simple water balance, appears to have been unwarranted. However, the practice of trying to establish a large soil moisture deficit by growing a deep rooted crop like lucerne appears to cause too much drying with the result that fracturs are established. At the Hudson Site, the water level in piezometers beneath the trial site was below 10 m. A small quantity of recharge appears to have moved through the unsaturated profile to this depth. The quantity of recharge would be much greater over a shallower clay profile.

Contents

List of Figures

List of Tables

A

B

C

Figure 1: Hudson site A) View toward the top of the ridge from the lower slope (248110) B) Lithological profile exposed in the gully that crosses the mid-lower slope C) Groundwater piezometer and OTT automatic groundwater level logger at the Hudson agricultural trial site, displayed by S. Heidenreich.

Figure 2: Magnesium (?) carbonate deposit in the gully wall.

Chapter 1

INTRODUCTION

1.1 Background to investigation

In the early 1990's, it was feared that rising groundwater levels beneath the Liverpool Plains indicated that dryland salinity was likely to develop extensively and that the agricultural productivity of the area was threatened. Federal and State resources were directed to research processes in the area in an effort to better understand the water balance of agricultural systems on the cracking clay soils (Vertosols) which dominate the region. The Hudson Trial site was established by NSW Agriculture to investigate the water balance of farming systems in what is believed to be a recharge area to the deeper aquifers under the Plains (Figure 1.1). It has been argued that agricultural practices in the upper parts of the catchment have increased recharge to deeper aquifers and that this recharge has caused elevated hydraulic heads and discharge at lower points in the catchment. The increased discharge was thought to have directly led to the development of water logging and dryland salinity.

The soils on the plains are derived from weathering of Tertiary age basalt on the Liverpool Ranges. The weathering of volcanic material (basalt) leads to the development of highly productive agricultural soils and explains why volcanic slopes in many parts of the world are highly developed. The Liverpool Plains is no exception with more than $200 million worth of agricultural production annually, despite some losses due to water logging and the presence of areas of saline soil.

The Liverpool Plains, part of the upper Namoi catchment in the Murray Darling Basin (Fig. 1.1), were a focus of the National Dryland Salinity Program and research has been conducted in the area since the early 1990s by various agencies (NSW Agriculture, NSW Department of Land and Water Conservation, CSIRO Land and Water and the UNSW Groundwater Centre). Intensive agronomic, soil and water balance studies have been completed at 2 non-saline sites in the partially salinised Yarramanbah/Pump Station Creek sub catchment:

1. Connamara in the lower Yarramanbah catchment, located on a yellow Sodosol of Triassic sandstone origin and
2. Hudson, located on a black cracking clay (Vertosol).

Early investigations concluded that no significant recharge to groundwater occurred at the Connamara Site, due mainly to the presence of an impermeable sodic B horizon. The lack of groundwater level response, and a hydraulic gradient suggesting groundwater flow into the hill slope, rather than towards the plains, contrasted strongly with findings at the hydrologically active Hudson Site (Timms 1998a). Subsequent investigations therefore were focused on recharge processes at the Hudson Site.

The research aims at these trial sites were to define profitable crop and pasture systems that would reduce surface runoff and deep drainage into groundwater and so alleviate the problems of water logging

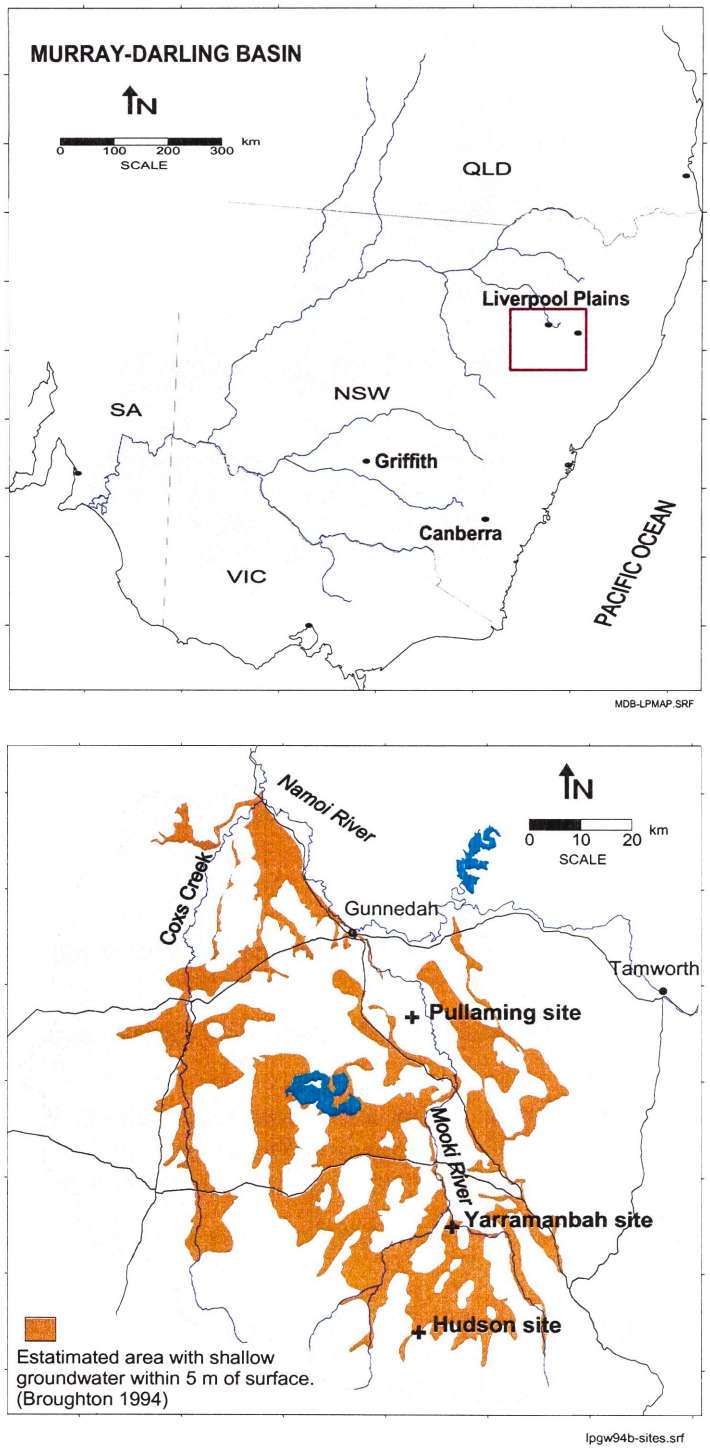

Figure 1.1: Location of the study site A) Murray-Darling Basin B) Liverpool Plains.

and dryland salinity further down the catchment. Deep drainage was defined as the quantity of water that passes downward beyond the root zone and may move into groundwater. Deep drainage can be represented by Equation 1.1.

$$\begin{aligned} \textit{Deep drainage} &= \textit{rainfall} - \textit{evaporation} - \textit{transpiration} \\ &\quad - \textit{runoff} \pm \textit{change in soil water storage} \end{aligned} \tag{1.1}$$

It was proposed that deep drainage to groundwater could be detected, and perhaps quantified, by monitoring of groundwater levels and by hydrochemical techniques. Such investigation at depths of between 5 and 30 m below ground, provide a context for agronomic and soil studies which focused on water balance components near the surface. In effect, the groundwater investigation describes the 'bucket' into which deep drainage episodically 'drips'.

1.2 Groundwater in the Upper Namoi

An overview of geology and hydrogeology for this area is provided by Broughton (1994). A broad stratigraphic framework for the unconsolidated sediments of the Mooki catchment was initially established by Gates (1980) for the purpose of estimating groundwater storage. Comprehensive stratigraphic and facies analysis by Lavitt (1999) defined a heterogeneous system with increasingly fine grained sediments from the proximal to distal alluvial fan and also a fining upwards trend towards the surface. The unconsolidated alluvial system may be simplified as a lower gravel dominated system and an upper system dominated by clay rich facies with a gradual fining up sequence.

Hydrographic evidence was presented by Broughton (1994) for rising piezometric heads in deep ($\sim$ 50–80 m) confined aquifers. Rises of upto 2–5 cm/year since the 1970s were documented. DLWC (1995) and subsequent status reports, show that in some areas groundwater levels in the confined aquifers have continued to rise, while in other areas where intense pumping of groundwater occurs, long term groundwater level decline has been noted.

1.2.1 Shallow groundwater and salinity

Salinity within the root zone of crops and grassland is manifest in two ways:

1. Saline (ECe 4-16 dS/m) and sometimes water logged, clay in the alluvial plains (Daniells et al. 2001) with effects varying from a slight reduction in plant growth and yield to completely bare areas with no yield over an area of several hectares and
2. Saline groundwater discharge at the junction of duplex and clay soils at the edge of sandstone hills.

Dryland salinity was recognised in the Liverpool Plains area following the wet winters in the late 1980s and early 1990s (Abbs & Littleboy 1998). Salinisation processes have been investigated by UNSW Groundwater Centre on a site specific basis near Breeza by Acworth & Jankowski (1997), at mound springs on the western margin of the Lake Goran basin (Kavanagh et al. 1998; Jones et al. 1998) and Acworth et al., submitted). The salinised Yarramanbah subcatchment has also received much attention, with investigations by Timms (1996), Crawford (1997), Timms (1998b) and Acworth & Beasley (1998).

Salt appears to be entrained within near surface clays and the poor distribution of salts and their concentration in clay argues against evaporative concentration as a source (Acworth & Jankowski 1997). Since weathering of basaltic material releases some Na but no Cl, the ultimate source of salt has been attributed to aeolian inputs over geological time. About 19 kg/ha/year of salt are currently deposited

by wet and dry precipitation of salt in the area (Blackburn and McLeod 1983). Local redistribution of these salts may have occurred during lunette formation and preferential leaching.

Erosion of saline clays has been recognised as a major land management problem in eastern Australia (Acworth & Jankowski 2001). Where surface soil cover has been lost, rainfall has dispersed exposed saline clay, releasing the load of entrained salt. Thus, in some situations, salinisation may be unrelated to groundwater flow processes.

Despite the fact that grain sorghum is highly sensitive to soil salinity under field conditions (Daniells et al. 2001), healthy crops are often observed above highly saline shallow groundwater. For example, crop stress was not always apparent at sites in the Yarramanbah sub catchment where saline groundwater was within 2 m of the ground surface, measured in a 5 m deep piezometer. This apparent conflict was explained by Timms et al. (2001) who noted that, due to overburden effects in compressible clay, the saturated zone was between 0.5 and 4 m deeper than groundwater levels measured in a 5 m deep piezometer. Furthermore, where the surface layers are not saline and if growing season rainfall is sufficient, crops do not need to access soil water at depth.

Temporal trends

In addition to temporal analysis of groundwater levels in confined aquifers, Broughton (1994) also documented the spatial extent of shallow groundwater at that time. Based on data from 230 newly installed shallow piezometers (<5 m depth), together with soils and topographic data, Broughton (1994) estimated that 195 000 ha (25% of the plains area) had water levels within 5 m of the ground surface. It was estimated at this time that 30 000 ha with water tables within 2 m of the ground surface suffered declines in crop yields. The episodic nature of climatic effects on shallow groundwater levels became evident when levels were found to have fallen in many of these piezometers during the drier years following 1992 (Timms 1997).

Analysis of monitoring data from a 7 year period to 1999, revealed that shallow groundwater was in hydrologic equilibrium over the medium term, despite short term response to rainfall events Timms et al. (2001). Long term trends are unknown. However, there is anecdotal evidence that groundwater occurred near the ground surface prior to cropping of the plain. An early NRMA road map of the area for instance, marks the Lower Yarramanbah valley as a swamp.

Since shallow groundwater levels fluctuate episodically, it is clear that the catch phrase *'rising water tables'* may well be a complete misnomer.

1.2.2 Groundwater abstraction issues

Evidence for declining groundwater quality due to groundwater abstraction in the Lower Mooki area was presented by Lavitt & Jankowksi (1998). It was noted that 81% of abstraction within Zone 3 (Lower Mooki - Breeza plain), occurred in the vicinity of the Pullaming stock route, such that vertical downward gradients from the middle (<30 m depth) aquifers to the deeper aquifers had increased between the late 1970s and mid 1990s. Timms & Acworth (2002) have presented results that indicate as much as 30% downward leakage of applied irrigation water in the Pullaming Area.

Hydrochemical and groundwater level data led Lavitt (1999) to the conclusion that large scale groundwater abstraction in the Pullaming area caused lateral flow northwards from Breeza, and southwards from the Namoi River alluvium. If the Mooki groundwater system once discharged into the Namoi alluvium, the direction of flow had since reversed due to groundwater abstraction becoming the dominant discharge process.

The impact of groundwater abstraction on groundwater quality over time has been determined from infrequent and sparse historic monitoring data by Lavitt (1999). The ratio Avg= TDS^{1990s} / $AvgTDS^{1970s}$ was determined from lumped groundwater quality data obtained from sampling of DLWC monitoring

bores. Ratios greater than 1, reflecting increased groundwater salinity, were evident in most areas, with ratios of up to 4.7 in aquifers to the east of the Mooki River. Increased salinity was attributed to downwards leakage of pore water from clay rich facies, which were thicker in the eastern foot slope areas (Lavitt 1999).

1.2.3 Recharge processes

The degree of vertical leakage to groundwater, otherwise known as diffuse recharge or deep drainage, is a key concern for resource management on the Liverpool Plains, particularly with respect to groundwater quantity and quality. However, a direct correlation between estimates of the volume of deep drainage (eg. Abbs & Littleboy 1998, Rigrose-Voase et al 2001) and increased groundwater storage has yet to be demonstrated at a scale meaningful for farm management. Furthermore, the outcome of hydrogeochemical studies and numerical groundwater flow models do not agree over the importance of diffuse recharge on the plains relative to direct foot slope recharge (Lavitt 1999).

The importance of foot slope recharge

A comprehensive hydrochemical study concluded that recharge predominately occurred on the foot slopes, both by diffuse and direct pathways Lavitt (1999), but that little recharge occurred through the plains. This finding was consistent with an early study by Gates (1980) who suggested that vertical leakage was <10 % of total recharge since recharge occurred predominately through preferential zones of the foot slopes.

Lavitt (1999) found that the hydrogeochemical recharge signature for foot slopes of the Liverpool Ranges were similar to that of recharge through foot slopes of the New England Fold Belt (NEFB) on the eastern margin of the Breeza plain. Recharge groundwater was saturated with respect to calcite and dolomite and had a composition that indicated stability with smectite clays. Minor levels of K were provided from mica dissolution, Na and Cl from halite dissolution and SO_4 from gypsum dissolution. Distinct $\delta^{13}C$ and dissolved inorganic carbon (DIC) signatures from recharge in the carbonate rich, open groundwater system at the foot slopes were retained along the flow path of confined aquifers, with some alteration due to ion exchange with smectite and zeolite.

Modelling of hydrochemical and isotopic data by Coram (1999) indicated that most recharge occurred on the foot slopes of the Liverpool Ranges, with minor recharge through creek beds. Diffuse recharge through the clay profile was found to be insignificant, although high nitrate concentrations and tritium was detected in several shallow bores. Groundwater from these shallow bores were also characterised by very low levels of ^{14}C. Mixing of old and young groundwater explained this discrepancy. Older groundwater north of Caroona was recharged under cooler and/or wetter conditions more than 1500 years ago (Lavitt 1999).

The importance of plains recharge

It has been argued that diffuse recharge on the plains is an important, and manageable component of the water balance (Timms 1998b) and that controlling deep drainage through the soil profile will slow salinisation (Stauffacher et al. 1997). A regional groundwater flow model for the northern Mooki River valley near Gunnedah concluded that vertical recharge through the plains was the dominant recharge source. It was assumed that net vertical recharge amounted to 4% of rainfall, although infiltration processes were not explicitly considered. During the 11 year calibration period, from 1979–1990, net vertical recharge from rainfall (and some flood irrigation) accounted for 60% of inputs, in contrast to 3% from direct river recharge and 7.5% from boundary inflow into the model area.

Hydrochemical evolution along the flow path of confined aquifers did not appear to be impacted by vertical recharge inputs, leading Lavitt (1999) to rule out piston flow to confined aquifers as a significant

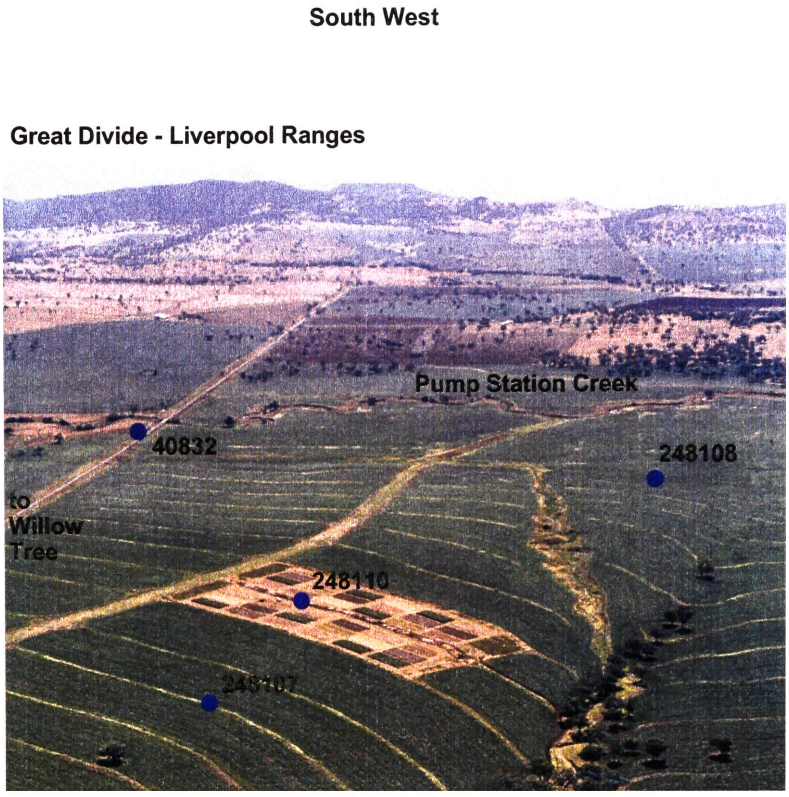

Figure 1.2: Oblique aerial photograph of the Hudson Site looking southwest and showing the Liverpool Ranges in the background

recharge process. However, it was conceded that piston style recharge to the clay dominated system may have occurred at some stage, with sluggish flow. The clay dominated system was recognised as a source of salts due to earlier aeolian accessions to the clay.

A bulk recharge rate for the Liverpool Plains was estimated on the basis on tritium activity measured on groundwater sampled from 30 shallow piezometers (Young et al. 1996). At a threshold depth of 5–6 m, no samples had a tritium activity >1 TU, compared with modern rainfall of 2.7 TU. By assuming piston recharge, a tritium generation date of 1964 and a porosity of <0.2, the rate of recent groundwater recharge was estimated to be 20–30 mm/year. It was also shown that all saline groundwater were old waters, with insignificant levels of tritium. Low levels of tritium were observed in shallow groundwater even in the upper catchment (Yarramanbah). However, as noted by Coram (1999), these estimates did not discriminate between different aquifer materials, or consider mixing influences.

1.3 Site description

The Hudson site is located on the Blackville Road, approximately 30 km west of Willow Tree and about 80 km south of Gunnedah. The site is in the upper catchment of the Yarramanbah-Pump Station creek sub catchment and is located on the alluvial/colluvial rim of the Liverpool Ranges which form part of the Great Dividing Range. Oblique aerial photographs of the site are shown in Fig 1.2 and Fig. 1.3.

The site is typical of highly productive farming country in the foothills of the Liverpool Range. Woodland on the site if it was present may have been cleared in the 1880s. No trees have been removed since 1924 (Robert Duddy pers. Comm.). The ground surface slopes at about 3% on site and about 2% below the trial site to Pump Station Creek. The soil to around 0.8 m depth is colluvial material with 75-80% clay of which 70% is smectite. The surface is self mulching. This overlies > 5 m of brown clay. The profile is classified as an Endocalcareous, Self- mulching, Black Vertosol; non-gravelly, very fine/very fine, giant (Isbell 1996); a Black Earth (Stace et al. 1968) or Ug5.15 (Northcote 1979).

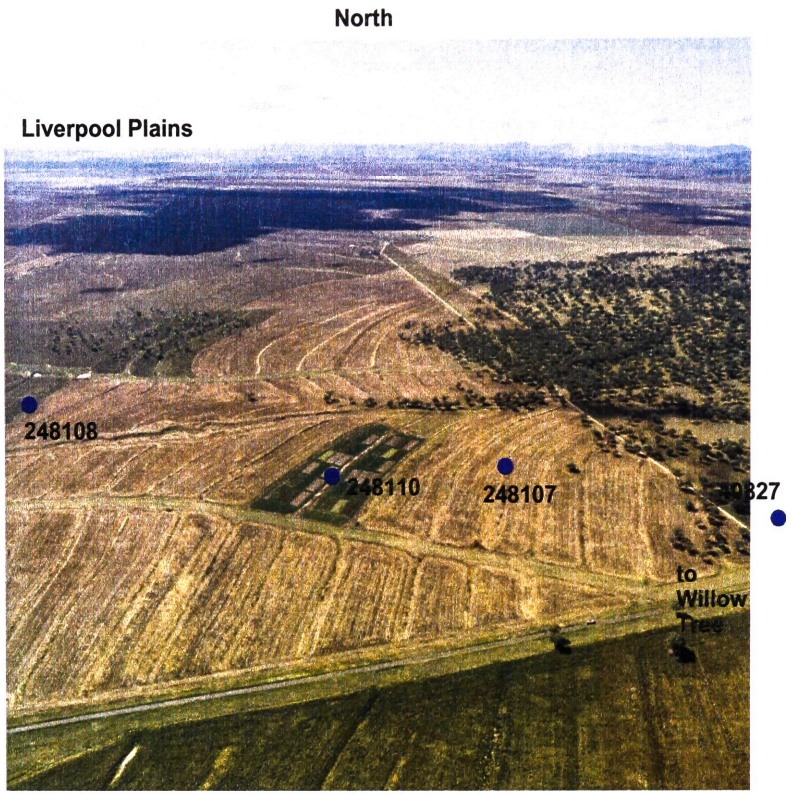

Figure 1.3: Oblique aerial photograph of the Hudson Site looking north towards the Liverpool Plains

The Hudson trial site was established in late 1994 by NSW Agriculture, but has now been decommissioned. The site covered around 6 ha over 2 interbank areas (Figs. 1.2 and 1.3). There were 4 replicate blocks of 9 crop and pasture treatment plots with 2 replicate blocks in each interbank area, see Fig. 1.4. Plots were 40 x 15 m situated between two contour banks. The plots were separated by a lucerne and phalaris buffer of 2 m along the plots and 10 m at the end. Experimental design and implementation are described by Ringrose-Voase & Cresswell (2000). The various applications in each plot are given in Table 1.1.

1.3.1 Data Collection by NSW Agriculture

Comprehensive weather, crop and pasture productivity, agronomy, surface runoff, soil water storage and soil chemistry data were collected by NSW Agriculture and CSIRO Land and Water (Ringrose-Voase & Cresswell 2000). Of direct relevance to these hydrogeologic studies, rainfall was measured both automatically and manually, barometric pressure was measured continuously, soil water (vol/vol%) to 3 m (6 m in lucerne plots) was measured monthly or more frequently with a neutron moisture probe (3 Al access tubes/plot), soil cores (to 3 m) were taken twice annually for water content (g/g%) and 1:5 Cl, NO_3 and EC. Selected cores were processed for CEC, PSA and clay type by XRD.

Elements of this data set are incorporated into this report but the majority is reported under separate cover by NSW Agriculture and CSIRO Land and Water (Young 1998; Ringrose-Voase & Cresswell 2000).

1.4 Previous site investigations

Groundwater investigations at the Hudson site were started in mid-1996 two years after the trial site was established by NSW Agriculture. Various, largely unpublished reports, on groundwater aspects of the study site are listed in Table 1.2.

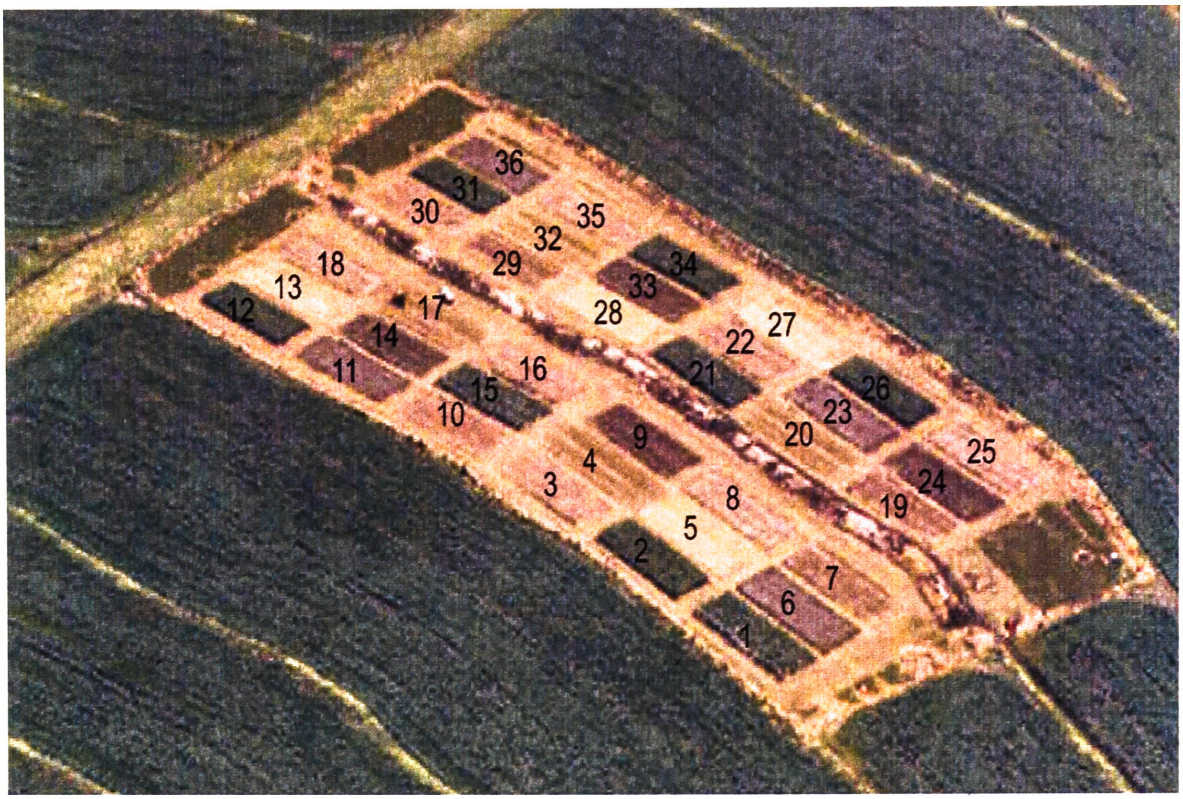

Figure 1.4: Plan of the experimental plot layout at Hudson

Table 1.1: Relation between plot numbers, replicates and crop types

Plot No.	Code	Crops	Plot No.	Code	Crops
1	LF3	Wheat - fallow	19	LF2	Fallow - sorghum stubble
2	OP2	Chickpeas - sorghum stubble	20	P1	Lucerne
3	W1	Barley - fallow	21	LF3	Wheat - fallow
4	Pi	Lucerne	22	W1	Barley - fallow
5	P3	Bambatsi - Natural sp.	23	LF1	Fallow - Wheat stubble
6	LF1	Fallow - wheat stubble	24	P2	Lucerne - Phalaris
7	LF2	Fallow - sorghum stubble	25	OP1	Barley - mung bean stubble
8	OP1	Barley - mung bean stubble	26	OP2	Chickpeas - sorghum stubble
9	P2	Lucerne - Phalaris	27	P3	Bambatsi - Natural sp.
10	LF1	Fallow - sorghum stubble	28	P3	Bambatsi - Natural sp.
11	LF1	Fallow - wheat stubble	29	LF2	Fallow - sorghum stubble
12	OP2	Chickpeas - sorghum stubble	30	W1	Barley - fallow
13	P3	Bambatsi - Natural sp.	31	OP2	Chickpeas - sorghum stubble
14	P2	Lucerne - Phallaris	32	P1	Lucerne
15	LF3	Wheat - fallow	33	P2	Lucerne - Phallaris
16	W1	Barley - fallow	34	LF3	Wheat - fallow
17	P1	Lucerne	35	OP1	Barley - mung bean stubble
18	OP1	Barley - mung bean stubble	36	LF1	Fallow - Wheat stubble

Table 1.2: Groundwater related studies at the Hudson site.

Description	Reference
Piezometer installation and sampling - stratigraphy, groundwater level and gradients, major ion, tritium and carbon-14 data	Timms, April 1998
Agronomy & water balance	Young et al. 1998
Groundwater levels data for 1998	Heidenreich, January 1998
Groundwater levels data for first half 1999	Heidenreich, June 1999
Electrical imaging, borehole logging, major ion sampling, mass balance hydrochemical modelling	Chambers 1999
Soil permeability	Ringrose-Voase & Creswell, June 2000
Hydrogeological appraisal	Minchin, September 2001

1.4.1 Piezometer installation

The preliminary piezometer installation and sampling report of Timms (1998b) compared and contrasted the Hudson site on a weathered basaltic hill slope with the Connamara trial site developed at Pine Ridge on a weathered sandstone profile developed over a Triassic bedrock (Fig. 1.1).

1.4.2 Hydrogeological analysis

A detailed hydrogeological appraisal of the Hudson site was first reported by Chambers (1999) who interpreted groundwater level, groundwater chemistry and geophysical data. Water level variability was used to estimate K_h to be between 0.8 and 1.5 m/day in the upper slopes on the site and 0.5 to 0.9 m/day on the lower parts of the site. Estimates of effective porosity of between 30 and 60% were used in this analysis. Water level data from the 3 deep bores was presented (Heideneich 1999a; Heideneich 1999b).

1.4.3 Hydrochemical analysis

Chambers (1999) provided a detailed hydrochemical description for the site based on samples taken in 1997 and May 1999. Analysis of major ions, ion ratios and saturation indices was used to explain hydrochemical variability down the slope due to mixing, dilution and ion exchange. Na:Cl ratios greater than 1 indicated that Na was released into groundwater in exchange for Ca and/or Mg, while reverse ion exchange is evident near the creek. High salinity of the creek water was attributed to influx of saline groundwater and the possibility of evaporative concentration.

Modelling of hydrochemical and isotopic data by Coram (1999) indicated that most recharge occurred on the foot slopes of the Liverpool Ranges, with minor recharge from creek beds. Diffuse recharge through the clay profile was found to be insignificant, although high nitrate concentrations and tritium was detected in several shallow bores. Groundwater from these shallow bores were also characterised by very low levels of ^{14}C. Mixing of old and young groundwater explained this discrepancy. Older groundwater north of Caroona was recharged prior to 1500 years ago under cooler and/or wetter conditions.

1.4.4 Geophysical measurements

Minchin (2001) reviewed the use of electrical image (Acworth 1999) measurements to determine soil moisture change beneath the trial plots at Hudson. Geophysical logs (gamma ray activity and apparent electrical conductivity) measured in each of 3 deep bores were also presented.

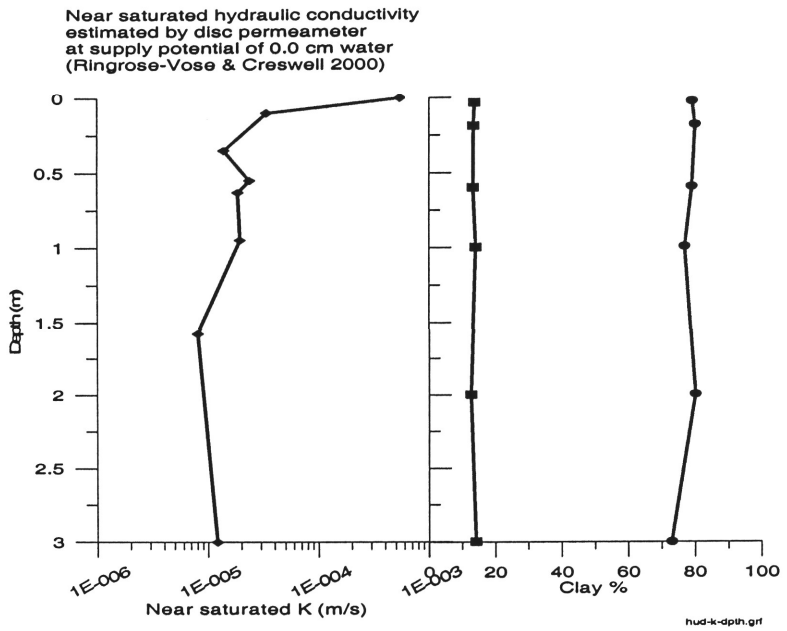

Figure 1.5: Hydraulic conductivity and clay-silt% to 3 depth at Hudson site. K of near-saturated soil was measured using disc infiltrometers (Source: Ringrose-Voase & Creswell 2000)

1.4.5 Hydraulic conductivity analysis

Crawford (1997) conducted falling head permeameter tests on a number of minimally disturbed clay cores from a site at Breeza on the Liverpool Plains. The cores were of similar material to that at Hudson. Values of hydraulic conductivity derived by (Crawford 1997) were approximately 1×10^{-5} ($\approx 1\,m/day$).

Vertical hydraulic conductivity (K_v) measurements were made to a depth of 3 m at the Hudson Site using disc infiltrometers (Ringrose-Voase & Cresswell 2000). This data is reproduced in Fig. 1.5.

1.4.6 Water use efficiency

Initial water balance studies at Hudson (Young et al. 1998) have indicated that it is not possible to close the water balance at the site (Equation 1.1) without allowing some component of deep drainage. This seems to be particularly the case for plots growing lucerne. This uncertainty has done much to promote the hydrogeological study reported upon here.

1.5 Aims

The hydrogeological setting and analysis of available data has not formed a significant reporting item in any of the State and Federal funding received for the Hudson Site to date. Land and Water Australia (LWRRDC) have funded one of the authors (Wendy Timms) to assemble the hydrogeological aspects of the study at the Hudson Site and to present the results as a Research Report. NSW Agriculture have strongly supported this additional work as it may lead to a resolution of the deep drainage question.

The aims of this report are therefore as follows:

- Compile and update hydrogeological information for the Hudson site from various unpublished sources.
- Develop an improved conceptual model for deep drainage to groundwater in a smectite clay.

- Revise estimates of deep drainage that are consistent with groundwater level variability and hydrochemical and isotopic data.

Chapter 2

REVIEW OF PHYSICAL AND CHEMICAL PROPERTIES OF SMECTITE CLAY

2.1 Occurrence of Smectite Clays

Swelling clays are widely distributed in Africa, India and Australia where they constitute a large proportion of agricultural soils. They typically develop as a weathering product of alkali rich basalts that are then distributed by flood waters throughout the catchment in which they occur. In Australia, Tertiary volcanic activity was extensive with several major eruptive centres typically occuring close to the Great Divide and along the eastern margin of the Murray Darling Basin (Sutherland 1995). Weathering products have been distributed widely throughout the Basin as a result. Acworth & Jankowski (2001) have argued that there has been significant additional aeolian redistribution of clay from the flat arid interior flood plains eastwards of the Darling back towards the mountains during the Pleistocene Period.

The result of this weathering and subsequent distribution is that in the Murray-Darling Basin there are estimated to be 250 000 km^2 of swelling clay soils which support $1500 billion in agricultural production annually (Smiles 2000).

In the local context of the Hudson Site, there are thought to have been at least 2 extrusive centres in the Tertiary period (32–40 Ma) extending from directly south of the site on the Liverpool Ranges, westwards to the Warrumbungles. Three types of lava flow have been described: massive 2–4 m thick flows; massive columnar flows and amygdaloidal flows up to 15 m thick (Schon 1986). Yarramanbah/Pump Station Creek sub catchment of the Upper Namoi occurs in the Colo Tops National Park at surface elevations of more than 1000 m. Erosion has cut into this volcanic pile with the development of nearly vertical cliffs at the head of the valley. A bore (40827) drilled just to the east of the Trial Site encountered basalt at a depth of a few metres and the site itself is underlain by basalt with basalt floaters regularly occurring in the soil.

The smectite clay that has developed by the in situ weathering of the basalt has a high calcium and magnesium cation exchange complex with local development of caliche in the deeper part of the weathered profile. The surface soil cracks extensively in dry weather and the complete weathered profile expands vertically in response to soil moisture changes.

A recent review paper by Matthew Bethune and Hugh Turral presented at an Australian workshop on water movement in cracking clay (Bethune & Kirby 2001) provides a summary of work to date concerned with modelling water movement in cracking soils.

The workshop concluded that there is insufficient information describing the water balance and drainage of

cracking/swelling soils and that there is insufficient general awareness amongst researchers and practioners of the impact of soil cracking and swelling on water movement in water balance studies. In particular, it was noted that at the Hudson Site, swelling of the surface clays could account for a large proportion (120 mm in one year) of water storage changes and that corrections to water balance calculations for swelling could be of the same order as deep drainage estimates.

The workshop (Bethune & Kirby 2001) concluded:

> we cannot currently develop or verify models for water movement in cracking and swelling soils, nor apply them to practical problems with any confidence.

2.2 Water Movement through Smectite Clay

Knowledge of the hydrology of swelling clay within the fractured vadose zone is incomplete, with various approaches adopted within agronomic, geotechnical and soil physics disciplines. Theoretical hydraulic behaviour of saturated deformable media has been described by groundwater hydrology and geotechnical engineering approaches, but is not widely applied.

The water table is a fundamental concept in hydrogeology and one that the general public is familiar with. The water table is defined as that point in the soil column where the water pressure in the soil is equal to the atmospheric pressure. It is widely assumed that deep drainage through a soil will sink down to the water table and the water will become part of the groundwater body. However, adopting classical hydrogeological assumptions based upon the transmission of hydrostatic pressure through a rigid soil/rock matrix is inappropriate in these highly deformable materials.

In a non-rigid or swelling clay soil the soil matrix is not capable of completely supporting the weight (stress) of the overlying media and some of this stress is transfered to the water column resulting in an overburden pressure. From a practical perspective, this means that water levels will always rise in a piezometer installed into a saturated clay (Timms et al. 2001) until the height of the water column inside a piezometer matches the overburden pressure in the formation. There is an important corollary to this water level rise and that is that the water level in the piezometer will respond to changes in weight of the overlying matrix. As the soil surface wets with rain, or dries due to evapotranspiration, the water level in the piezometer will respond to the change in overburden pressure. This is a pressure response and does not indicate a flow of water from the soil surface to depth as normally occurs in groundwater recharge to a rigid unconfined aquifer.

Another complication is that there is an extensive (several metres) wide zone above the water table that is also fully saturated. Water is held in this zone by surface tension and will move in response to gradients in matric potential. Above the top of the tension saturated zone (capillary fringe) the clay will still contain large amounts of water and may in fact be almost saturated. Again, water is held in the pore space by surface tension but some of the larger pores are air filled.

A further complication is cracking and movement of the matrix in the unsaturated zone in response to drying of the clay. At the end of a long dry period, the cracks may extend down to the top of the tension saturated zone. It may well be that the interface between the unsaturated zone and the top of the tension saturated zone will not be horizontal and may even include closed surfaces.

Intense rain falling on top of the soil will initially fill open cracks and will then form a saturated zone above the unsaturated zone (perched aquifer) as the surface clay swells in response to the increased water content.

Clearly, the response of a swelling clay soil to rainfall will be complex with pressure variations variously transmitted through the soil matrix. It is highly probable that there is limited direct flow of water down to the saturated zone under these circumstances, especially if the degree of cracking of the soil at depth is maintained at a minimum.

The concept of a water table in swelling clays is not particularly useful and further research is required to describe the way in which the water pressure at depth responds to different external loads. Later in this report we describe the response to atmospheric and overburden pressure changes for a piezometer at the trial site.

2.2.1 Physical properties of swelling clay

Smectite is a group of common swelling clay minerals including bentonite and montmorillonite. It is a 2:1 layer clay comprised of a two tetrahedral silica sheets either side of a hydroxyl octahedral sheet. The thickness through these 3 layers, or along the c-axis, varies between 1.7 to 10 nm, of which only 0.93 nm is solid mineral and the remainder is interlayer water. A Ca-smectite has a typical thickness of 1.8 nm, while a dilute monovalent solution increases the thickness to 10 nm. The total water content of such a clay is then made up of interlayer water, double-layer water (surrounding the charged clay mineral) and free pore water between the clay particles.

Another useful model for smectite clay was developed by Quirk & Aylmore (1971) who considered smectite clay to be comprised of structural domains. Each domain is formed from several quasi-crystals containing 5 to 10 platelets. The relatively high permeability of the clay is attributed to heterogeneous pore size distribution formed from intra-domain pores (2 - 5 nm), inter-domain pores (1 - 2 nm) and transmission pores ($< 0.05\,mm$). For example, Choi & Oscarson (1996) observed a bimodal pore size distribution for Ca-smectite clay, with large pores that were absent in Na-smectite. Since hydraulic conductivity is proportinal to the square of the pore size, Ca-smectite is relatively permeable when compared to Na-smectite.

A number of physical and chemical factors determine the bulk clay permeability. These include fracturing, the proportion of silt and sand, the consolidation history of the deposit, the cation exchange capacity and the pore water chemistry (Mitchell 1993). Due to the very small particle size, smectite can be cmpacted wet to a hydraulic conductivity between 10^{-10} and 10^{-15} m/s (Rowe et al. 1995). In natural environments however, K_v typically varies beween 10^{-7} and 10^{-10} (Mitchell 1993). The hydraulic conductivity may change with a decrease in exchangeable sodium (Na^+) and an increase in pore water concentration.

2.3 Fracture flow in a dual porosity medium

Fractured media were classified by Streltsova (1976) based on the relative storage and hydraulic conductivity of fractures and matrix. A purely fractured medium (eg. limestone) consists of continuous fracture porosity with zero matrix storage and permeability. In a fractured formation (eg. weathered granite) flow occurs through fractures, despite storage mainly within matrix porosity. A third model for fractured media is the dual-porosity medium (eg. claystone or sandstone) where flow occurs through both the matrix and the fractures.

Under some conditions fractures may provide a conduit for water flux to deep aquifers. Rapid bypass flow may occur through macro pores such as fractures, animal burrows and root tubes (Wood et al. 1997). Micro fractures may not be visible in cores (eg. Keller et al. 1986) but may be revealed by X-ray radiographs (eg. Doser et al. 1998) and deep fractures have been observed to penetrate far below surficial weathered zones. The crack depth and inflow of water into the crack are of paramount importance, although models are not currently capable of incorporating the latter (Bethune & Kirby 2001).

The effective hydraulic conductivity, K_e, of fractured deposits may be several orders of magnitude greater than unfractured medium. Snow (1969) showed that K_e is sensitive to fracture aperture, and less sensitive to fracture spacing.

$$K_e = \left(\frac{\rho g}{\mu}\right)\left(\frac{N(2b)^3}{12}\right) \tag{2.1}$$

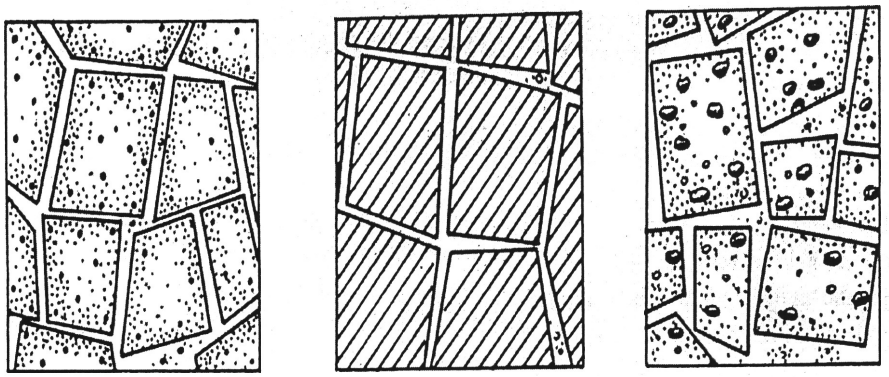

Figure 2.1: Fracture formation, purely fractured medium and dual porosity system (Streltsova, 1976)

Where:

ρ is fluid density,

μ is dynamic viscosity,

b is fracture aperture and

N is the number of fractures per unit length of medium.

This means that small fractures (eg. 30 μm) may significantly increase K, but impart a negligible effect on bulk porosity or bulk storage. Harrison et al. (1992) found that 80% of total flow through an aquitard could be attributed to fracture flow, even when fracture porosity (fracture volume/bulk volume) was only 1.3×10^{-5}. In a semi-arid area of Texas and New Mexico, macro pore flow accounted for between 60% and 80% of annual average recharge of 11 mm (Wood et al. 1997).

Fracture flow is commonly identified by scale independence of hydraulic conductivity determined by different methods. For example, Rudolph et al. (1991) calculated K_e of 1.5×10^{-8} m/s from depth profiles of major ions, 2.7 times higher than K obtained by consolidation testing of 5.5×10^{-9} m/s. In a glacial till, field hydraulic conductivity was up to 3 orders of magnitude greater than that determined by oedometer tests for the clay matrix (2×10^{-10} m/s (McKay et al. 1993)).

2.3.1 Flushing of salt from fracture surfaces

Evaporation from crack surfaces can be large despite the rate of evaporation being less than for surface soils, since surface areas may be between 2.9 to 4.6 times the exposed surface area of soil (Adams & Hanks 1964). Subsequent recharge events may then flush these accumulated salts to groundwater. Drever & Smith (1978) showed that evaporation followed by resolution could result in a solution depleted in SO_4 and Mg relative to Cl.

Enhanced recharge of fresh water in a dual porosity system in the Clare Valley of South Australia, has resulted in back diffusion of solutes from the matrix to fractures (Love & Herzceg 2001). Salt fluxes were increased through the upper flow system which was characterised by high fracture density with apertures of 200 to 600 μm.

Models have been developed to describe the flushing of solutes from fracture surfaces into groundwater in the Chalk aquifer of southern England, in response to recharge events and inundation of fracture surfaces by seasonally high water tables (Wright & Barker 2001). In this case, increased groundwater salinity was directly proportional to increased groundwater levels.

2.4 Groundwater recharge - The Betwa River Basin Study

2.4.1 Introduction

Detailed physical studies were carried out on soils derived from weathering of the Deccan Trap basalts of the Betwa River basin above Dhukwan. The study was a joint endeavour by the Central Groundwtaer Board of India, The Institute of Geological Sciences and the Institute of Hydrology from the UK. The work was carried out between 1977 and 1980 and reported by Hodnett & Bell (1981). The type of soil and the quantification of deep drainage through soils of this type present a very similar problem to the measurement of recharge at Hudson. For this reason, a review of the methodology and results of the Betwa Basin Study is given below. The review is based entirely upon Hodnett & Bell (1981).

The work involved an extensive network of 26 neutron probe measurement sites covering soil depths up to 2 m (Area I); and between 2 m and 12 m (Areas II and III). Mercury manometer tensiometers were installed at various depths to 2.4 m to characterise soil water potential at one of the sites.

Black cotton soils are the major agricultural soil covering a large proportion of the 500,000 km^2 of Deccan Trap basalts over much of Madhya Pradesh, Maharastra and Gujarat Staes in India. The soils show marked swelling and shrinking properties and an extensive pattern of cracks forms during the dry season. The cracks may be up to 75 mm wide at the surface and extend to 6 m depth beneath areas of perennial grass and scrub. Crack depths of 1.5 - 2.0 m are more typical beneath cutivated soils. The soils are stone free except where shallow weathered blocks of basalt occur. All the basalt soils contain small concretions.

2.4.2 Physical properties

The surface soil colour is very uniform (2.5Y 4/2) dark greyish brown and the colour is uniform throughout the upper 2 m of profile. Below this depth the colour becomes gradually paler, changing to 2.5Y 5/3, light olive brown (yellow clay). There is no apparent textural change. The dry bulk density of the upper 0.6 m of the profile is areally very uniform with a mean value of 1.527 g/cm^3.

Soil moisture depletion in the upper 2.5 m at the end of the dry season was established using the neutron gauge sites. The average depletion under 8 wheat sites grown on the deeper soils was 239 mm (standard deviation of 54 mm). The average under 3 dal sites was 223 mm. There was a marked difference between the cultivated sites and the naturally vegetated sites with depletion of as much as 508 mm extending down to 3.0 m - with possibly greater depletion below 3 m.

Very marked variability of wetting was noted early in the wet season caused by recharge being channelled to cracks. Areas with little recharge were thought to be protected by early swelling and closure of smaller crack networks.

Weathered basalt had a specific yield of between 5 and 10%, compared with the black cotton soil (1 - 2%) and the yellow clay (<0.5%), and therefore drains more readily.

Actual daily mean evapotranspiration rates calculated from the water balance data for three periods covering the end of the monsoon are shown in Table 2.1. These data show that the actual evapotranspiration can exceed the potential when the soils are wet - possibly the impact of a much reduced albedo for wet soil, but that the rate drops rapidly to 40% of potential within 3 weeks of the end of the rains and to only 14% aftr 6 weeks (Hodnett & Bell 1981).

The total actual evapotranspiration from the cropped sites calculated from the water balance for the bulk of the depletion period between 14 October 1977 to 2 June 1978 was 307.1 mm. This was 31% of the potential evaporation of 999 mm. Post monsoonal drainage losses from the deep soils were small. A figure of 28 mm (10%) moisture loss from the upper 2.5 m was noted. The evapotranspiration rate did not appear to be impacted by the size of the soil moisture deficit. If this is the case, then annual

Table 2.1: Relationship between actual and potential daily evapotranspiration at Betwa, Deccan Plateau, India

Period 1978	Actual ET (mm)	Potential ET (mm)
2 to 8 September	4.1	2.9
8 to 21 September	1.9	4.9
7 to 28 October	0.6	4.4

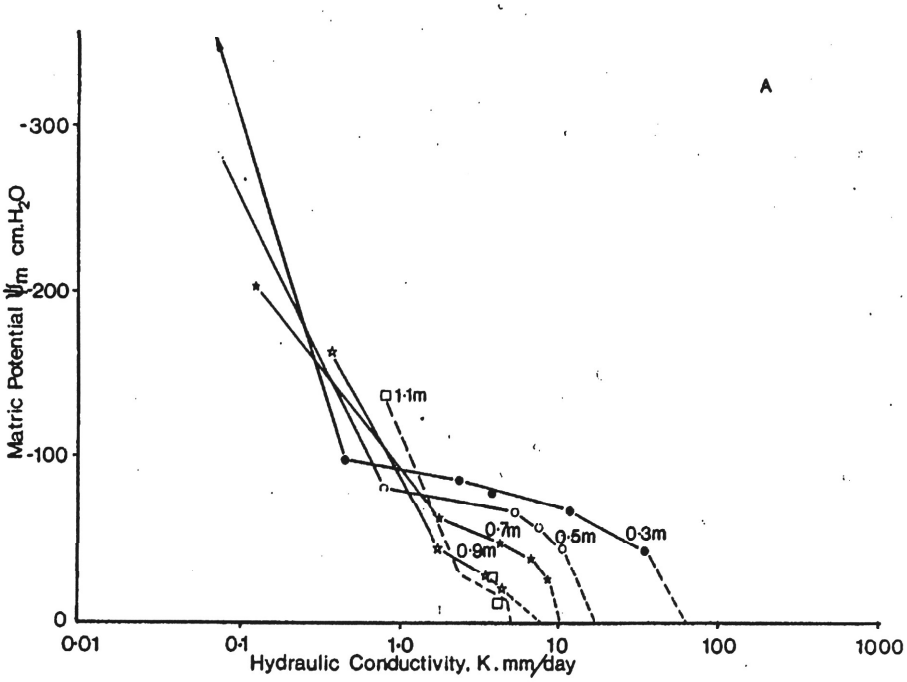

Figure 2.2: Unsaturated hydraulic conductivity variation at Dhaturi Site

evapotranspiration will be fairly constant in most years.

2.4.3 Unsaturated hydraulic conductivity determination

Unsaturated hydraulic conductivity data were obtained using the instantaneous profile method of Watson (1966) where moisture flux (υ) was determined by neutron probe measurement and matric potentials (ψ) by the mercury manometers. Equation 2.2 was then used to solve for hydraulic conductivity at different moisture and matric potentials.

$$\upsilon = -K_{(\psi_m,\theta)} \frac{d\psi}{dz} \tag{2.2}$$

Replicate plots 6 m apart were established in two areas of deeper soils. One of the plots was allowed to be farmed as normal while the second plot was covered with sheets of plastic and used to determine the hydraulic conductivity as the profile drained. Each plot comprised two sets of neutron probes and 1 set of manometers.

A rapid decrease in hydraulic conductivity with depth was observed at both sites for any given value of matric potential between 0 and 800 mm head. Results from Hodnett & Bell (1981) are shown in Figure 2.2 and Figure 2.3.

Figure 2.2 and Figure 2.3 demonstrate that large decreases in hydraulic conductivity occur for initial

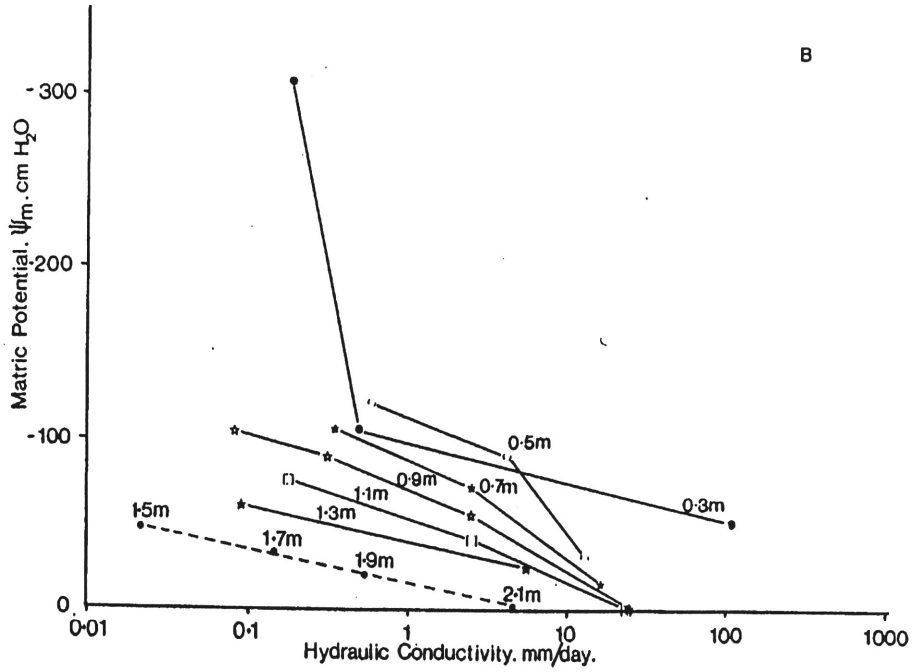

Figure 2.3: Unsaturated hydraulic conductivity variation at Nabibag Site

decreases in matric potential. This may indicate the draining of initial pore space in the fractured soil. At both sites a reduction in volumetric moisture content (θ_v) of 0.02 reduces the hydraulic conductivity by two orders of magnitude or more.

2.4.4 Hydrological significance of the shrinkage cracks

The shrinkage cracks facilitate the early re-wetting of the soil (Hodnett & Bell 1981). The wide open cracks presented to the early rains of the monsoon allow water to freely enter the soil down to the base of the fissure system. This allows the soil to rewet quickly and rainfall goes preferentially into removing soil moisture deficit rather than to surface runoff. Initial wetting is very sporadic however with a clear picture emerging only when the matric potential rises above -500 cm (water). As wetting of the profile proceeded a zone of saturation appears in the middle of the soil profile between 0.6 m and 1.5 m with unsaturated conditions both above and below. This is particularly well shown in the profile for 29/7/1979 shown in Figure 2.5. The saturated zone then gradually expands upward and downward until the complete profile is saturated

The hydraulic conductivity data show that conductivity decreases with depth in the upper 1.5 - 2.0 m of the profile. The shrinkage cracking beneath crops also follows this pattern. In areas beneath natural vegetation, enhanced hydraulic conductivity extends to depths of 4 m or greater. The rapid decrease in hydraulic conductivity in the range of matric potential between zero and -1000 mm is evidence that the principal conductive pathways for water movement are large pores or fractures which are full only at potentials greater than -1000 mm. The rapid decrease in conductivity in this range of matric potential is associated with moisture content reduction of about 0.02 and this indicates that these large pores (diameter 0.03 - 0.3 mm) only occupy about 2% of the soil volume.

The matric potential data clearly indicate that little deep drainage occurs once the soil profile is saturated. Drainage through cracks appears to be the main process of water movement therefore and will diminish as the cracks close due to soil expansion.

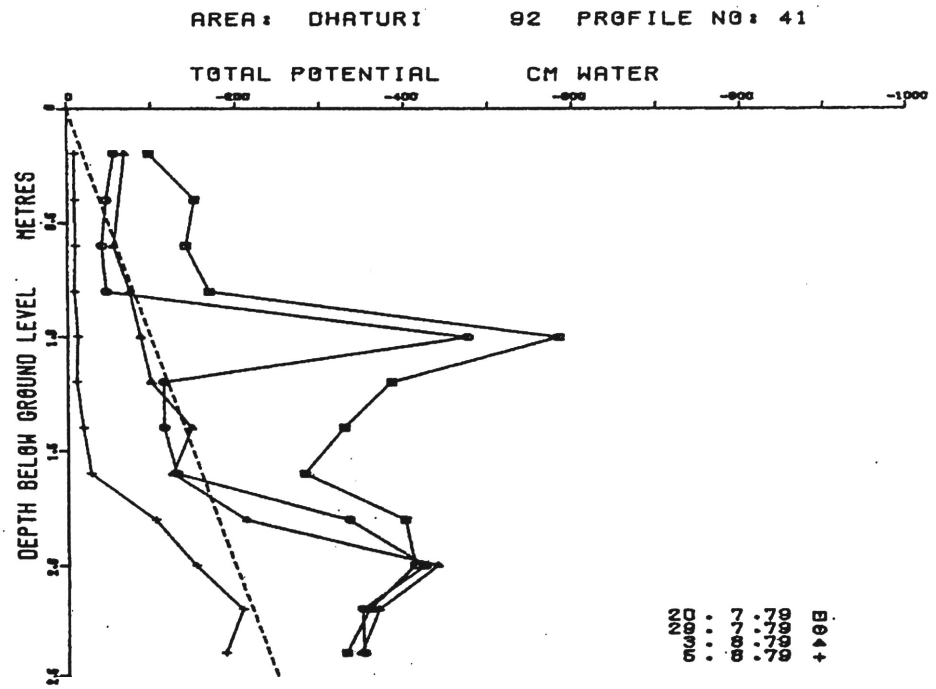

Figure 2.4: Total potential vs depth at Dhaturi Site (A) during wetting of the profile

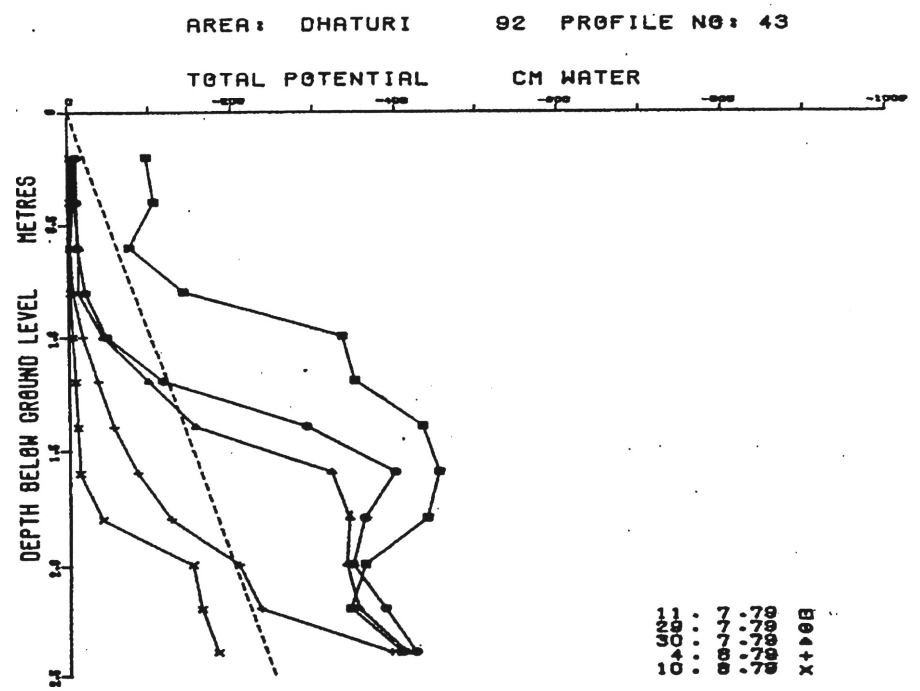

Figure 2.5: Total potential vs depth at Dhaturi Site (B) during wetting of the profile

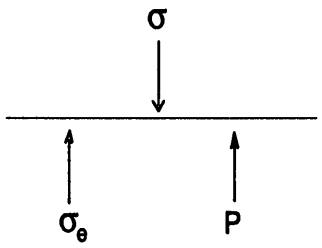

Figure 2.6: Stress balance about a horizontal plane

2.5 Flux through deformable media

The theory of fluid flow in a deformable matrix is developed in this section as it is not widely available in the literature and must be included to understand the observed hydrographic responses reported in later chapters. The discussion is based on work by Domenico & Schwartz (1990) and Smiles (2000).

2.5.1 Compressibility of the Rock Matrix: The Effective Stress Concept

For a saturated porous material to undergo compression there must be an increase in the grain-to-grain pressures within the matrix and/or an increase in the water pressure. Without such pressure changes, no volumetric change can occur.

The total vertical stress (pressure) acting on a horizontal plane at any depth can be resolved into two components (Fig. 2.6 and Equation 2.3).

$$\sigma = P + \sigma_e \tag{2.3}$$

Where:

σ is the total stress acting downwards and is the weight of all the overlying material,

σ_e is the effective stress - the component of σ supported by the grain to grain contact of the media,

P is the neutral stress or water pressure

The stress balance represented by Equation 2.3 is important in understanding much of what occurs in deformable media. Consider the way in which this balance would change as the total stress changes. Differentiating Equation 2.3 with respect to σ gives:

$$\frac{\partial \sigma}{\partial \sigma} = 1 = \frac{\partial P}{\partial \sigma} + \frac{\partial \sigma_e}{\partial \sigma} \tag{2.4}$$

Where:

$\frac{\partial P}{\partial \sigma}$ is called the pore pressure coefficient and represents the percentage of the load that is carried by the fluid provided that the fluid is not allowed to drain. This term is also known as the Tidal Efficiency.

$\frac{\partial \sigma_e}{\partial \sigma}$ must then represent the percentage of the load carried by the matrix. This term is also known as the Barometric Efficiency.

2.5.2 Development of the Flow Equation

The normal Darcy Equation is based on the flow of water in response to a gradient in hydrostatic head in a rigid matrix. As described above, the Hudson clays are deformable and therefore a more extensive theoretical development is required to understand the flow of water that also occurs as a result of a gradient of excess pressure. Following the discussion on effective stress we can write:

$$\sigma + \Delta\sigma = \sigma_e + (P_s + P_{ex}) \tag{2.5}$$

Where the total pore water pressure comprises 2 parts, P_s being the hydrostatic pressure and P_{ex} is a transient pore water pressure in excess of the hydrostatic pressure and is related to the increased downward total stress component ($\Delta\sigma$).

In a similar fashion, the total hydraulic head can be restated (Domenico & Schwartz 1990) as:

$$h = z + \frac{P_s}{\rho g} + \frac{P_{ex}}{\rho g} \tag{2.6}$$

where:

h is hydraulic head

z is distance above some datum plane - normally sea level

ρ is the density of water

g is acceleration due to gravity

Darcy's Law relates the flux of water to the gradient in hydraulic head.

$$\frac{Q}{A} = v \approx \frac{\Delta h}{\Delta L} \tag{2.7}$$

Where:

v is the specific discharge derived from the flow through a particular cross sectional area. This term can also be thought of as a volume flux of water.

L is distance in a generalised direction.

Introducing a proportionality constant, which we call *hydraulic conductivity* gives:

$$v = -K\frac{\partial h}{\partial L} \tag{2.8}$$

The negative sign indicates that water moves from areas of higher hydraulic head to areas of lower hydraulic head.

For one-dimensional flow in the vertical direction, Darcy's Law can be restated as:

$$v_z = -K_z\frac{\partial h}{\partial z} = -K_z\frac{\partial}{\partial z}\left(z + \frac{P_s}{\rho g} + \frac{P_{ex}}{\rho g}\right) \tag{2.9}$$

Following the approach of Domenico & Schwartz (1990), when considering the flow that occurs in response to excess pressure change only, Equation 2.9 can be simplified to:

$$v_z = -\frac{K_z}{\rho g}\frac{\partial P_{ex}}{\partial z} \tag{2.10}$$

We need to develop a relationship that describes the way in which mass is conserved within a representative control volume of the material under consideration. How does v_z change with respect to distance and time. We either have a steady state approach where $\frac{\partial v_z}{\partial z} = 0$ - mass moves into and out of the control volume at the same rate and there is no change in the mass stored within the control volume, or $\frac{\partial v_z}{\partial z} \neq 0$ and mass can be stored or lost from the control volume. Clearly, for the clays that are capable of deformation, there will be some change in the storage and we need to consider the second case.

The derivation of a mass conservation equation for this relationship has been the subject of considerable discussion in the literature. A relationship that describes the way in which the flux (v) changes with space and time is required. Early attempts at this (Jacob 1940) ignored the fact that the co-ordinate system had to deform if there was to be a change in σ_e due to compression. This was overcome by the use of material derivatives that followed the motion of the solid phase rather than using a fixed Cartesian co-ordinate system. The approach is described fully by Domenico & Schwartz (1990) and has been recently invoked in the soil physics literature by Smiles (2000).

The result of using the material derivative approach to take account of the deforming medium is that the conservation equation for a homogeneous fluid moving in the vertical dimension can be written as:

$$-\frac{\partial v_z}{\partial z} = \frac{\phi}{\rho}\frac{\partial \rho}{\partial t} + \frac{1}{1-\phi}\frac{\partial \phi}{\partial t} \tag{2.11}$$

The RHS of equation 2.11 describes 2 terms. The first relates to the way in which the density of water (ρ) changes with time. The second describes the way in which the porosity (ϕ) changes with time. If water is to be added to or removed from storage, it has to either change the density of the water or the volume of the pore space.

The change in density of water is related to the pressure and the compressibility of water, viz:

$$\frac{\partial \rho}{\partial t} = \rho \beta_w \frac{\partial P}{\partial t} \tag{2.12}$$

The change in porosity can be written (Domenico & Schwartz 1990) as:

$$\frac{1}{1-\phi}\frac{\partial \phi}{\partial t} = \beta_p \left(\frac{\partial P_{ex}}{\partial t} - \frac{\partial \sigma}{\partial t} \right) \tag{2.13}$$

Where:

β_w is the compressibility of the water and

β_p is the compressibility of the matrix

For completeness, the compressibility of water at constant temperature and mass is defined as:

$$\beta_w = \frac{1}{K_w} = -\frac{1}{V_w}\left(\frac{\partial V_w}{\partial P}\right)_{T,M} \tag{2.14}$$

where:

β_w is the compressibility of water with units of reciprocal pressure $(m^2/newtons)$ $\frac{m \cdot s^2}{kg}$

K_w is the bulk modulus of compression for the fluid,

V_w is the bulk fluid volume

P is the pressure (Pa) or $(newtons/m^2)$ $\frac{kg}{m \cdot s^2}$

The compressibility of the matrix, assuming that the grains themselves are incompressible, is given by:

$$\beta_p = \frac{1}{K_b} = -\frac{1}{V_b}\left(\frac{\partial V_b}{\partial \sigma_e}\right)_{P,T} = \frac{1}{V_b}\left(\frac{\partial V_p}{\partial \sigma_e}\right)_{P,T} = \beta_p = \frac{1}{H_p} \tag{2.15}$$

where $\Delta V_b = \Delta V_p$ for the special case of incompressible grains. Note that the clay grains are compressible as water is driven out of them and this term will need further definition. Notwithstanding that, the remaining terms are:

β_b is the total bulk compressibility of the matrix. Units of $(m^2/newtons)$ $\frac{m \cdot s^2}{kg}$

K_b is a bulk modulus of compression

β_p is the vertical compressibility

H_p is a modulus of compression referring only to the pore space

V_b is the bulk volume

V_p is the pore volume and

σ_e is the effective stress

Returning to Equation 2.13, the quantity $\partial\sigma/\partial t$ can be thought of as the vertical stress that gives rise to the excess pressure development. Substituting the relationships for density change with time (Equation 2.12) and porosity change with time (Equation 2.13) into the 1-D conservation of mass equation (Equation 2.11) gives:

$$\frac{\partial v_z}{\partial z} = \phi\beta_w \frac{\partial P}{\partial t} + \beta_p \left[\frac{\partial P_{ex}}{\partial t} - \frac{\partial \sigma}{\partial t}\right] \tag{2.16}$$

Substituting Darcy's Law (Equation 2.10) into Equation 2.16 and rearranging terms on the RHS gives:

$$K_z \frac{\partial^2 P_{ex}}{\partial z^2} = \rho g \left(\phi\beta_w + \beta_p\right) \frac{\partial P_{ex}}{\partial t} - \left(\rho g \beta_p\right) \frac{\partial \sigma}{\partial t} \tag{2.17}$$

The term $\rho g(\phi\beta_w + \beta_p)$ is known as the specific storage, whereas the quantity $\rho g \beta_p$ is the component of specific storage due exclusively to pore compressibility.

In some problems it can be assumed that the stress is applied rapidly and then held constant. This could occur as the result of a considerable quantity of rain added to the top of a soil column - or a vehicle moving onto the soil and staying there. In this case, the second term on the RHS of Equation 2.17 diminishes to zero. If we also consider that the compressibility of water is so much less than the compressibility of the soil skeleton that it can be ignored, Equation 2.17 can be collapsed to:

$$\frac{\partial^2 P_{ex}}{\partial z^2} = \frac{\rho g \beta_p}{K_z} \frac{\partial P_{ex}}{\partial t} = \left(\frac{1}{C_v}\right) \frac{\partial P_{ex}}{\partial t} \tag{2.18}$$

This is the 1-D consolidation equation (Terzaghi & Peck 1948) where the hydraulic diffusivity C_v is also known as the coefficient of consolidation and is given by:

$$C_v = \frac{K_z}{S_s} \tag{2.19}$$

Using equation 2.17 we can calculate the rate at which a hydraulic change will propagate through an aquifer. Rearranging we get:

$$\frac{\partial P_{ex}}{\partial t} = C_v \frac{\partial^2 P_{ex}}{\partial z^2} \tag{2.20}$$

Equation 2.20 is analogous to Fick's 2nd Law that allows the calculation of the rate of movement of a solute front in terms of the concentration gradient, viz:

$$\frac{\partial C}{\partial t} = D \frac{\partial^2 C}{\partial x^2} \tag{2.21}$$

Where:

D is the diffusion coefficient

2.6 Undrained Response of Water Levels to Natural Loading Events

The way in which the water level in a piezometer reacts to changes in load can be used to determine the storage (compressibility) characteristics of the matrix (aquifer). Some loads, such as atmospheric pressure, act on both the formation and the water in the piezometer at the same time, while other loads, such as additional weight of rain, floods or tides act only on the matrix and not on the water level in the piezometer. This difference leads to important variations in the observed response.

It is also important to consider the boundary conditions under which the loading takes place. There are two possibilities:

- For field deformations that are slower than the characteristic time for diffusion of fluid through the matrix - a *drained response* occurs. This can be seen where a load is applied to a sandy aquifer. There is an initial increase in water pressure, but water then moves away and the load shifts to the grains - so the water pressure returns to the initial level.
- When the application of the load is rapid in comparison to the time taken for diffusion of the pore fluid the local fluid mass remains essentially the same and an *undrained response* is noted.

The undrained response is elastically stiffer than the drained response so that the respective deformations are characterised by different coefficients.

All water-level fluctuations as observed at a point that are caused by rapid loading such as tidal or atmospheric variation can be treated as constant mass phenomena. This implies that no fluid flow occurs and therefore the fluid flow term in equation 2.18 can be set to zero leaving, after rearrangement:

$$\left(\frac{\partial P_{ex}}{\partial \sigma}\right)_M = \frac{\beta_p}{\beta_p + \phi\beta_w} \tag{2.22}$$

This equation is called the pore pressure coefficient equation (refer also to equation 2.4) and defines the change in fluid pressure at constant mass (undrained) as the stress increases. Literally speaking, it represents the proportion of an incremental load that is carried by the pore fluid assuming that the pore fluid is not allowed to drain. Jacob (1940) referred to this quantity as the *tidal efficiency (T.E.)*. As used by Jacob (1940), the TE is defined as the ratio of a piezometric level amplitude as measured in a well to the oceanic tidal amplitude, or:

$$T.E. = \frac{dP}{\rho g \Delta h} = \frac{\beta_p}{\beta_p + \phi\beta_w} \tag{2.23}$$

Loading of clay can occur due to flooding or to rainfall moisture induced changes in the weight of the top soil. The above theory suggests that the water level in a piezometer will respond to these changes as an additional stress is applied to the surface. Note that the water level change will occur even though there is no movement of the water down into the clay!

Barometric pressure has an inverse relationship with water levels in a piezometer. As the atmospheric pressure increases, the water level decreases. For a rock with a very low compressibility (lower than water), the rock matrix takes all the additional pressure and the well acts as a perfect barometer. Returning to equation 2.4 it can be seen that if $\partial P/\partial \sigma$ represents the tidal efficiency, the other term in this equation $(\partial \sigma_e/\partial \sigma)$ represents the barometric efficiency, and that:

$$1 = TE + BE \tag{2.24}$$

so that

$$BE = 1 - TE = 1 - \frac{\beta_p}{\beta_p + \phi\beta_w} = \frac{\phi\beta_w}{\beta_p + \phi\beta_w} \tag{2.25}$$

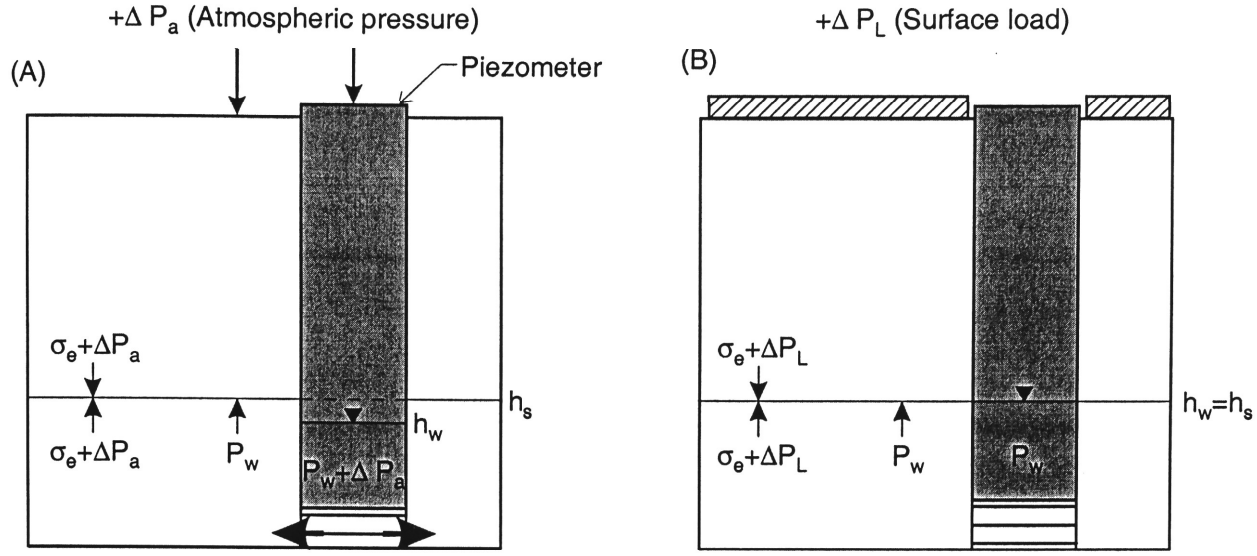

Figure 2.7: (a) Rigid and confined matrix subject to atmospheric pressure increase - Water level falls (b) Rigid and confined matrix subject to additional surface loading - No change in water level.

Thus as $\beta_p \rightarrow 0$ for a rigid aquifer, $BE \rightarrow 1$ and $TE \rightarrow 0$. Conversely, as β_p becomes larger (less small), $BE \rightarrow 0$ and $TE \rightarrow 1$. BE is closely related to the compressibility of the fluid and TE is closely related to the compressibility of the matrix. It follows then that we *would* expect TE responses in deformable clays such as those at Hudson.

In a rigid system, the changes in σ will be completely supported by change in σ_e and the value of $\frac{\partial \sigma_e}{\partial \sigma}$ will $\rightarrow 1$. As the rock matrix is rigid, it has a very low compressibility ($\beta_P \rightarrow 0$). Consider what happens in a borehole drilled into a rigid aquifer, such as a limestone, to change in atmospheric pressure. A schematic is given in Figure 2.7.

In Fig. 2.7(a), an increase in ΔP_a (a high pressure area approaching) is transferred to σ_e as the value of β_p is very small and the rock supports any change in weight. This leaves P_w in the formation less than the pressure in the well $P_w + \Delta P_a$ as the atmospheric pressure change is transmitted instantaneously to the water in the well. Water then moves into the formation in response to the pressure differential between the well and the formation. The water level in the piezometer falls as the atmospheric pressure increases. A barometric efficiency (BE) can be calculated as a ratio of the fall in water level (Δh) computed as a pressure, to the change in atmospheric pressure. $BE = \Delta h \rho g / \Delta P_a$. In terms of compressibilities as $\beta_p \rightarrow 0$ then:

$$BE = \frac{\phi \beta_w}{\beta_p + \phi \beta_w} = 1 \tag{2.26}$$

It is also useful to see what happens to a rigid aquifer system in response to an applied load - such as a train or building. In Fig. 2.7(b), the additional stress from the surface loading is carried by the matrix, leaving P_w unchanged. The loading on the surface is not transferred to the water in the well and therefore there is no hydraulic gradient set up and no water level change occurs.

The BE can be used as an indication of the compressibility of the rock. As $BE \rightarrow 1$ the rock must be incompressible and $\beta_p \ll \beta$. Conversely, the degree to which BE falls short of unity is an indication of the compressibility of the formation. If $\beta_p \gg \beta$ another type of response occurs.

In a system that can deform, where the $\beta_p \gg \beta$, increases in total stress are shared differently. Figure 2.8(b) indicates the repsonse to an increase in surface loading indicated by ΔP_L. The formation compresses elastically and leaves the water to take the load. As the surface of the water in the piezometer is not subject to the increased load, a gradient in water pressure exists around the piezometer with water moving into the well in response to this gradient. A tidal efficiency (TE) can be defined (Jacob

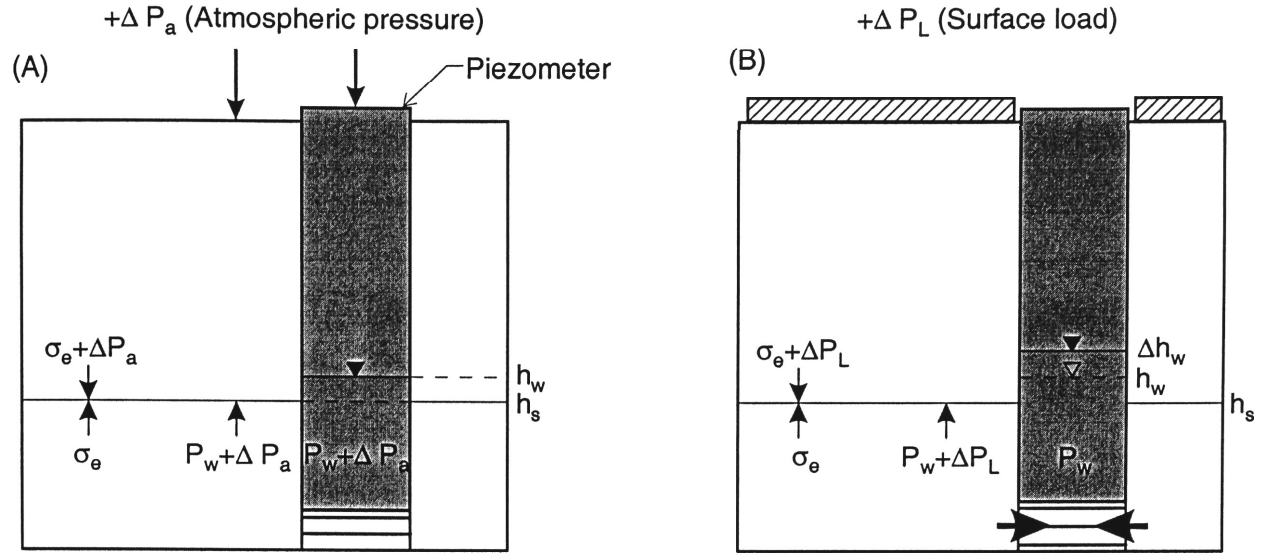

Figure 2.8: (a) Compressible and confined matrix subject to atmospheric pressure increase - No change to water level in piezometer (b) Compressible and confined matrix subject to increased surface loading - Water level rises in response to the increase in total stress.

1940) as:

$$T.E. = \frac{dP}{\rho g \Delta h} \tag{2.27}$$

It is of interest to see what would happen in a compressible aquifer to a change in atmospheric pressure. The schematic is shown in Figure 2.8(a). As the increase in total stess due to the atmospheric pressure change is transfered to the water around the piezometer at the same time as to the water in the piezometer - there is no gradient in water pressure between the piezometer and the ground around and therefore no flow of water and no change in water level in the well.

Chapter 3

INVESTIGATION METHODS

3.1 Drilling and piezometer installation

Piezometers at the Hudson site were installed in two phases. On the 25–26^{th} of June 1996, 3 nested piezometers were installed on the upper, mid and lower slope. These were installed by Ray Tyndall of Afrac Drilling using a Mayhew 1500 rotary rig, without the aid of drilling mud.

An exploratory hole was later drilled through bedrock above the site. Since it was powder dry, the hole was abandoned and backfilled. In May 1997, 2 additional nested piezometers were installed, one located in the woodland above the site, and another adjacent to Pump Station Creek. Although the woodland site was also drilled through basalt rock, some weathered horizons were detected at this location that justified the installation of piezometers. These piezometers were installed using a rotary mud drilling rig Mayhew 15W, by Gary Smit of DLWC Groundwater Drilling.

All piezometers were constructed using 50 mm PVC casing (Class 9 and 12 for phase I and II piezometers respectively). Machine slotted screen was gravel packed in the hole and 1 m thick bentonite seals placed between the piezometer screens. Filter socks were not fitted. Detailed construction diagrams are provided in Appendix A and the piezometer locations are shown on Fig. 1.2.

3.2 Downhole geophysical logging

Gamma ray activity and bulk electrical conductivity logs were obtained using a GEONICS EM-39 downhole logging device (McNeil 1986). The gamma ray activity log was run at a speed of 0.015 m/s using a time constant of 8 seconds. An electromagnetic induction logging tool was then run at a speed of 0.050 m/s to produce a bulk electrical conductivity (ECa) log. Data was sampled at 25 mm depth increments.

3.3 Electrical Image Acquisition

Three 122.5 m long electrical images (Acworth 1999) were measured after lucerne had been planted in September 2000. Measurements were repeated in November 2000, January 2001, March 2001, June 2001 and August 2001 to investigate the change in soil moisture status beneath the plots as the lucerne crop developed. Line locations are shown on Fig. 4.3.

Two 25 multi core cables were used in this work with takeouts on each cable arranged every 5 m. The cables were laid overlapping by 2.5 m. Stainless steel or brass electrodes were pushed approximately 20 cm into the soil and connected to the multi-core cables. Electrical images were measured using a

LUND automatic electrode selector connected to an ABEM 4000 Terrameter. The data was interpreted using the RES2DINV code of Loke (2001).

3.4 Groundwater level data collection

DATAFLOW capacitance probe loggers were installed in 4 piezometers but were replaced by OTT pressure transducer loggers early in 1999. Unfortunately, the reliability and accuracy of DATAFLOW loggers was less than acceptable, particularly at saline sites further north in the Yarramanbah/Pump Station catchment where a level drift of 0.3 m within a few weeks was common. Comparison tests of DATAFLOW, GREENSPAN and OTT loggers were then carried out by Heidenreich (pers. com. Jan 1998), which confirmed that investment in pressure transducer loggers could be justified by increased accuracy, reliability and reduced maintenance costs, despite a 10 fold higher initial capital expense.

Groundwater level results for 1998 and the first half of 1999 were reported by Heideneich (1999a). Groundwater level data between June 1999 and November 2001 were compiled for this report from logger files provided by DLWC.

3.5 Sampling and analysis of water

Sampling and analysis of groundwater from the Hudson site was opportunistic, in the sense that sampling events occurred whenever personnel, funding and access permitted. Access to piezometers on the lower slope for example, was often prevented by crops or by lack of access over wet black soil. Although 6 sampling events occurred, the number of samples from individual piezometers varies from 2 to 6, with the focus of activity at piezometer 248110-3, below the trial plots.

The first samples that were taken in March 1997 were analysed by the Tamworth Environmental Laboratory, with bicarbonate analysed at the DLWC Gunnedah Research Centre within 24 hours of sampling. The results were characterised by large charge balance errors.

In April 1997, piezometer 248110 and piezometers 248108-1, -2 and -3 were sampled for isotope analysis. CSIRO Adelaide laboratory provided carbon-14, and carbon-13 values for 248108-3. ANSTO laboratories at Lucus Heights, Sydney analysed 4 samples from the above piezometers for tritium.

Testing of field parameters and major ion chemistry was carried out by UNSW Groundwater Centre in May, 1999 and March and July 2000, with the results from the first of these tests reported by Chambers (1999). The July 2000 sampling included analysis for oxygen-18, deuterium, carbon-13, carbon-14 and tritium isotopes. Radio isotopes were analysed by the Institute for Nuclear Sciences, New Zealand. Detailed sampling procedures adopted by UNSW Groundwater Centre are provided below. Finally, in November, 2001 field parameters and selected major ion chemistry was tested at various stages of purging piezometer 248110-3.

A submersible pump (GRUNDFOS MP1) was required to recover water samples from higher yielding piezometers at the lower slope, and adjacent to the creek. Samples from the upper and mid slope were obtained by hand bailer.

3.5.1 Unstable chemistry

Electrodes were calibrated in the field according to standard WRL procedures (Beck 1999). EC measurements were temperature corrected to 25 °C . A salinity correction was not applied to measured DO given the relatively low salinity groundwater encountered. EH measurements from the Ag/AgCl electrode (E_0) were converted to the standard normal hydrogen electrode (E_{NHE}). Water samples were taken for

analysis when these parameters stabilised, to ensure that stagnant casing water was removed, and that representative groundwater samples were obtained.

Bicarbonate (HCO_3) was determined by titration of an aliquot of sample with 0.01 M HCl down to an endpoint of pH 4.3. Acidity due to free carbon dioxide ($CO_2(aq)$) and undissolved H_2CO_3 was measured by titration of a sample aliquot with 0.025 M NaOH to pH 8.3. These titrations were performed with an ORION meter that was fitted with a Ross Sureflow pH electrode to ensure rapid equilibration.

3.5.2 Inorganic chemistry

A sample for cation determination was preserved after filtering through a 0.45 μm filter into a 50 ml plastic screw top jar, and acidified with 2–3 drops of concentrated HCl. An unfiltered and unacidified sample of at least 200 ml was retained in a triple rinsed HPT bottle for chloride analysis and silica testing.

All the above samples were cooled, either in the refrigerator of the mobile laboratory van, or in chilly boxes.

Major cations, trace elements, and total Fe and total S were determined by inductively couple plasma atomic emission spectroscopy (ICP-AES) at the UNSW Geography Laboratory. Samples with high EC were diluted prior to analysis and the results corrected as necessary. Sulphate was assumed equal to total sulphur (×2.994).

Chloride and reactive silica were analysed at the UNSW Water Research Laboratory, by standard methods described by Beck (1999). For Cl, this involved argentometric titration, and for reactive silica, spectrophotometric analysis by the heteropoly blue method.

3.5.3 Environmental isotopes

Samples were also collected for stable isotope analysis at selected sites. Duplicate samples for $\delta^{18}O$ and $\delta^{2}H$ analysis were collected in 28 ml glass McCartney bottles, ensuring no head space. The bottles were periodically tightened and stored inverted against the insert rubber seals to ensure an air-tight seal. Samples for $\delta^{13}C$ analysis were collected by precipitating all available DIC in a 2 L samples, using saturated $SrCl_2$ under alkaline conditions. This was achieved by addition of 4 ml of freshly prepared 11 M NaOH.

Selected samples were collected for radioisotope analysis. Samples for $\delta^{3}H$ analysis were collected in 1.0 L glass Schott bottles, taking care that the tops were sufficiently tightened to prevent atmospheric exchange. Samples for carbon-14 analysis were obtained according to guidelines supplied by the Institute of Geological & Nuclear Sciences (C. Taylor, pers. com., March 2000). Saturated $SrCl_2$ and NaOH solutions were pre-prepared in numbered and weighed 50 ml Schott bottles using anlaytical grade reagents. Samples were collected in accurately pre-weighed and numbered 1 L Schott bottles. The contents of partnered 50 ml Schott bottles was added to each sample bottle, with care that any precipitated impurities were left in the 50 ml bottle. The bottles were then filled to the rim to exclude as much air as possible. Lids on both bottles were periodically tightened.

3.5.4 Rainfall chemistry and stable isotopes

A simple rainfall sampler was designed using a modified 50 L plastic drum (Figure 3.1). A 0.5 m diameter plastic funnel fed into a 1.0 L glass Schott bottle nested within the drum. This design ensured a sample volume of about 1.0 L from a 5 mm rainfall event. To ensure a pure rainfall sample, the funnel was covered by a lid between rainfall events and was fitted with an insect screen constructed from wire mesh.

The rainfall sampler was installed within the meteorological enclosure at the DLWC Gunnedah Research Centre. The lid was removed prior to an imminent rainfall event and the sample collected within 24 hours

Figure 3.1: Cost effective rainfall sampling device.

so as to mimimise effects of evaporation and atmospheric exchange on the sample. On site measurement of pH and EC were undertaken. Samples were transferred to duplicate McCartney bottles for $\delta^{18}O$ and $\delta^{2}H$ analysis by CSIRO Adelaide. Excess sample was transferred into a plastic bottle for subsequent major ion analysis by ICP-AES at UNSW.

3.6 Cation exchange capacity of solid phase

Cation exchange capacity ($CEC_{effective}$) was determined on solid phase samples collected in 0.2 m increments from the ground surface to 3.0 m depth. These were collected from Plots 4, 14, 23 and 32 (Locations shown on Fig. 1.4 in July 1995.

Analysis was conducted by NSW Agriculture laboratories in Rydalmere by the $BaCl_2$ extraction method.

Chapter 4

RESULTS

4.1 Bedrock and colluvial-alluvial profiles

A cross-section of the Liverpool Range foot slope at the Hudson site is depicted in Figure 4.1.

Basalt bedrock, in a variable but relatively unweathered state, was encountered during drilling of the uppermost piezometer nest (40827) and an abandoned test hole (40825), between 3 m to 50 m depth and 6 m to 50 m depth respectively. Alternate layers of blue and red (stained) basalt, with minor clay rich layers suggested that the bedrock is not massive but comprised of a series of volcanic flows. Since basalt bedrock was recorded at similar elevation at both piezometer nests 248107 and 248110, these volcanic flows are only gently dipping.

Clay rich colluvium-alluvium was at least 21 m thick at the piezometer on the lower slope, compared with about 10 m thick below the agricultural trial site and less than 2 m depth below woodland on the upper slope. Weathered basalt was observed below the colluvium-alluvium at two piezometer nests on the upper slope. The angle of the interface between fresh and weathered basalt is steeper than the dip of the basalt surface and indicates that the weathered profile cuts across the flow boundaries.

4.2 Piezometer installation details

Installation details for 12 monitoring points at 5 nested piezometer sites are outlined in Table 4.1. Of these piezometers, the following have remained dry:

- all piezometers at the woodland nested piezometer site (40827-1, 40827-2) and
- shallow piezometers at the sites above and within the Agricultural trial site (248107-1, 248107-2, 248110-1, 248110-2).

Groundwater influx in the deep piezometers (248107-3 and 248110-3) was slow. In contrast, there was a large groundwater influx to piezometers below the Agricultural trial site, and near the creek. The driller estimated influx to piezometer 248108-2 at 0.013 L/s (100 gallons/hour), and to piezometer 248108-3 at 0.06 L/s (50 gallons/hour) (R. Tyndall, Afrac Drilling, pers. com., June 1996).

Table 4.1: Piezometer installation details for Hudson site

Bore ID	Easting [a]	Northing	Elevation ground m RL [b]	Elevation top piezo m RL	Piezo Screen m	Install date	Lithology [c]
40825 [d]	257700	6486570	-	-	-	Feb-97	B
40827-1 [e]	257930	6486690	137.12	138.01	10-13	May-97	WB
40827-2	257930	6486690	137.12	138.01	28-40	May-97	partly WB
248107-1[f]	257664	6487157		110.29	5.7-6.7	Jun-96	WB
248107-2	257664	6487157		110.29	12.0-13.0	Jun-96	WB
248107-3	257664	6487157		110.29	22.5-23.5	Jun-96	B
248110-1[g]	257190	6487168		100.6	6.0-7.0	Jun-96	CA
248110-2	257190	6487168		100.6	9.0-10.0	Jun-96	WB
248110-3	257190	6487168		100.6	16-17	Jun-96	B
248108-1[h]	256654	6487784		81.52	6.0-7.0	Jun-96	CA
248108-2	256654	6487784		81.52	9.0-10.0	Jun-96	CA
248108-3	256654	6487784		81.52	20.7-21.7	Jun-96	WB
40832-1[i]	256050	6486820	82.93	84.05	5-7	May-97	CGRAV
40832-2	256050	6486820	82.93	84.05	18-21	May-97	WB

[a] determined by hand held GPS
[b] relative to BM = 100 m on tree (survey courtesy of NSW Agriculture)
[c] WB = weathered basalt, B = basalt, CA = colluvium-alluvium, CGRAV = clayey gravel
[d] located opposite Hudson gate, abandoned and backfilled
[e] located in woodland above Ag site, 100 m north of Blackville road fence
[f] located above Ag site on downhill side of contour bank
[g] located in centre of Ag site
[h] located below Ag site, on fence line
[i] located on SW bank of Pump Station Creek

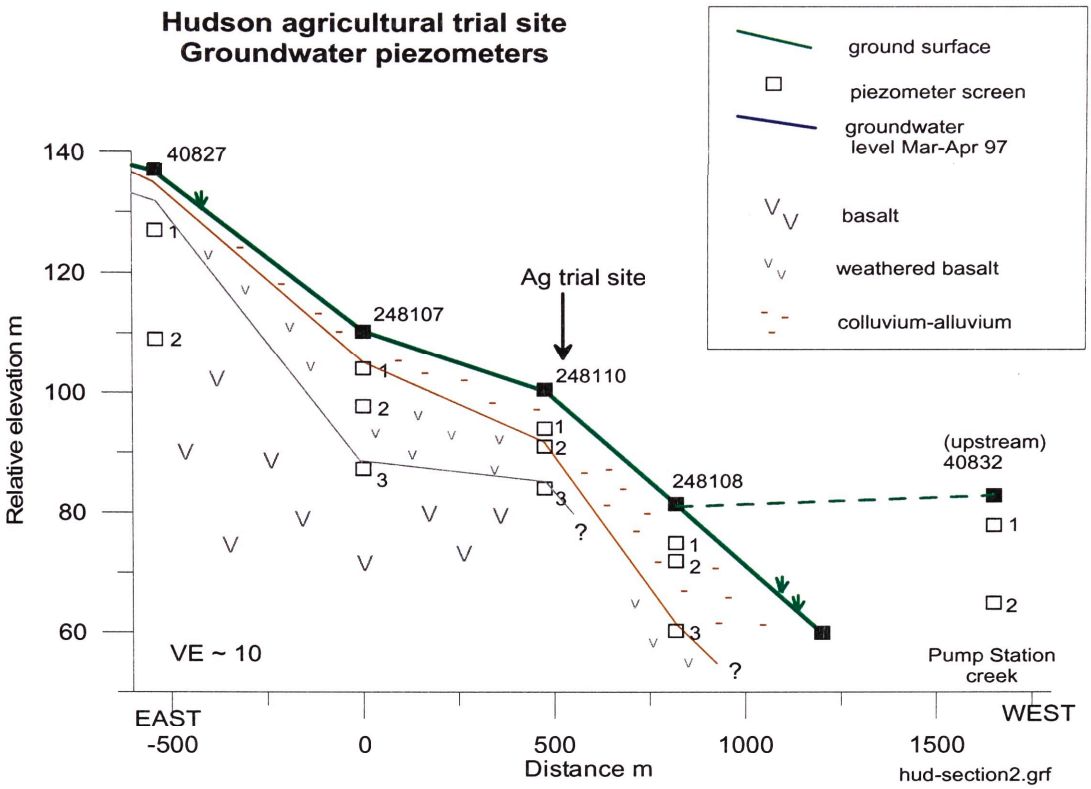

Figure 4.1: Cross-section of the Hudson foot slope showing subsurface lithology and piezometer installations.

4.3 Downhole geophysical logging

Downhole geophysical logging of natural gamma and apparent bulk electrical conductivity (ECa) correlated with lithological boundaries that were identified during drilling (Figure 4.2). The depth of weathered basalt at one site, piezometer 248110, was redefined by geophysical interpretation at 6 m depth (+1 m).

4.4 Electrical Image Data

Electrical image data was acquired along the 3 lines shown on Figure 4.3 on a regular basis between September 2000 and August 2001.

An additional single 245 m long line (Line 5 in Fig 4.3) with a depth penetration of approximately 35 m was taken through Plots 6 to 17 in September 2000 using an electrode separation of 5 m. This data is shown in Fig. 4.4. The top image in this figure is the field measurement of apparent resistivity/conductivity. The bottom image is the distribution of true resistivity/conductivity arrived at by a least squares constrained inversion of the field data. The inversion program seeks to produce a match between the apparent resistivity/conductivity (middle image) produced by the model distribution in the bottom image. The goodness of fit is indicated in the figure. If a fit of better than a few percent is achieved then the model distribution (bottom image) is taken as a satisfactory inversion of the field data.

4.4.1 Line A - 2.5m electrode spacing

Line A extended from the northern fence of the Trial Farm above the access gate, across Plot 6 (Young Lucerne), and Plot 5 (native grasses) to end in the lucerne/phalaris buffer between Plots 5 and 4. Measurements were repeated along this line during each field trip. The data is shown in Fig. 4.5.

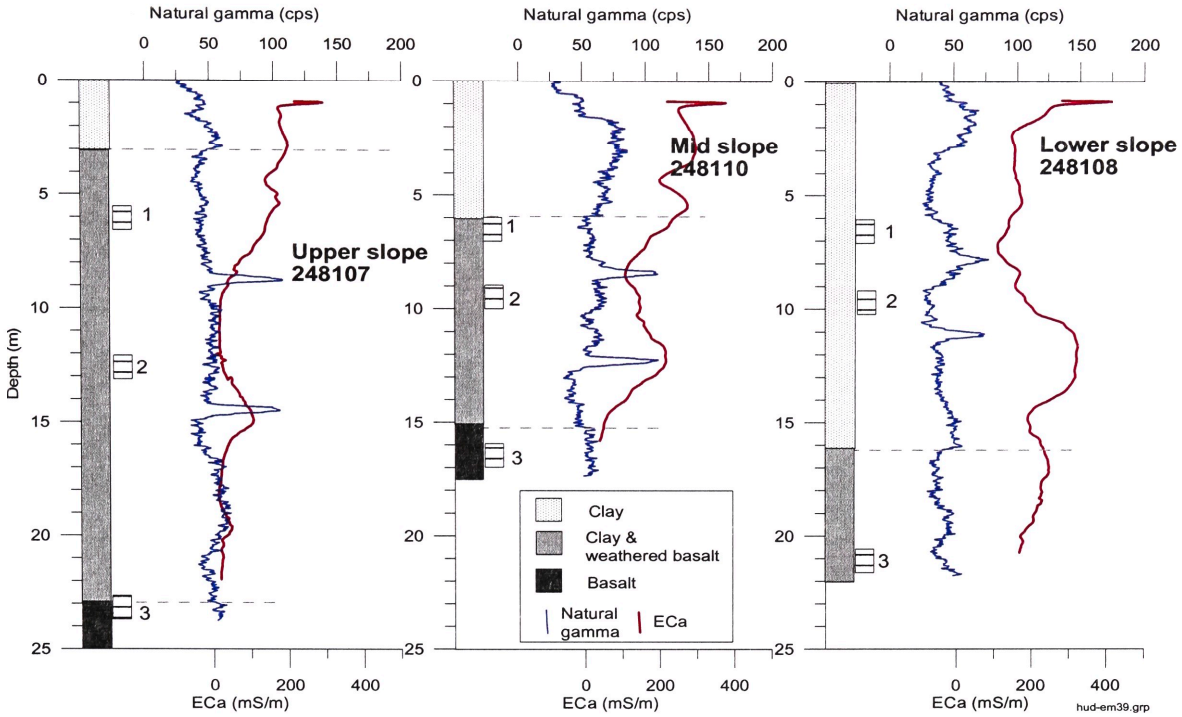

Figure 4.2: Downhole geophysical logs correlated with lithology for upper, mid and lower slope piezometers.

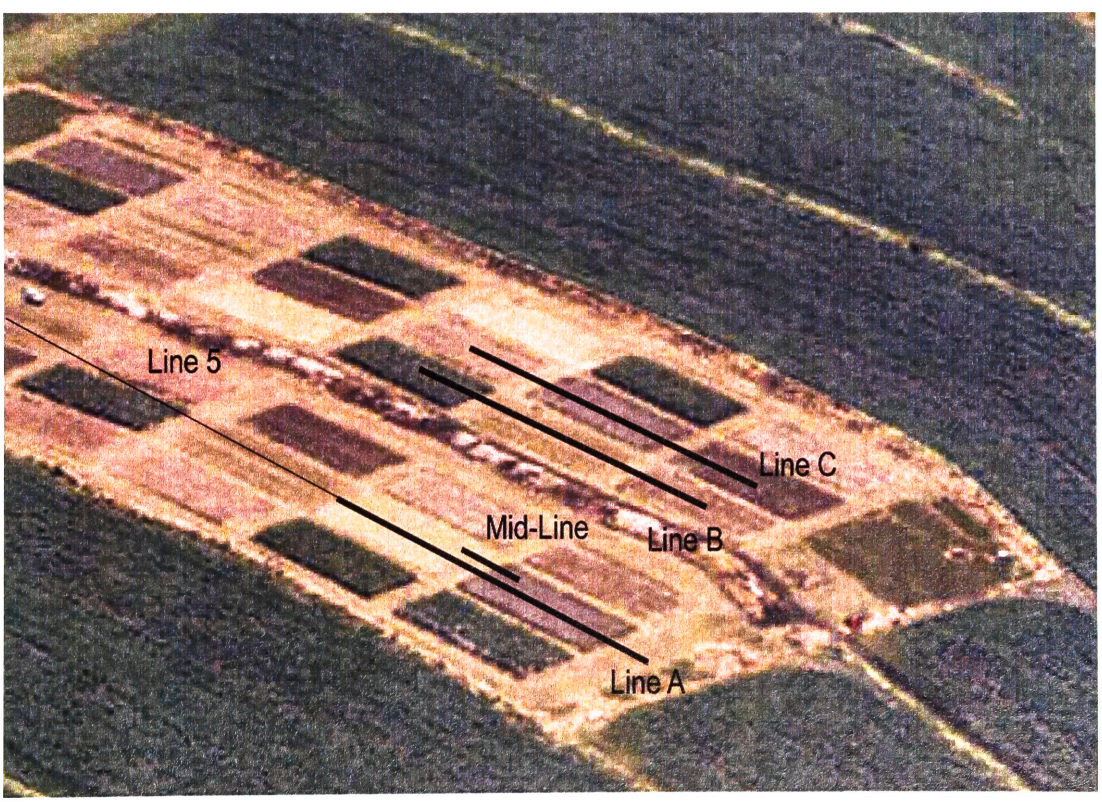

Figure 4.3: Location of Electrical image lines

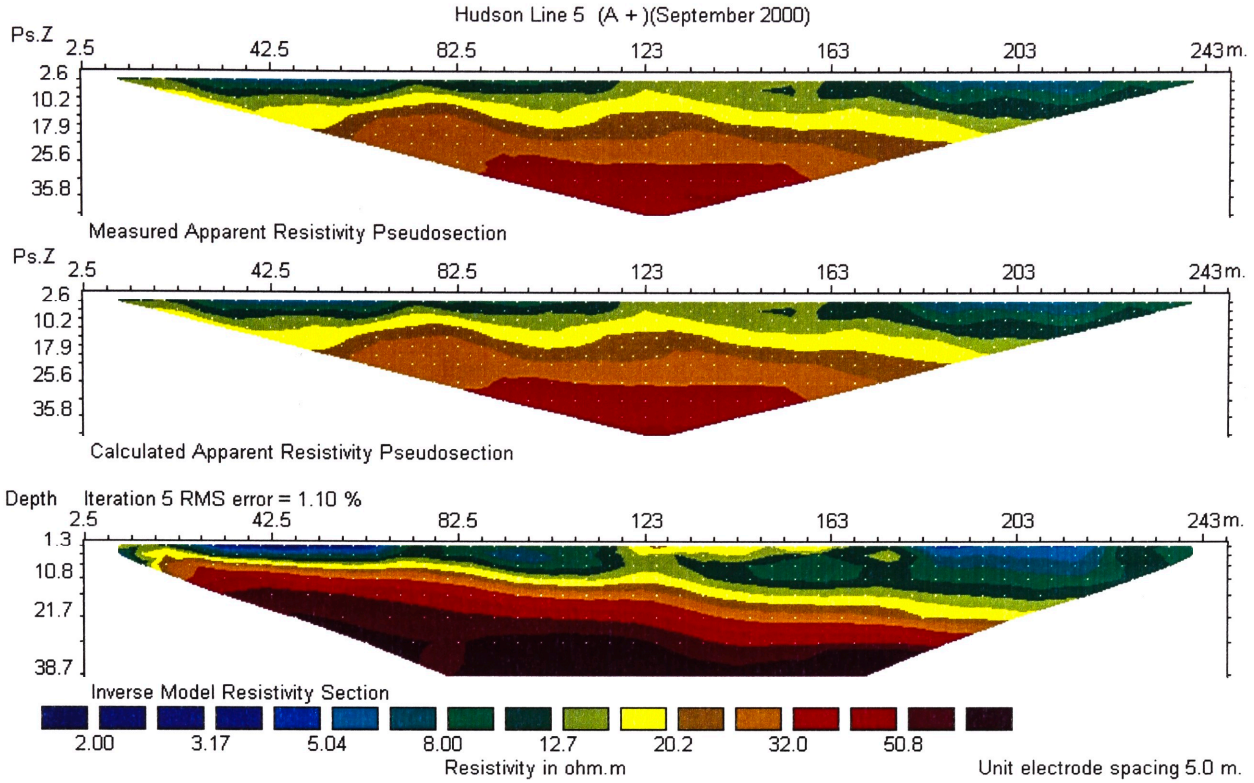

Figure 4.4: Line 5 data

4.4.2 Line B - 2.5m electrode spacing

Line B extended from the northern fence of the Trial Farm down slope from the access gate, across Plot 14 (Fallow), and Plot 20 (sprayed out lucerne) to end in the sorghum stubble of Plot 21. The data is shown in Fig. 4.6.

4.4.3 Line C - 2.5m electrode spacing

Line C was parallel to Line B and ran through the next set of plots down slope from Line B. The line commenced in Plot 24 (Fallow) and ran through Plot 23 (lucerne planted in September 2000) to Plot 22 (Fallow). The data is shown in Fig. 4.7.

4.4.4 Part of Line A - 1.0m electrode spacing

The image lines previously shown have been measured using a base electrode spacing of either 5 m or 2.5 m. This resulted in images that extended to either 40 m or 20 m. A final line (mid-line on fig. 4.3) was measured at the end of July 2001 using an electrode separation of 1.0 m. This will have a total depth penetration of approximately 10 m with a better near surface resolution. The results are shown in Fig. 5.8.

4.5 Groundwater levels

The complete data set available for groundwater levels at the Trial Site is shown in Fig. 4.8. Rainfall data from the same site is also shown. In Fig 4.9 the same data is shown against cumulative rainfall.

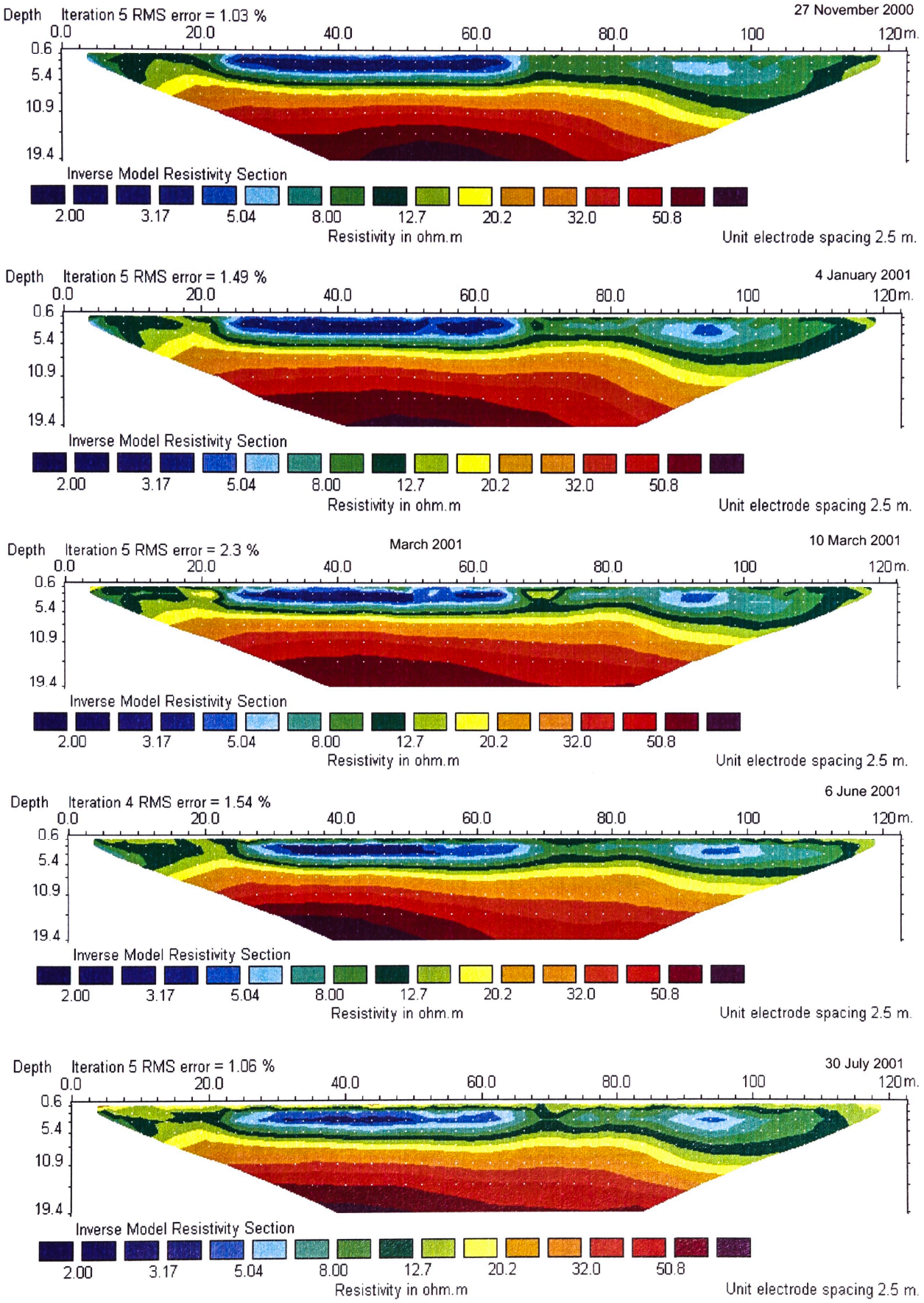

Figure 4.5: Image lines through the lucerne (Plot 6) planted in September 2000

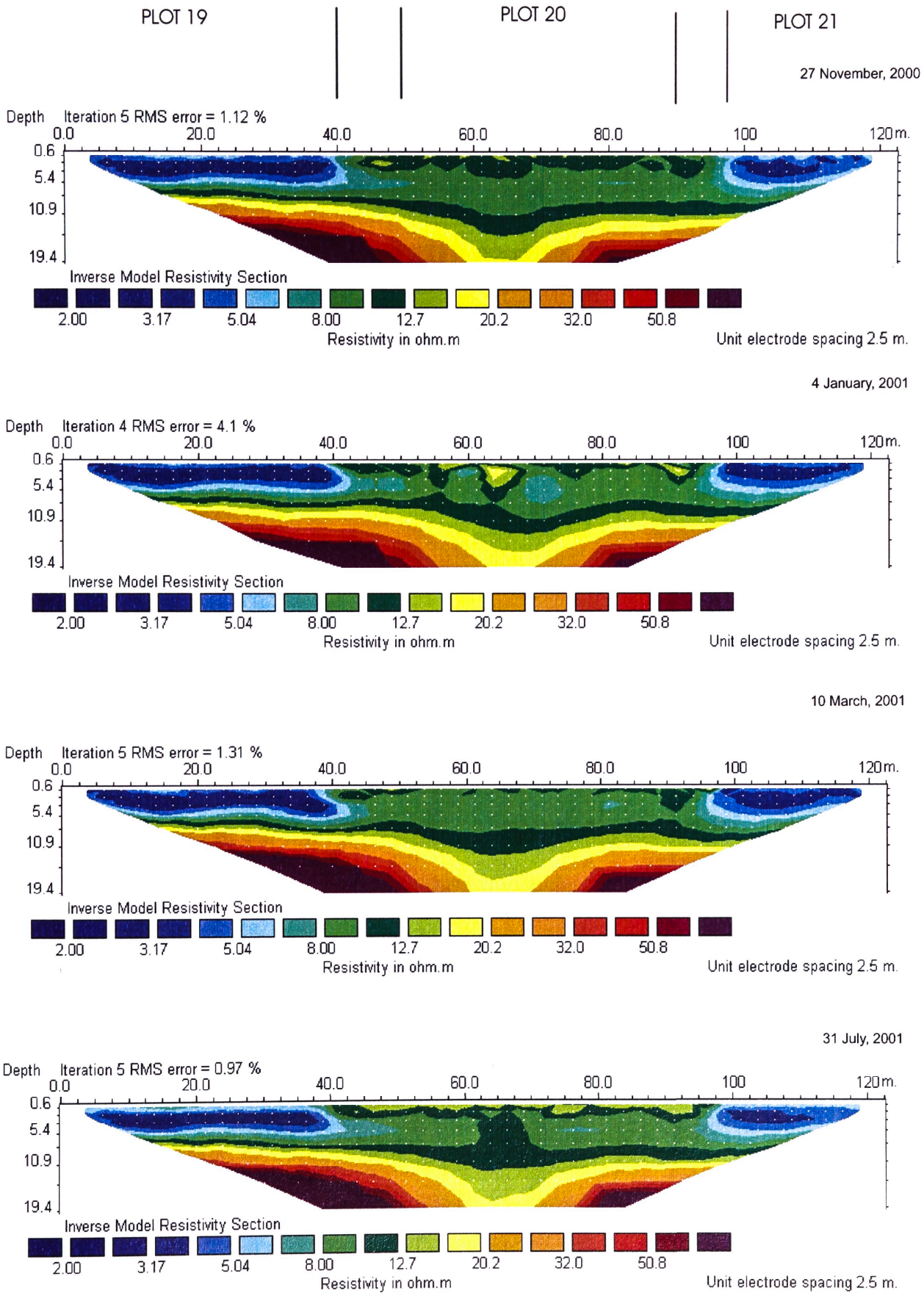

Figure 4.6: Image line B

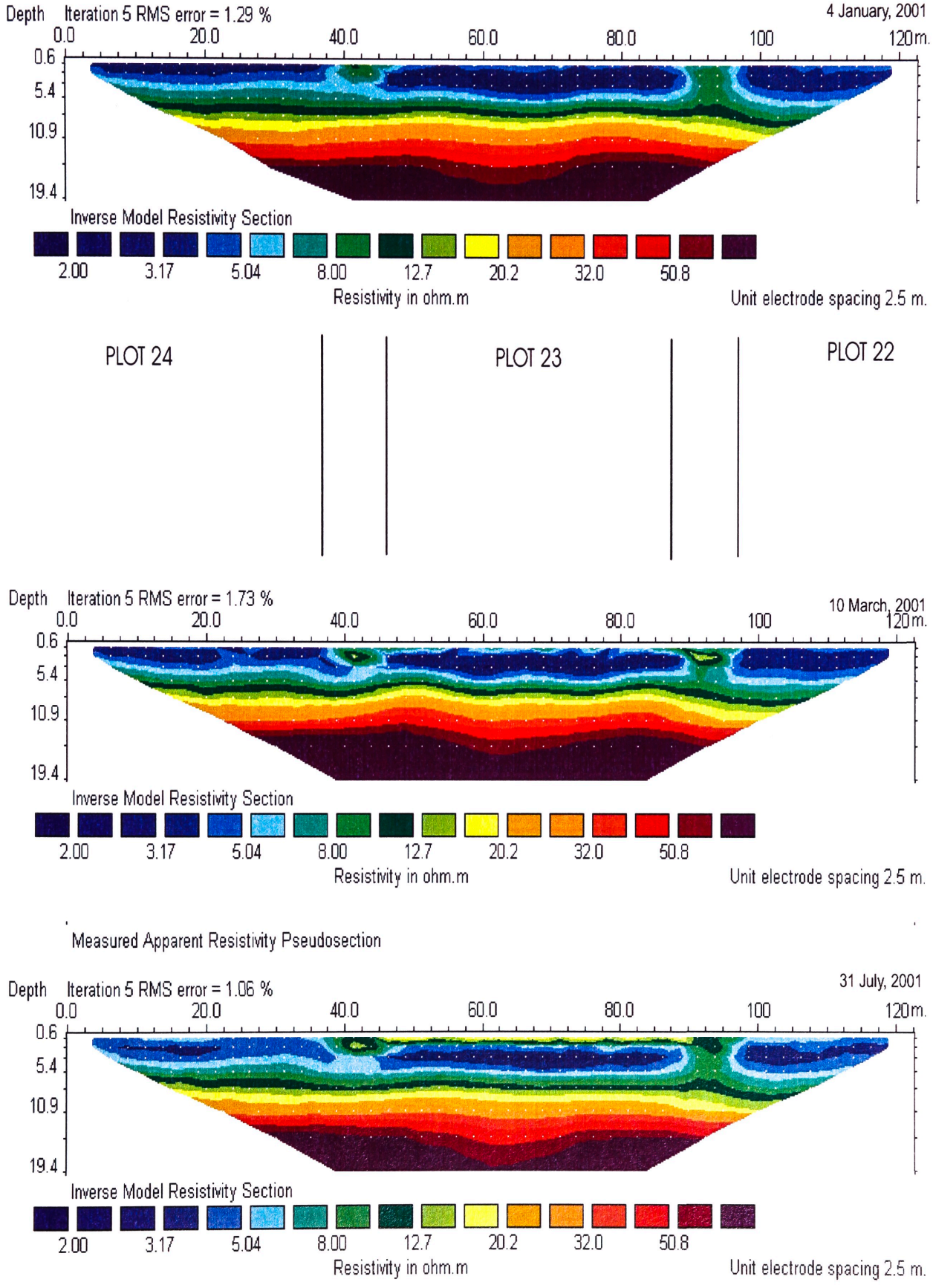

Figure 4.7: Image line C

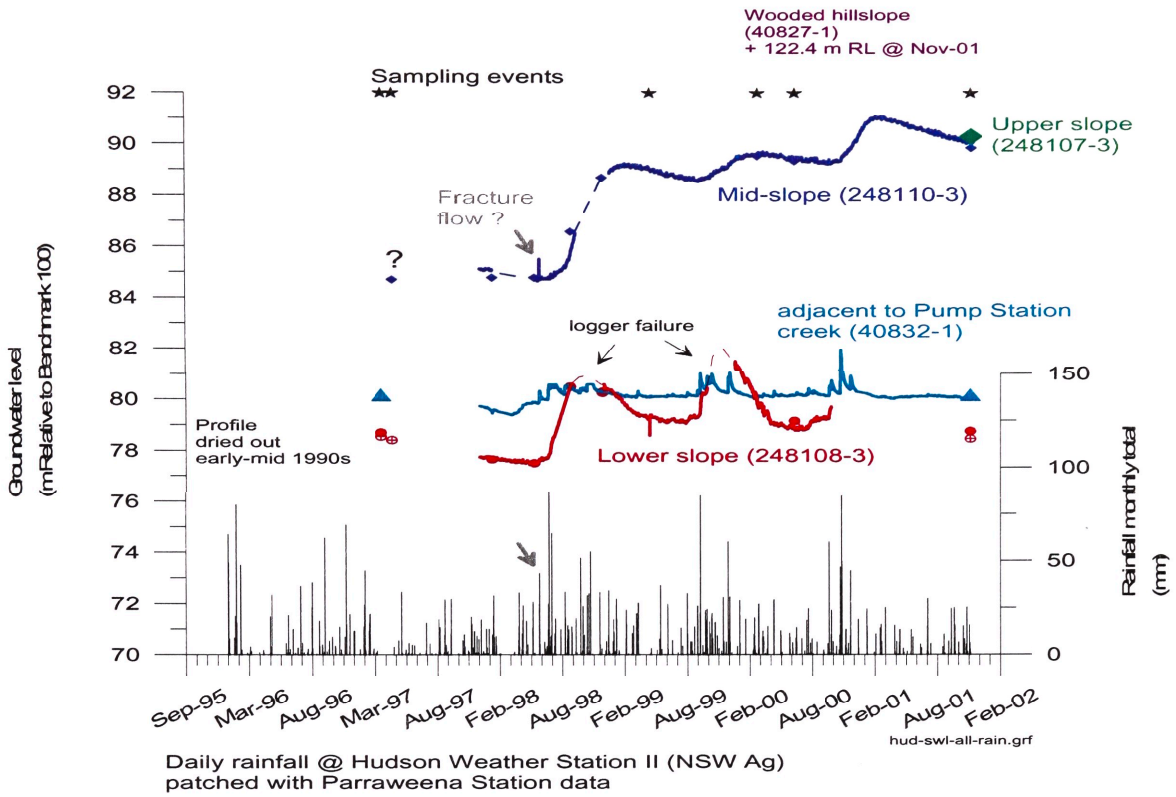

Figure 4.8: Groundwater levels at the Hudson site, 1997-2001.

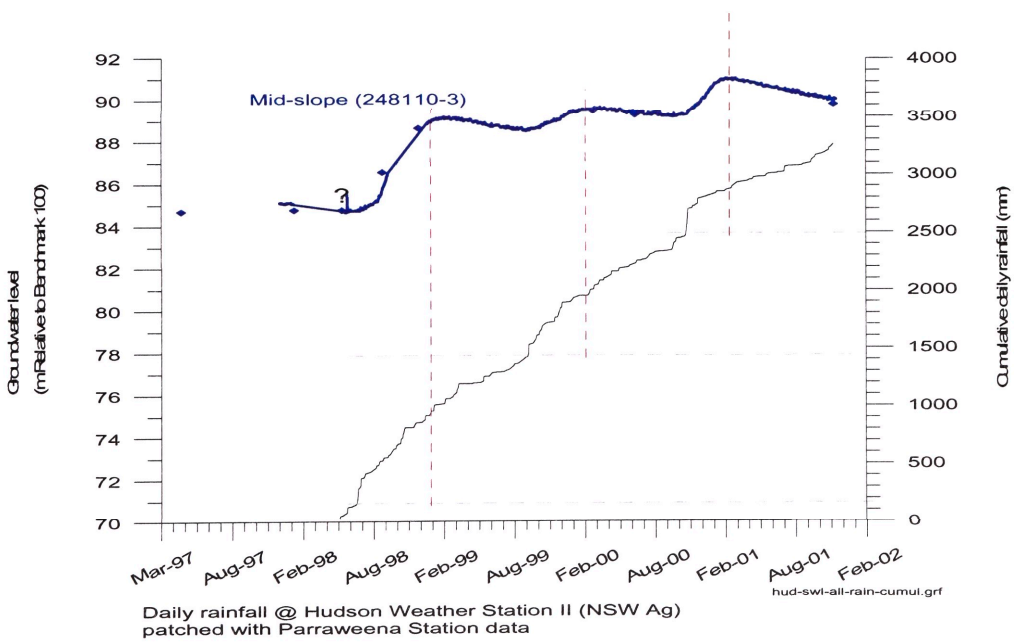

Figure 4.9: Groundwater levels at the Hudson site, 1997-2001, compared with cumulative rainfall.

4.6 Rainfall hydrochemistry and stable isotopes

A total of 18 rainfall samples from events between October 1999 and January 2001 were analysed for pH, EC, major ions and oxygen-18 and deuterium isotopes. These results, along with estimated total dissolved solids and data from comparative studies are provided in Table 4.2.

Table 4.2: Rainfall stable isotope and hydrochemical data, Gunnedah Research Centre, October 1999 to January 2001.

Sample date	Rain (mm)	$\delta^{18}O$ ±0.2 ‰ SMOW	$\delta^{2}H$ ±1‰ SMOW	pH	EC (μS/cm)	SO_4	Na	Ca	K	Cl[a]	TDS[b]
						(mg/L)					
31-Mar-98[c]	–	-2.81	-10.5	–	–	–	–	–	–	–	–
23-Oct-99	3.6	-4.16	-11.9	–	–	–	–	–	–	–	–
9-Nov-99	16	-2.97	-3.8	–	–	–	–	–	–	–	–
28-Jan-00	3.6	-4.22	-14.1	–	20.3	2.49	0.27	0.04	0.22	–	–
9-Mar-00	38.4	-8.28	-60.9	5	18.8	<0.6	0.04	3.32	<0.01	–	–
4-May-00	8	-2.66	-11.8	5.4	14.5	<0.6	0.70	0.05	0.48	–	–
9-Aug-00	9.8	-1.66	3.3	5	11.0	<0.6	0.5	<0.005	0.23	0.66	2.0
14-Oct-00	57.6	-2.47	-0.5	5.4	12.9	<0.6	0.35	0.18	0.07	–	–
26-Oct-00	28.6	-5.14	-30.1	4	3.9	<0.6	0.14	0.08	<0.01	–	–
15-Nov-00	26.0 [d]	-4.53	-21.4	4.4	3.4	<0.6	0.06	<0.005	<0.01	–	–
16-Nov-00	31.6	-4.76	-24.7	4.2	1.7	<0.6	0.05	<0.005	<0.01	–	–
18-Nov-00	12.6	-3	-14.2	4.3	3.9	<0.6	0.07	<0.005	0.03	–	–
19-Nov-00	29.2	-4.06	-19.9	3.6	3.2	<0.6	0.12	<0.005	<0.01	–	–
1-Dec-00	9.4	1.52	22.1	3.9	11.2	<0.6	0.16	<0.005	0.02	–	–
14-Dec-00	31.2	0.77	27.8	3.8	4.2	<0.6	0.08	<0.005	<0.01	0.01	0.08
31-Jan-01	33.4	-10.4	-69.2	4.9	2.2	<0.6	0.07	<0.005	<0.01	–	–
12-Jan-01	30.8	-11.04	-76.1	3.7	1.8	<0.6	0.06	<0.005	<0.01	–	–
Rainfall average		-4.1	-18.6								
1974–75[e]	–	–	–	–	–	0.4	0.8	0.1	0.2	1.10	3.2

[a]Cl estimated by assuming HCO_3 of zero, and CBE of zero
[b]TDS calculated from major ions
[c]Coram, in preparation
[d]rainfall of 4.2 and 21.8 mm on consecutive days
[e]wet & dry deposition (Blackburn et al. 1983)

4.7 Groundwater hydrochemistry

The complete hydrochemical dataset for groundwater and Pump Station creek is provided in Tables 4.3, 4.4 and 4.5.

4.8 Groundwater stable and radio isotopes

A limited number of samples were collected for stable and radioisotope analysis. Results for stable isotopes oxygen-18 and deuterium are given in Table 4.6. Data for radioisotope carbon-14 and tritium, together with associated data on dissolved inorganic carbon (DIC) and carbon-13 are given in Table 4.7.

Table 4.3: Groundwater field hydrochemical data for the Hudson site, 1997 to 2000

Site	Date	SWL (m bc) [b]	pH	Eh_{NHE} [a] (mV)	Temp (°C)	EC25 °C (μS/cm)	CO_2 (mg/L)	O_2 (mg/L)
248107-3	10-May-99		7.7	485	19.2	1338	–	4.5
	5-Jul-00		7.5	–	20.2	1355	68.2	4.5
248108-1	18-Mar-97	2.96	7.6	316	27.9	990	–	–
	21-Apr-97	3.1	7.6	–	20.2	1200	–	–
	10-May-99		7.7	434	19.8	890	–	2.5
	5-Jul-00	3.35	7.4	–	17.9	832	–	5.0
248108-2	20-Mar-97	2.96	7.5	–	24.3	990	–	–
	21-Apr-97	3.1	7.6	–	20.5	1210	–	–
	10-May-99		7.6	424	19.7	865	–	4.5
	5-Jul-00	3.34	7.1	–	19.5	822	34.3	4.6
248108-3	20-Mar-97	2.79	7.6	–	24.2	860	–	–
	21-Apr-97		7.6	–	20.1	1070	–	–
	10-May-99		8.4	433	21.6	845	–	6.8
	5-Jul-00	3.14	7.5	–	17.9	805	–	4.1
248110-3	20-Mar-97		7.8	–	24.3	1210	–	–
	21-Apr-97	15.88	7.6	–	21	2710	–	–
	10-May-99		7.8	481	18.9	1089	–	8.4
	19-Mar-00	11.05	6.9	345	20.2	2000	–	4.8
	5-Jul-00	11.25	7.3	–	17.7	1110	21.2	7.8
40832-1	10-May-99		8.3	442	18	1765	–	2.2
	19-Mar-00	3.94	7.5	309	19.1	1952	–	2.0
40832-2	10-May-99		8.3	465	18.7	1950	–	2.1
	19-Mar-00	3.95	7.4	340	19.4	1880	–	0.6
Creek	10-May-99		8.3	469	17.6	1963	–	2.4
	19-Mar-00		7.7	349	248	1920	–	5.1
	5-Jul-00		7.6	–	17.4	824	–	5.3
Windmill	10-May-99		7.8	471	15.7	5720	–	3.5

[a] Eh_{pt} converted to Eh_{NHE}
[b] m bc = metres below steel casing

Table 4.4: Groundwater major ion data for the Hudson site, 1997 to 2000

Site	Date	TDS[a]	Na	K	Mg	Ca	Cl	SO_4[b]	HCO_3 [c]	CBE [d]
		(mg/L)								%
248107-3	10-May-99	1120	102.54	2.76	85.47	79.18	91.92	6.22	751.71	1.5
	5-Jul-00	1112	86	2.05	90.2	77.2	135.59	6.95	714.37	-1.9
248108-1	18-Mar-97	1134	163.8	5.1	106.9	80.2	216.8	11.6	550	13.2
	10-May-99	717	108.98	1.34	41.61	31.84	76.94	4.36	452.05	0.6
	5-Jul-00	686	83.8	1.11	47	33.4	73.75	4.46	442.86	-1.1
248108-2	20-Mar-97	929	117.4	5.9	58.3	96.2	177.4	7.2	466.1	7.5
	10-May-99	699	97.47	0.92	44.23	35.71	76.8	3.83	440.09	1.2
	5-Jul-00	673	80.5	0.86	45.3	32.7	74.47	4.58	434.32	-2.3
248108-3	20-Mar-97	1667	68	8.7	194.4	144.3	197.1	4.4	1050	7.2
	10-May-99	674	69.76	1.66	51.47	41.59	71.69	4.38	433.41	0.9
	5-Jul-00	676	60	1.28	55.4	42.1	68.51	4.31	444.69	0.1
248110-3	20-Mar-97	1148	138	6.6	97.2	96.2	197.1	16.1	597.04	9.5
	10-May-99	878	139.57	1.42	49.78	36.63	90.14	9.33	551.45	1.1
	19-Mar-00	1303	210.87	2.38	89.93	49.56	395.59	44.57	509.96	-3.2
	5-Jul-00	888	124	1.61	54.2	36.9	121.12	7.84	542.3	-2.9
40832-1	10-May-99	1338	116.77	1.77	147.65	52.59	238.97	4.68	775.66	0.9
	19-Mar-00	1513	123.43	1.63	191.27	60.77	285.31	11.89	839.06	4.7
40832-2	10-May-99	1467	125.67	3.26	160.52	66.22	261.55	5.92	843.52	1.7
	19-Mar-00	1421	103.05	2.64	168.01	61.05	263.42	5.07	817.4	1.2
Creek	10-May-99	1444	123.16	2.5	164.08	79.71	321.72	8.01	744.78	3.3
	19-Mar-00	1403	97.96	2.53	167	77.25	326.74	10.25	721.02	1.6
	5-Jul-00	1089	96.7	1.81	152	79.2	316.26	11.59	431.88	12.1
Windmill	10-May-99	3417	332.88	2.47	447.97	179.71	1556.81	24.86	872.16	1.4

[a]TDS calculated from major ions
[b]SO_4 assumed equal to S_T
[c]HCO_3 was measured in the field, except for March 1997 samples
[d]CBE is charge balance error

Table 4.5: Groundwater minor and trace element data for the Hudson site, 1997 to 2000

Site	Date	Fe	Al	B	Li	SiO_2	F
		(mg/L)					
248107-3	5-Jul-00	0.02	0.03	0.07	0.02	–	–
248108-1	18-Mar-97	0.02	–	–	–	17.5	0.24
	5-Jul-00	0.02	0.04	0.05	0.02	–	–
248108-2	20-Mar-97	0.06	–	–	–	20.8	0.2
	5-Jul-00	0.02	0.03	0.03	0.01	–	–
248108-3	20-Mar-97	0.01	–	–	–	20.6	0.17
	5-Jul-00	0.02	0.03	0.05	0.02	–	–
248110-3	20-Mar-97	0.03	–	–	–	16.1	0.25
	19-Mar-00	0.02	0.03	0.14	0.06	–	–
	5-Jul-00	0.52	0.56	0.09	0.02	–	–
40832-1	19-Mar-00	0.02	0.03	0.07	0.04	–	–
40832-2	19-Mar-00	0.02	0.03	0.02	0.04	–	–
Creek	19-Mar-00	0.02	0.03	0.02	0.03	–	–
	5-Jul-00	0.02	0.03	0.02	0.01	–	–

Table 4.6: Oxygen and deuterium stable isotope data for Hudson site, July, 2000.

Site	$\delta^{18}O$ ±0.2 ‰ SMOW	$\delta^{2}H$ ±1 ‰ SMOW
248110-3	-4.69	-33.4
248108-3	-4.95	-34.7
248108-1	-4.89	-34.4
Average Gunnedah rainfall	-4.1	-18.6

Table 4.7: Dissolved inorganic carbon, carbon-13, carbon-14 and tritium data for Hudson site.

Site	Date	TDIC[a] (mmol/kg)	$\delta^{13}C$ ±0.2 ‰ V-PDB	pMC	TU[b]
248110-3	Apr-97	–	–	–	0.3 ± 0.2
	Jul-00	7.063	-8.92	80.08	0.027 ± 0.021
248108-1	Apr-97	–	–	–	0.3 ± 0.2
	Jul-00	6.608	-12.9	58.48	0.005 ± 0.021
248108-2	Apr-97	–	–	–	< 0.3
248108-3	Apr-97	–	-13.7	55.3	0.3 ± 0.2
	Jul-00	8.940	-12.47	45.49	–

[a]TDIC, total dissolved inorganic carbon, determined by gravimetric analysis
[b]TU is tritium unit where TU=1 corresponds to a ratio T/H = 1E-18

4.9 Cation exchange capacity of solid phase

The cation exchange capacity of the solid phase (dominantly clay) from the ground surface to a depth of 3.0 m is detailed in Table 4.8. Black clays on the Liverpool Plains are typically saturated with cations and there are no absorbed H^+, meaning that $CEC_{effective} = CEC_{total}$ (D. Dight, pers.com. 26.11.01).

Total CEC varied from 126–150 meq/100g, which is very high. Typical CEC for montmorillonite is 80–120 meq/100g (Appelo & Postma 1994). The very high values, may in part reflect soluble salts which may not have been leached from the samples prior to testing.

Table 4.8: Cation exchange variation with depth, Hudson plots 5 and 14, July 1995.

Depth (m)	Mg	Ca	K	Na	$CEC_{effective}$
	(meq/100 g)				
Plot 5					
0.1	51.4	73.2	1.01	0.7	126.31
0.2	56.4	78.2	0.52	0.9	136.02
0.4	58.4	75.6	0.47	1.3	135.77
0.6	61.8	77.4	0.48	2	141.68
0.8	61.4	72.4	0.44	2.3	136.54
1	61.6	68.4	0.44	2.8	133.24
1.2	59.8	70	0.52	2.7	133.02
1.4	61.2	68.4	0.56	2.9	133.06
1.6	59.4	68	0.52	2.8	130.72
1.8	59.4	68.6	0.53	2.8	131.33
2	66.8	77.8	0.56	3.8	148.96
2.2	64.6	74.2	0.49	3.6	142.89
2.4	63	75	0.48	3.4	141.88
2.6	62	74.8	0.48	3.4	140.68
2.8	66.4	77.4	0.48	3.7	147.98
3	67.8	79	0.45	3.6	150.85
Plot 14					
0.1	53.8	72	1.15	0.4	127.35
0.2	58.2	78	0.72	1	137.92
0.4	58.2	75	0.58	1.5	135.28
0.6	59.2	72.4	0.57	2.2	134.37
0.8	63.2	76.2	0.56	2.9	142.86
1	66	73.6	0.56	3.6	143.76
1.2	65	72.6	0.59	3.9	142.09
1.4	64.6	65.6	0.57	3.9	134.67
1.6	65.2	68.4	0.53	4.1	138.23
1.8	69	72.2	0.57	4.2	145.97
2	64.4	68.4	0.5	3.9	137.2
2.2	66.6	70.8	0.49	4.1	141.99
2.4	65.8	69.2	0.45	3.9	139.35
2.6	65.2	69.4	0.47	3.8	138.87
2.8	64.2	71	0.52	3.9	139.62
3	63.2	71.2	0.48	3.7	138.58

Chapter 5

DATA INTERPRETATION

Various aspects of the data presented in the previous chapter will be interpreted in this section. Where appropriate, corroborating data sets from other investigations will be included to aid the interpretation. A synthesis of the available data will be presented in the following section.

5.1 Water Balance Models

A mosaic of sometimes deep (1 - 2 m) cracks is characteristic of dry Vertosols (cracking clay soils). These cracks have invited speculation as to whether they might provide rapid access to the subsoil for water and solutes. Certainly this may happen with high rates of flood or irrigation run-on onto a deeply dried profile until the clays swell and the cracks close. The detailed experiments in India (Hodnett & Bell 1981) tend to confirm this speculation. Such 'by pass' or 'preferential flow' is the process often used to explain an observed or perceived greater rate of flow of water and solutes than is predicted by matrix flow theory. Generally, bypass flow may occur down cracks, old root channels, along the surface of tree roots fed by trunk flow, ped surfaces and slickenside faces.

In Fig. 5.1 the soil water (mm) in profiles under crop and pasture treatments are shown. The data has been derived from 4 replicates for each treatment. The evapotranspiration and rainfall data were summed over the periods between soil water measurements. The treatments comprised:

LF1, 2 and 3 phased long fallow wheat/sorghum rotation (2 crops in 3 years);

W short fallow wheat/barley rotation (1 crop per year);

RC 1 and 2 crops sown in response to a planting rule of 0.5 m wet soil in the appropriate planting window (virtually 2 crops per year),

P1 and 2 lucerne cv Aurora pasture;

P3 Bambatsi panic, wallaby grass and Queensland blue grass pasture.

Water balance data for the Hudson Site during the winter of 1998 is shown in Table 5.1. The calculation has been worked for each of the 9 different plot types for which soil moisture data is available.

A constant rainfall of 327 mm has been assumed based upon the on-site rain gauges. In this calculation, a constant value of actual evapotranspiration (ET_p) has been assumed for each plot. This is based on the assumption that soil moisture was not limiting during the wet winter and therefore that the actual evapotranspiration would have been the same as the potential evapotranspirration calculated from the on-site climate station data. The change is soil moisture storage (ΔS_w) was caculated from the neutron soil moisture gauge measurements (an average of 3 holes at each plot spaced at 10 m 20 m and 30 m from

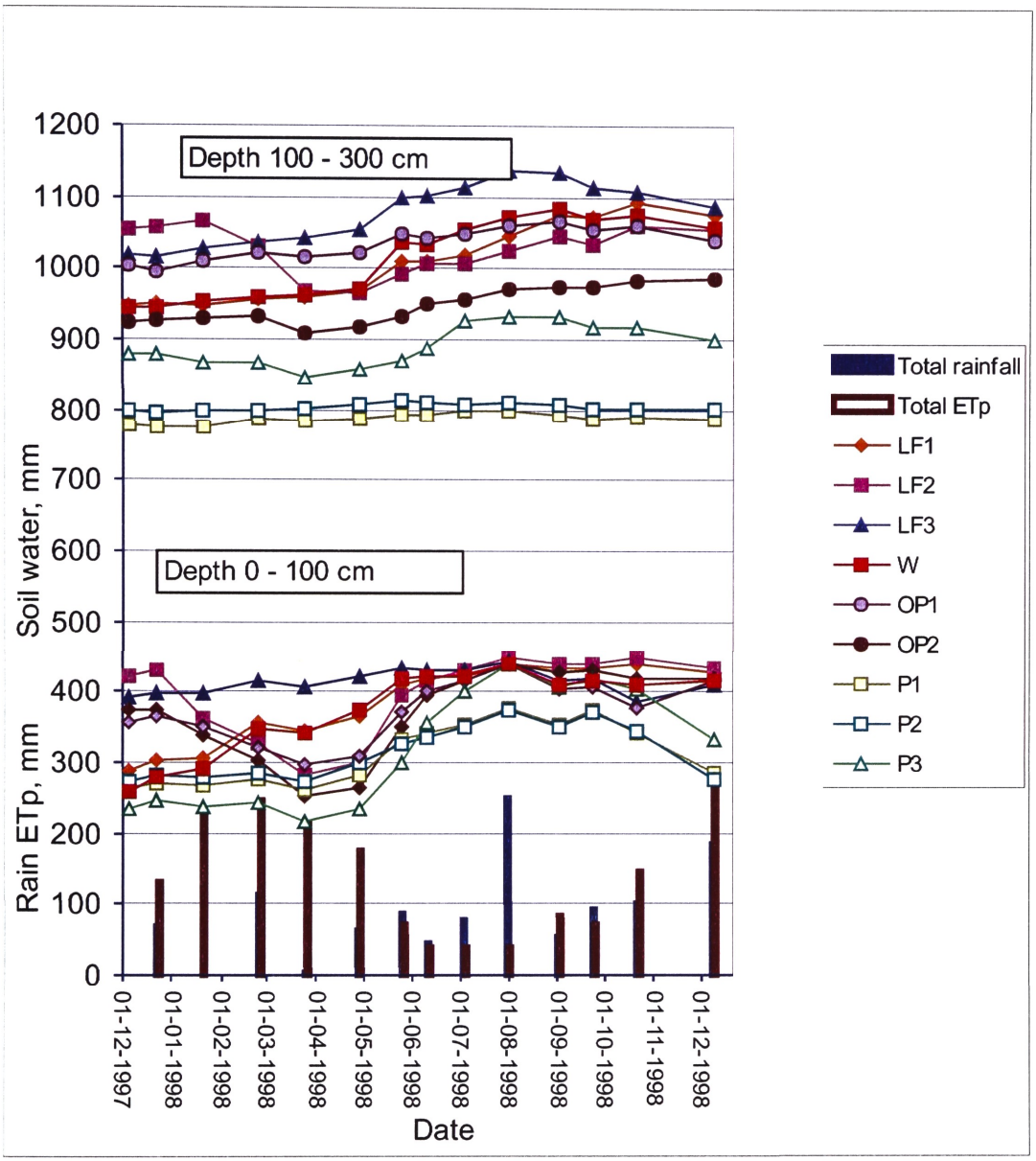

Figure 5.1: Water balance data for 1998

Table 5.1: Water Balance, June - July, 1998 at Hudson

System	Stubble type and growing crop	Stubble, litter mass t/ha	Rain	ETp	RO	ΔSW	ΔW	Unused storage mm on 31 July 97	Δ SW mm 25 March - 31 July
			mm between 10/6/98 to 31/07/98						
LF 1	Wheat stubble	3.5	327	75	89	55	108	-35	149
LF 2	Sorghum stubble	4.8	327	75	90	54	108	-25	210
LF 3	Sorghum stubble + wheat crop	1.5	327	75	31	47	174	-131	104
W	Wheat stubble + wheat crop	3.0	327	75	35	55	162	-61	166
RC 1	Mungbean stubble + barley crop	0.3	327	75	49	56	147	-49	168
RC 2	Sorghum stubble + chickpea crop	2.1	327	75	49	67	136	37	232
P 1	Lucerne + litter	0.2	327	75	188	40	24	273	106
P 2	Lucerne + litter	0.3	327	75	82	39	131	263	80
P 3	Grass + litter	0.3	327	75	27	127	98	78	280

the edge of the plot), corrected for a deforming soil matrix as described by Ringrose-Voase & Cresswell (2000). Run off (RO) was measured at each of the representative plots using a tipping bucket raingauge installed in the run off line. Changes in soil moisture (ΔW) were then calculated from Equation 5.1.

$$\Delta W = Rain - E_p - RO - \Delta SW \tag{5.1}$$

The total soil profile available moisture was estimated to be 1450 mm. The maximum soil moisture deficit (SMD) was observed to be 250 - 300 mm for annual crops, 360 mm for perennial grass and approximately 500 mm for lucerne. The difference beteen saturation and field capacity (equivalent to the specific yield) was estimated to be 130 mm. An estimate of the available residual moisture beneath each of the plots is given in Table 5.1.

On the Hudson research site during the record wet winter of 1998, the driest soil profiles, especially those under lucerne, failed to wet up at all at depths between 1 and 3 m (Figure 5.1). The water balance calculation shows that there should have been significant additional water available to add to storage. The inbalance suggests that deep drainage may have occurred without the soil wetting up, with water by-passing the unsaturated soil matrix along ped surfaces in the depth range 1 to 3 m. It is possible that this additional water was added to soil moisture storage at depths greater than 3 m.

5.2 Downhole geophysical logging

Apparent electrical conductivity (ECa) was relatively low at each site, averaging about 200 mS/m (Figure 4.2), compared with 400 mS/m at the saline Yarramanbah site. Near surface ECa was slightly higher on the upper slope than the mid and lower slope. ECa generally decreased with increasing depth except for distinctive bulges at about 6 and 12 m on the upper slope, 15 m on the mid slope and 11 m to 13 m on the lower slope. Relatively high ECa at these depths occurred within the weathered basalt, or on the mid slope, directly above basalt rock.

Natural gamma peaks of 50 cps above background were detected at all sites in discrete 0.5 m thick bands within the weathered basalt. At the upper slope, these features were located at 9 and 14.5 m depth, at the mid slope at 8.5 and 9 m depth and at the lower slope at 11 m depth. The upper gamma peak at each site coincided with decreased ECa, while the lower gamma peak was associated with increased ECa. The cause of these features is uncertain, but indicates that high gamma emitting radio isotopes such as

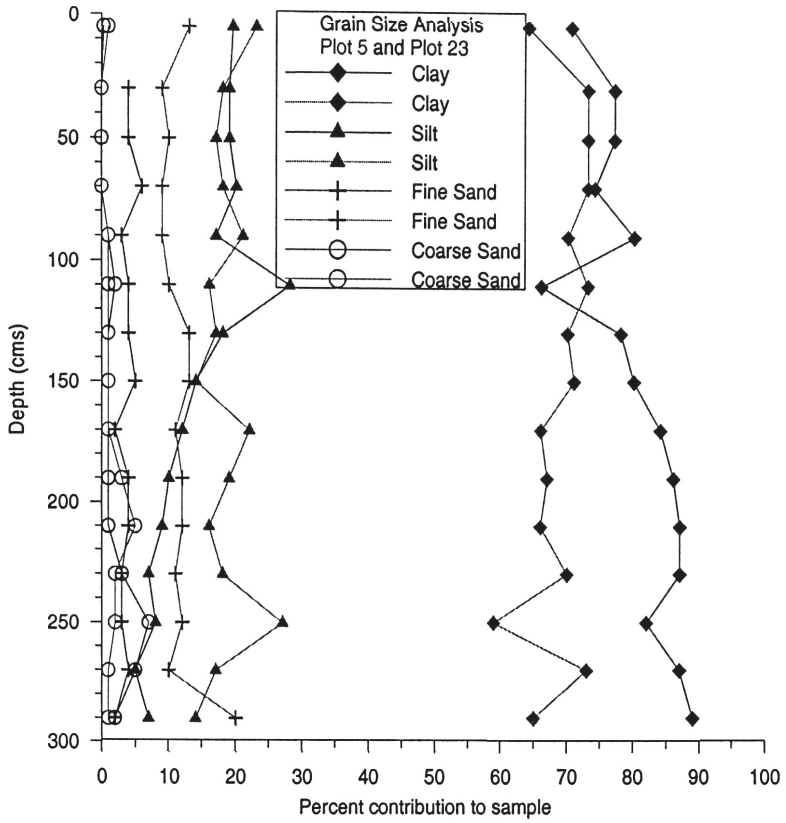

Figure 5.2: Grain-size analyses for plots 5 and 23 - to 3 m depth

K^{40}, U^{238} or Th^{232} are concentrated in these zones. Drilling records revealed that the upper gamma peak occurred within a hardened zone which included white precipitate (caliche?). This evidence, together with the position of these features within the landscape, suggests that the upper feature in particular is a sub-horizontal preferential flow horizon. The variation in ECa occurs above the depth of saturation, as indicated from the water level and chemical sampling data sets.

5.3 Electrical Image Data Interpretation

The electrical image data clearly shows anomalies relating to the lay out of the plots. Figure 4.4 extends over 5 different plots and samples the bulk ECa to a depth of 40 m. There appears to be a fairly uniform bulk ECa in the inverted data at depth that correlates well with the depth to unweathered basalt. Of greater interest is the shallow depth variability associated with the different plots. It is clear that significant differences extend through the soil profile down to bed rock. These differences must be related to soil property variation and show every indication of being closely related to crop type and management. There is a clear high resistivity/low conductivity zone at each of the 10 m buffer zones between the plots. The anomaly extends at least to 7 m on the image sections. Both image lines passing through the young lucerne show clear indications of increasing resistivity as the growing season extends.

Changes in bulk resistivity can be a function of clay type, moisture content, salt content and soil porosity. The clays are known to be dominantly (> 85%) smectite, based upon the X-ray diffraction data reported by NSW Agriculture. Particle size analysis was carried out on 2 plots (5 and 23). The results are shown in Fig. 5.2 and confirm that the soils are dominantly silty clays with minor fine sand.

The salt content of the soils is not known. However, the EM39 data indicates a low salt content in the saturated sections measured and the area has high agricultural productivity so salinity is clearly not a major issue. The remaining variable that can impact the bulk electrical resistivity to the extent observed is the moisture content. Clearly, as moisture is removed from the clay, electrical current will find fewer

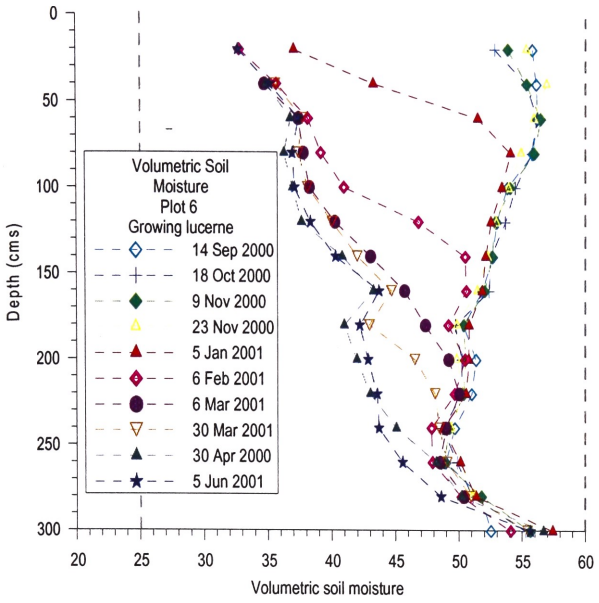

Figure 5.3: Neutron probe soil moisture measurements for Plot 6

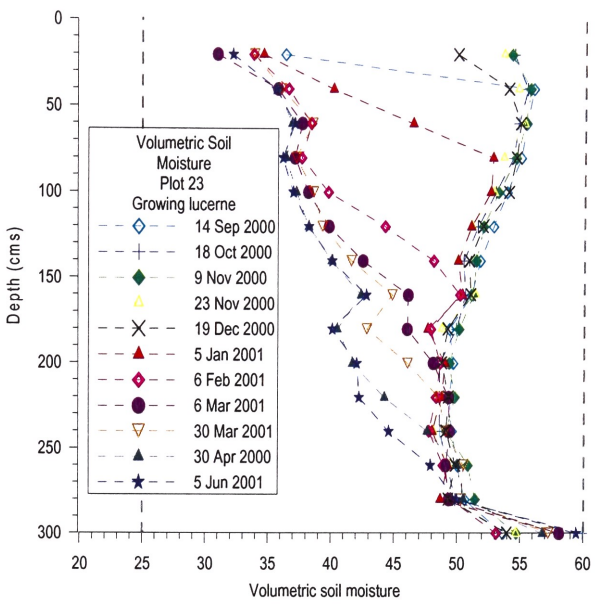

Figure 5.4: Neutron probe soil moisture measurements for Plot 23

continuous pathways in which to pass and the ECa will decrease. There is an extensive data base of measurements from the neutron soil moisture access tubes available. Each plot has been sampled fairly regularly with Plots 6 and 23 sampled each month. Data for these 2 plots are shown in Figs. 5.3 and 5.4.

The plots that have been prepared for lucerne in September 2000 (Plot 6 and 23) have the lowest resistivity (highest conductivity). The volumetric moisture content (θ_v) is approximately 55% in the top metre and then falls slowly to 50% at 2.75 m depth. There is a sharp rise towards 60% in the final 200 mm but this could be related to moisture collection at the base of the access tube. There is a clear reduction in θ_v as the crop grows (Fig. 5.3 for example) and this relates to the rainfall and evapotranspiration that occurred at the time. Figure 5.5 shows that significant rainfall occurred in October and November that probably supplied all the crop requirements and delayed drying of the soil until January 2001. From the beginning of January onwards the soil profile dries down with increasing depth up to the last measurements made in June 2001. There is an interesting small reversal in this trend that occurs at the end of January and is particularly marked at a soil depth of 160 mm. The reversal occurs in both plots growing lucerne and indicates that rain may have infiltrated to this depth during storms on 31 January and 1 February. In June 2001, the surface soil moisture (θ_v) has been reduced to 30% with a steady increase with depth to between 55% and 60% at 3.0 m.

Data for the 2 deep (6 m) profiles at plots 20 (Sprayed out lucerne) and 24 (Fallow) are shown in Figs. 5.6 and 5.7. It is significant that both these plots show little change with depth apart from an increase in soil moisture in Plot 24 (Fallow) that occurred between 1.8 m and 3.2 m depth during the heavy rain in November 2000. The sprayed out lucerne (plot 20) has volumetric moisture between 30% and 40% for the complete profile to 6 m depth. By contrast, the fallow plot 24 shows much higher moisture content with the top of the profile between 50% and 55%. There is a significant decrease in moisture at 5 m depth.

There is a clear correlation between volumetric moisture content and ECa. The spatial resolution of the electrical image lines is not sufficient to obtain a direct correlation between individual soil moisture measurements and individual equivalent zones of bulk resistivity derived from the inversion. However, Fig. 4.5 clearly shows an increase in resistivity (conductivity decrease) between line spacing 22 m and 62 m as the lucerne crop grows proceeds. Values of resistivity of approximately 3 Ωm (dark blue on the colour scale) occur at 1 m depth in November. By the end of July 2001, this value had increased to approximately 20 Ωm. Corresponding volumetric moisture contents change between 55% and 30%.

The variation noted for the lucerne plots is supported by data for the other plots. Plot 20 had lucerne growing previously before the crop was killed by spraying. The moisture content appears to have been reduced to between 35% and 42% to 4 m depth and 30% to 35% between 4 m and 6 m. Inspection of Fig. 4.6

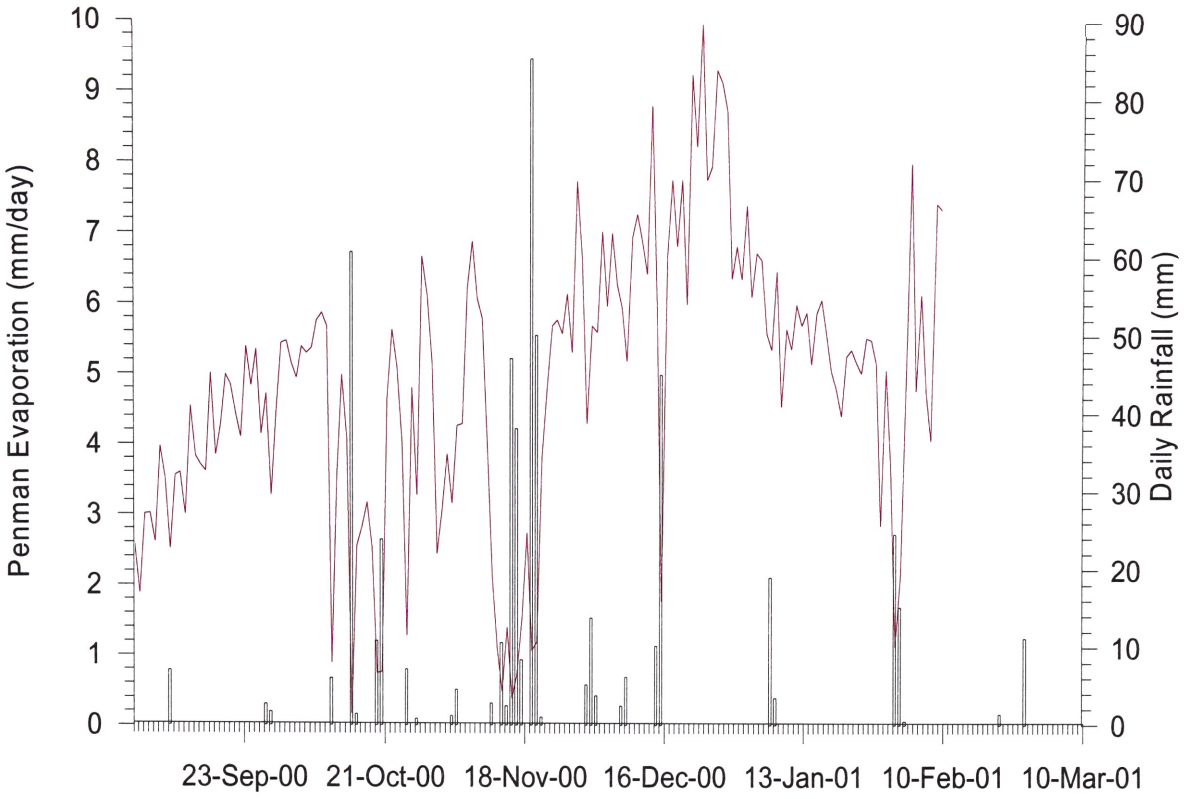

Figure 5.5: Daily Penman evaporation and rainfall for the period September 2000 to February 2001

shows that the central part of the image between 45 m and 85 m shows higher resistivity ($\approx 15\,\Omega m$). In a similar manner, the fallow Plot 24 shows low resistivity at the surface ($\approx 3\,\Omega m$)increasing with depth to $\approx 12\,\Omega m$ at 6 m depth. These changes correlate with the soil moisture changing between 53% and 30%.

The correlation is best shown in Fig. 5.8 where a base electrode separation of 1 m was used. The line was measured on 31 July 2001, a little later than the last neutron access measurement, but the change from low resistivity material below 2.2 m to higher resistivity surface zones clearly matches the moisture content change for the 5 July survey.

5.4 Groundwater level variability

The way in which groundwater levels respond to rainfall or to changes in confining stress can be used to determine the hydraulic status of the aquifer. For example, a confined aquifer with a rigid matrix (Fig. 2.7) will respond to changes in atmospheric pressure whereas an aquifer with a compressible matrix will not respond to atmospheric changes but will respond to applied loads (Fig. 2.8). An unconfined aquifer in a rigid permeable matrix will be recharged by deep drainage whereas an unconfined aquifer in a low permeability clay will not respond as readily. The Hudson data set can be analysed to determine the most appropriate conceptual model of the compressible clay.

5.4.1 Groundwater level response to rainfall recharge

Groundwater levels in piezometers on the lower slope responded to rainfall events before piezometers on the mid slope (Figure 5.9 and Figure 5.10, Table 5.2). However, the magnitude of the response on the mid slope was greater than that on the lower slope. At the lower slope, groundwater levels tended to increase significantly immediately after rainfall, in contrast to a muted, slow rise evident in the mid-slope piezometer. After rainfall in October 1999, the mid-slope piezometer took 210 days to reach maximum

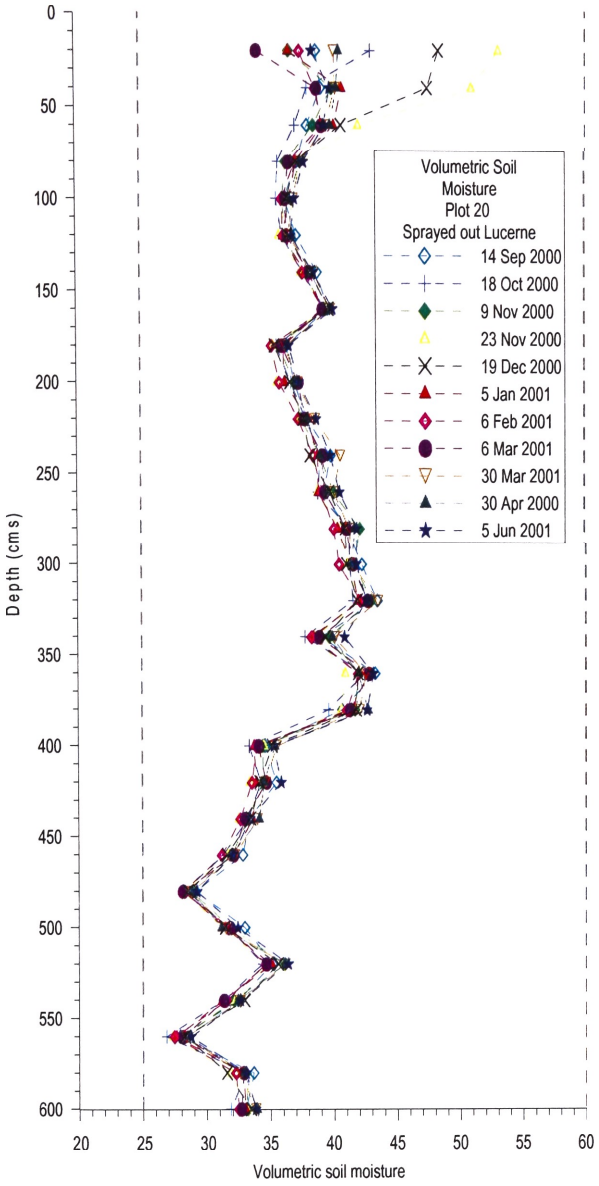

Figure 5.6: Neutron probe soil moisture measurements for Plot 20

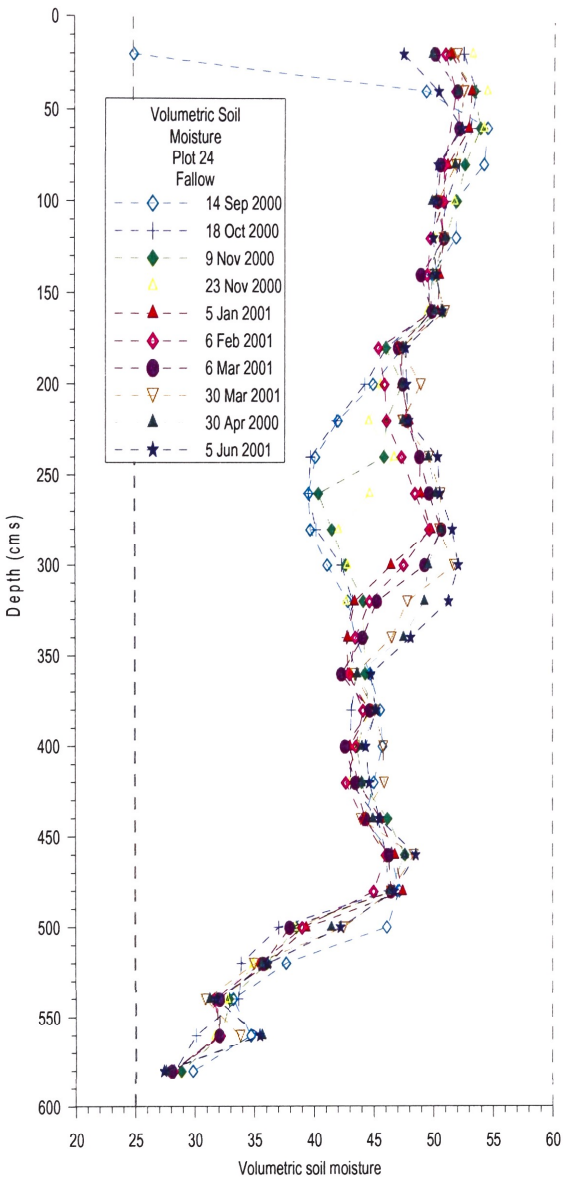

Figure 5.7: Neutron probe soil moisture measurements for Plot 24

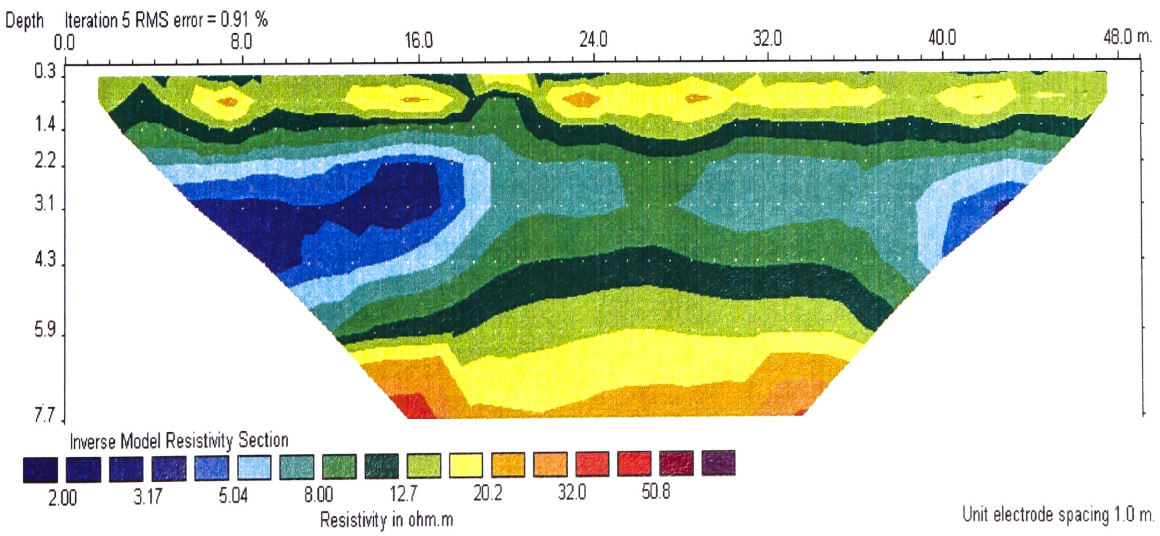

Figure 5.8: Electrical image line centered on the buffer between Plot 6 and Plot 5

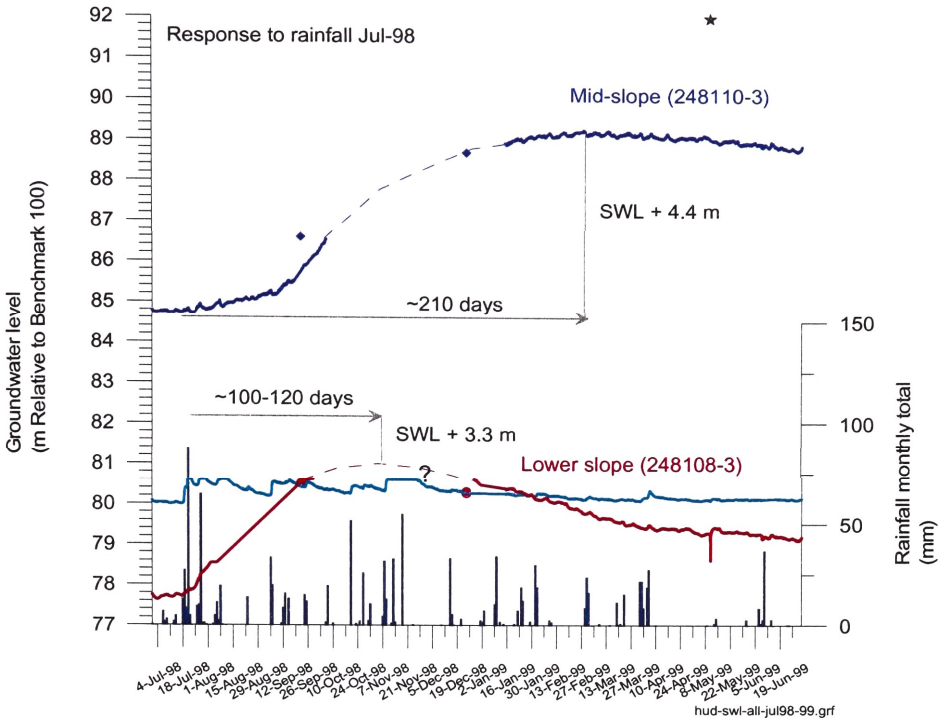

Figure 5.9: Groundwater response to rainfall 1998 - 1999

groundwater level, whereas the lower slope piezometer reached a maximum water level in approximately 115 days.

Table 5.2: Groundwater level response to major rainfall events.

Rain event	Rain event (mm)	Piezo	Time lag ΔSWL_f (days)	ΔSWL (m)
18 to 21-Jul-99	136.4	248110-3	210	4.4
		248108-3	100-120	3.3
3 and 4-Oct-99	107.6	248110-3	175	1
		248108-3	70-80	1.6 ?
15 to 19-Nov-00	178.4	248110-3	100-110	1.6

Groundwater level increases at the mid slope (248110-3) were 4.4, 1.0 and 1.6 m for major recharge events in July 1999, October 1999 and November 2000 respectively. At the lower slope piezometer (248108-3), groundwater level rise was 3.3, and <1.6 m for July 1999, and October 1999 respectively.

Groundwater rise and recession slopes are different for each of the 3 major recharge events. However, additional rainfall was recorded during the period of increase and decrease. Figure 4.9 shows that the lower recession rate after October, 1999 can be attributed to increasing cumulative rainfall. These smaller events are evidently superimposed on groundwater level response to major events.

The data indicates that the water level in the clay responds as an unconfined aquifer with an immediate response to rainfall on the lower slopes but a delayed response on the upper slopes. The choice of conceptual model for the silty-clay aquifer is important if the correct management strategy is to be followed. It is therefore important to evaluate all available data sets to test this hypothesis.

Hydrographic evidence for fracture flow

A possible example of rapid recharge (bypass flow) was recorded in the mid-slope bore (248110-3) and is shown in Fig. 5.11. The rate of change in ground-water level is shown in Fig. 5.12.

A distinctive spike in groundwater level is evident for piezometer 248110-3 in Figure 5.12, marked by

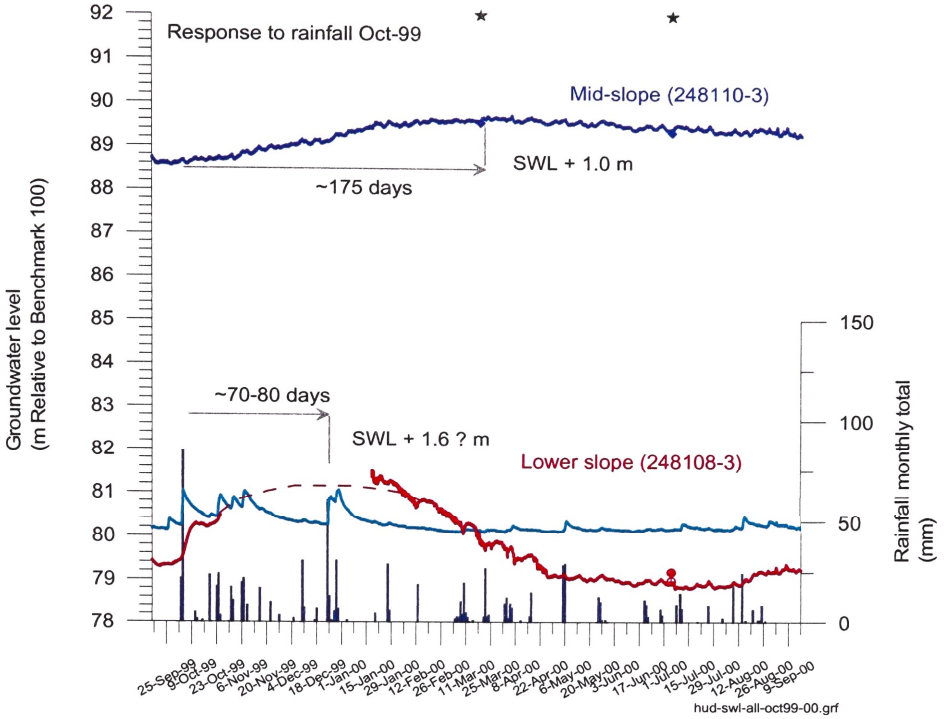

Figure 5.10: Groundwater level response to rainfall 1999 - 2000

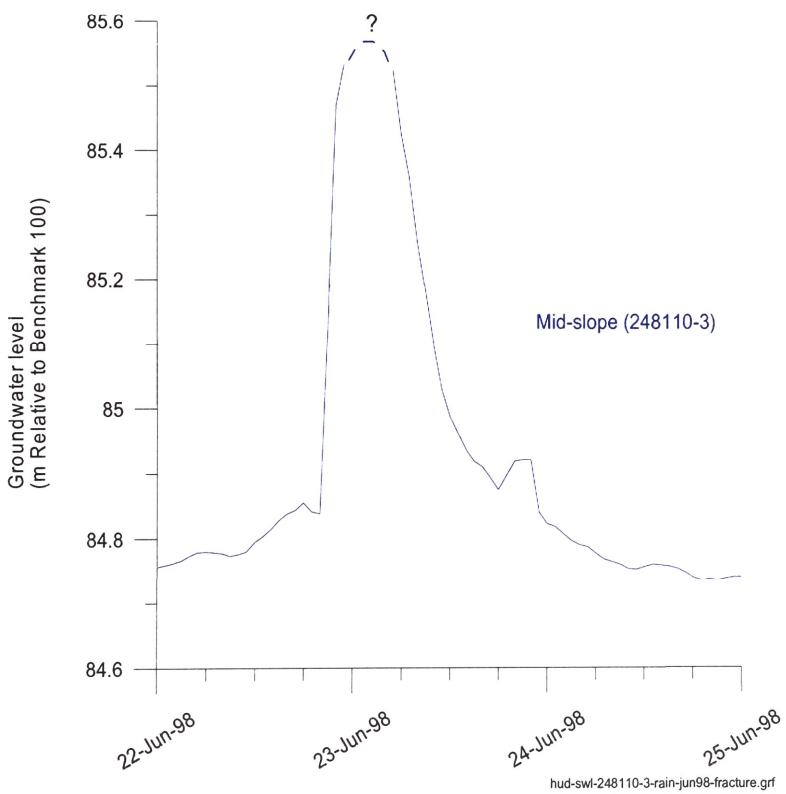

Figure 5.11: Groundwater level response to rapid-recharge event at the mid-slope bore

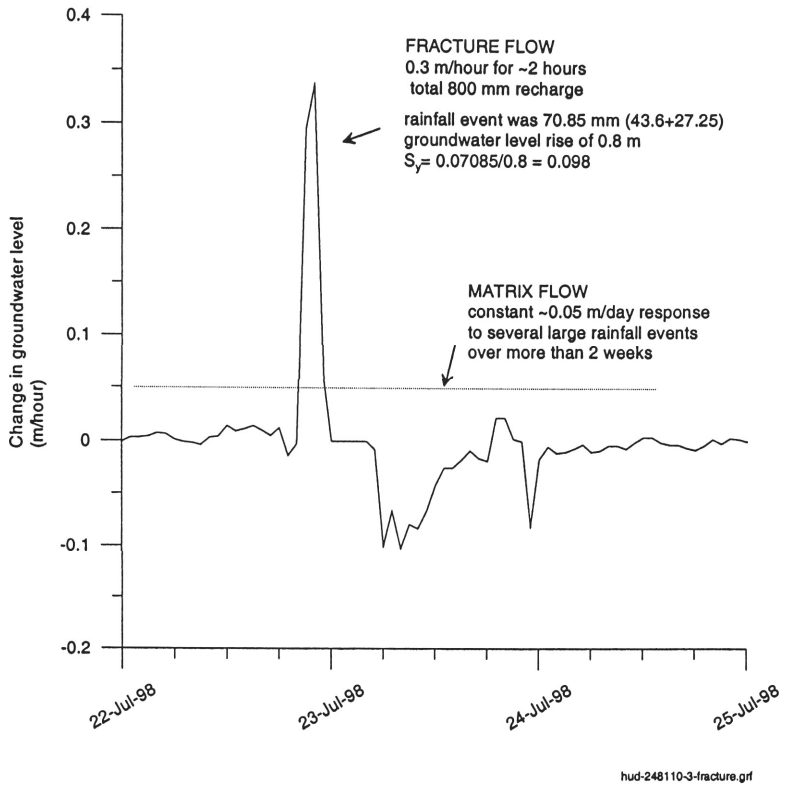

Figure 5.12: Rate of ground-water level change for the rapid-recharge event

an arrow. The intake to piezometer 248110-3 is at 15 m and the response immediately after rain could not be achieved by a downward movement of water through the soil matrix. It is significant that this feature occurs after a prolonged dry period with relatively low groundwater levels. Groundwater level in piezometer 248110-3 increased by 0.8 m, at a maximum rate of increase of 0.3 m/hour for about 2 hours. Within 6 hours, groundwater levels began to fall and within a day, had fully receded, prior to a sustained groundwater level increase of about 5 m over the following 6 months. During each of 3 rising limbs on the hydrograph of Figure 5.9, the rate of rise was about 0.05 m/day.

The groundwater level began to increase between 20:00 and 21:00 pm on the 22nd of June, 1998. Rainfall on site, up to 09:00 on the 22nd and 23rd of June was 27.25 and 43.6 mm respectively (total 71 mm). This data suggests that fracture flow did not occur immediately on the 22nd of June, 1998, although hourly rainfall data is not available for a more detailed analysis. It is possible that significant fracture systems had developed with wide appertures that were unable to seal within the time frame of this rainfall event.

The spiky pattern, superimposed on an otherwise smooth hydrograph, is similar to that observed below mottled clay in Western Australia by Johnston (1987). In that case, a spike response to rainfall in a small number of piezometers, over a time scale of a week, was attributed to bypass flow. Groundwater levels had typically receded sometime prior to subsequent weekly measurements. This work recommended that these events be given greater attention in view of the inability of fracture flow to leach salts from the matrix.

5.4.2 Barometric pressure effects

The analysis of aquifer response to varying applied stresses (Chapter 2) indicated that a compressible unconfined aquifer should not respond to atmospheric variation. Close comparison of the hydrograph data to the barometric pressure data from the climate station shows that a barometric response often occurs and that the barometric efficiency (Equation 2.25) approaches (and sometimes exceeds) 1. Fig. 5.13 shows a clear barometric efficiency in the lower slope bore. Fig. 5.14 shows a similar response in the early part of the record for the mid-slope bore. The barometric response becomes muted as the groundwater

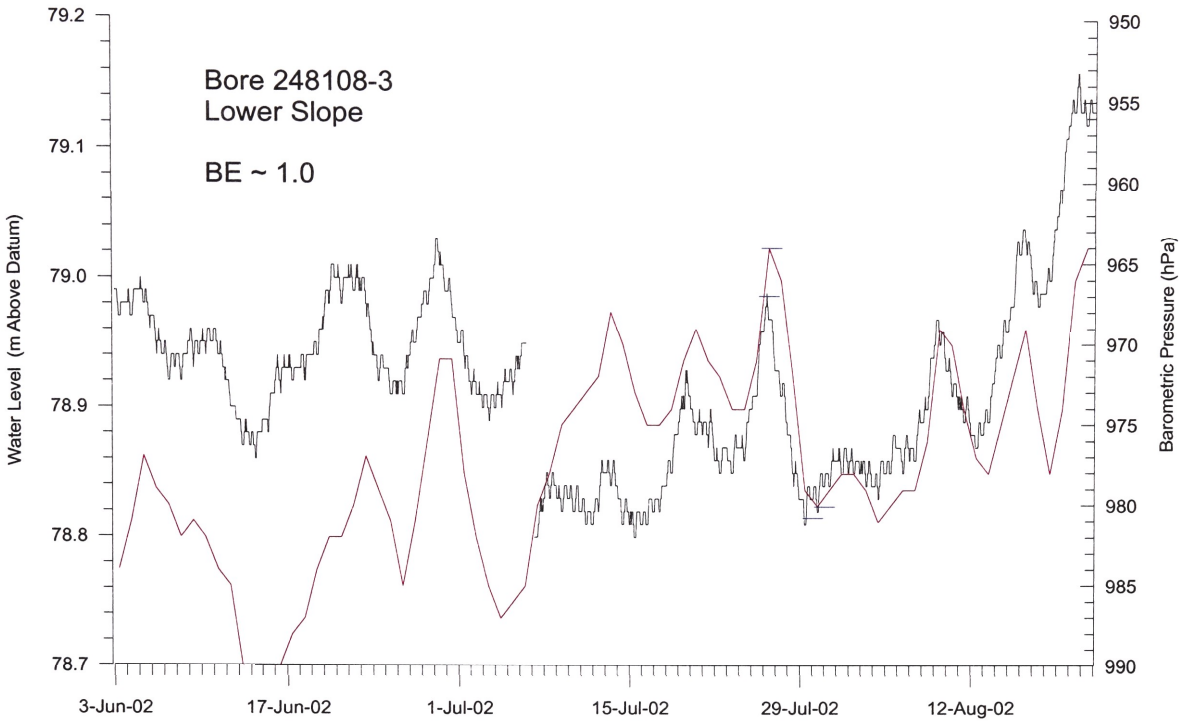

Figure 5.13: Barometric efficiency of 1 on the lower slopes (Bore 248108-3)

level responds to rainfall (Fig. 5.14). A detailed analysis of the barometric response for mid-slope bore in a dry period shows a barometric response close to 1 (Fig. 5.15).

The field data strongly indicates that the silty clay does have a barometric response, contrary to the initial analysis. Discussion of the possible reasons for this important observation is presented in the following chapter as it forms an important component of the conceptual model presented.

5.5 Groundwater flow

Volumetric groundwater flux may be determined by Darcy's law, if hydraulic gradient and hydraulic conductivity are known. The number of data points is very small at Hudson for such an analysis however, sensible deductions can still be made based on the available data.

5.5.1 Hydraulic gradients

The gradient in hydraulic head indicates the probable direction of groundwater flow. Hydraulic gradients and potential flow directions, which were observed at the site in November 2001 are illustrated in Figure 5.16. Lateral and vertical gradients were generally low, but were higher than the hydraulic gradient of 0.001 for shallow groundwater observed on the plains of the Yarramanbah sub catchment by Timms et al. (2001).

Lateral hydraulic gradient

The lateral hydraulic gradient was greatest between piezometers on the mid to lower slope. Over this interval, hydraulic gradient varied between 0.012 and 0.03 in May, 1999 and November 2001 respectively. By contrast the hydraulic gradient over the upper to mid slope was 0.004 to 0.01 in May, 1999 and November 2001 respectively.

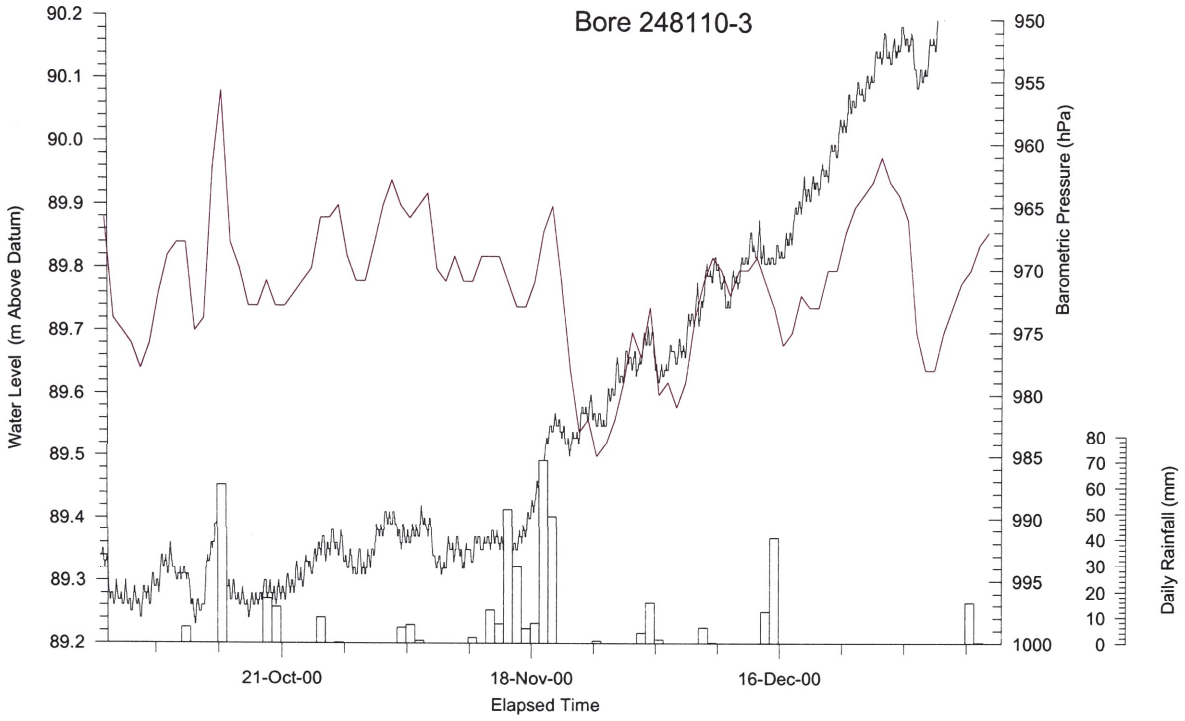

Figure 5.14: Changing barometric efficiency on the mid slopes (Bore 248100-3)

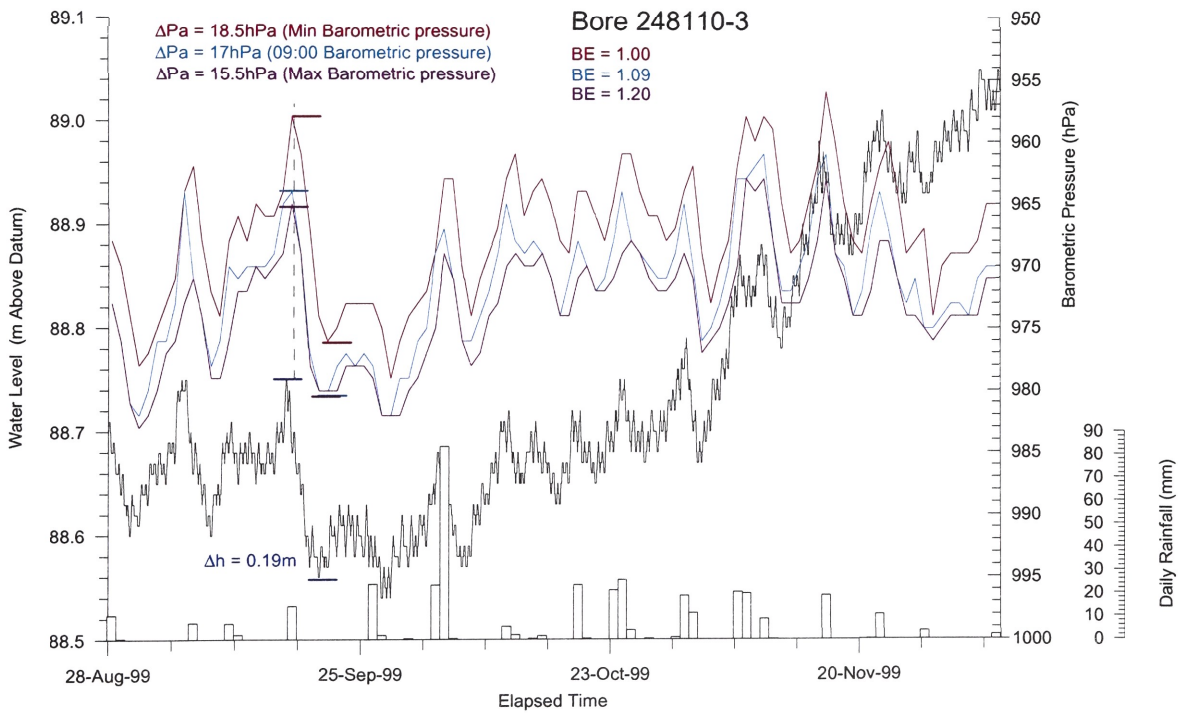

Figure 5.15: Detailed analysis of BE on the mid slope for alternate values of barometric pressure

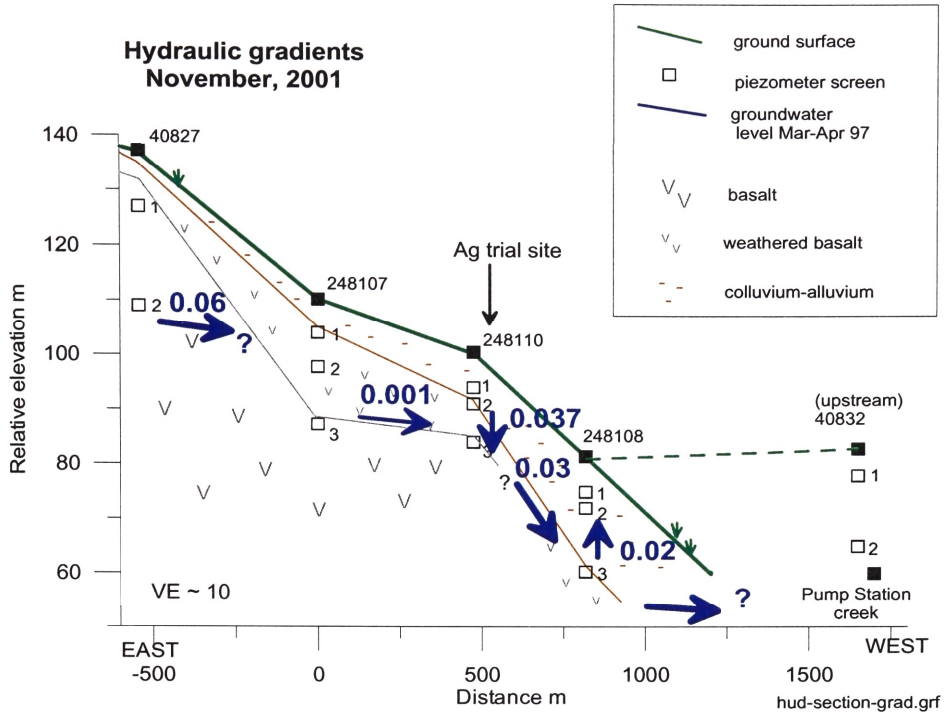

Figure 5.16: Hydraulic gradients, November, 2001.

Water observed occasionally in piezometer 40827 in the woodland above the hill slope was at a much great elevation head. This water was probably in a perched aquifer zone or occurred at the top of another basalt flow.

Vertical hydraulic gradient

The vertical hydraulic gradient was determined for each nested piezometer that contained water. At the lower slope, an upwards vertical gradient of 0.01 to 0.02 was present in March 1997 and November 2001, respectively. Shallow piezometers at the mid slope were generally dry, except in November 2001, when water was also observed in 248110-2. At this time a downwards hydraulic gradient of 0.037 between piezometers 248110-2 and 248110-3 was observed.

The downwards hydraulic gradient at the mid slope was greater than the upwards hydraulic gradient at the lower slope. The increased hydraulic head down gradient may be interpreted as the effect of a confining zone. While discharge probably occurs closer to the creek, discharge may potentially occur through the soil profile on the lower slope.

Vertical hydraulic gradients were similar in magnitude to horizontal hydraulic gradients.

5.5.2 Estimation of hydraulic conductivity

A relatively high hydraulic conductivity was observed for clay at both the Hudson Site and the nearby Claremont Site.

Smectite clay

The hydraulic conductivity of smectite clay varies according to effective stress (confining loads), the chemistry of interstitial water and also the moisture content which may be reflected in fracturing. Although

compacted smectite may is known to have a hydraulic conductivity as low as $10\times^{-10}$ m/s (Rowe et al. 1995), there is evidence that K_v of smectite clay on the Hudson site is considerably higher. Ringrose-Voase & Cresswell (2000) measured K_v of 8.1×10^{-6} to 2.4×10^{-5} m/s at depths between 0.5 and 3.0 m. For these measurements, a constant head was applied through a disc infiltrometer of 0.3 to 0.4 m diameter, positioned on a thin bed of sand, at the desired depth within an excavated trench on the site.

These values are similar to K_v determined on minimally disturbed clay cores (0.06 m diameter) from the nearby Claremont site by Crawford (1997). For these, K_v ranged from 9.3×10^{-7} to 3.8×10^{-5} m/s, using synthesised saline water (1000 μS/cm). The smallest initial K_v value was for a core from 8.4 m depth at the saline N1 piezometer where groundwater was 33 500 μS/cm. K_v was observed to decrease by 2 to 3 orders of magnitude during flushing with fresh water (20 μS/cm). Sorption of solutes was shown to be active when flushed by relatively saline water, while leaching was demonstrated when flushed with water fresher than native pore water.

The similar range of values determined on heavy black soils by these two methods suggests that the relatively high K_v may be attributed to the flocculated particle state. If fracturing were a major factor, it would be expected that K_v for a 0.4 m diameter sample (disc permeameter) would be greater than that for the 0.06 m sample (falling head permeameter). However the laboratory results are not directly comparable with field results, partly because different individual samples were tested, so no firm conclusion can be drawn on the importance of fracture flow from the available permeability data. It is clear however that smectite clay in the area has a relatively high hydraulic conductivity, within the range normally expected for silt (10^{-9} to 10^{-5} m/s) rather than for clay (10^{-11} to 10^{-9} m/s) (Domenico & Schwartz 1990).

Weathered basalt aquifer

According to Freeze & Cherry (1979), typical hydraulic conductivity for permeable basalt is in the range 0.01 m/s to 10^{-7} m/s. It is noted in Fetter (1994), that hydraulic conductivity tends to be high in similar Miocene age fissure flood basalt in the Columbia River. Weathered basalt aquifers have a hydraulic conductivity that exhibits very large anisotropy with $K_h >> K_v$. The enhanced horizontal hydraulic conductivity is associated with the top of each flow as it weathers prior to the next flow. A new flow will cover the young soil profile that has developed and the associated fires will burn existing vegetation often leaving voids. In extreme cases, lava tunnels can develop. Vertical hydraulic conductivity can also develop as a result of sub-vertical cooling cracks that often form.

5.5.3 Lateral and vertical water fluxes.

Darcy's law may be used to calculate the volume of groundwater which is transmitted laterally through the saturated weathered basalt aquifer. The differences in flux through a series of planes provides a crude estimate of recharge to groundwater. Such an approach assumes that flow occurs via piston flow in the matrix.

Table 5.3: Range of deep drainage estimates for given K_h, November, 2001. Estimates are given in mm/month and (mm/year).

Slope section	K_h (m/s)		
	Low 8×10^{-6}	Median 1×10^{-5}	High 2×10^{-5}
Upper to mid	7 (80)	8 (100)	16 (190)
Mid to lower	18 (220)	23 (270)	46 (550)

Flux through a unit width vertical plane at the upper, mid and lower slope was estimated based on saturated zone thickness estimates and hydraulic gradients from November, 2001 (Figure 5.17). The

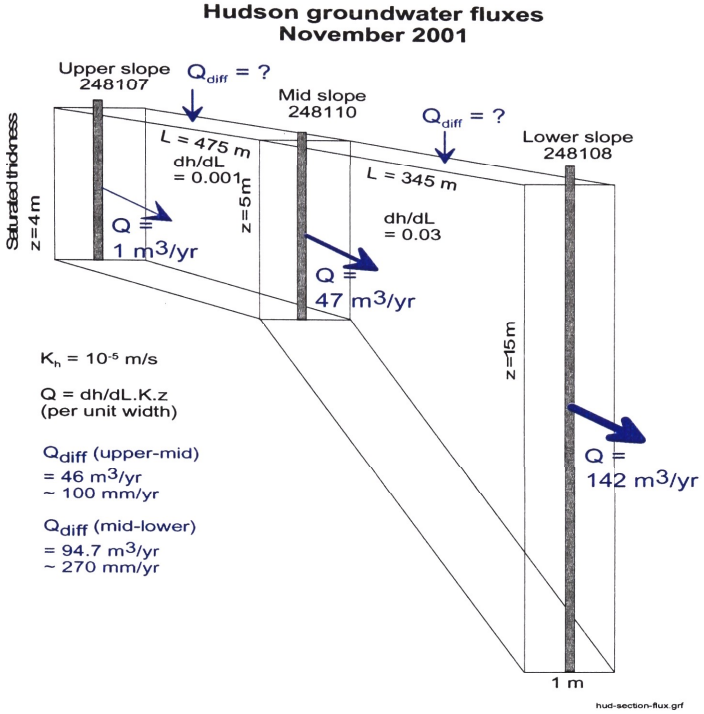

Figure 5.17: Method for estimating deep drainage to groundwater by flux plane method, November, 2001.

difference in lateral flux through each plane, Q_{diff} was attributed to recharge into the groundwater system. The results for a range of horizontal hydraulic conductivities are shown in Table 5.3.

A large increase in ground-water flow is indicated between the upper slopes and the lower slopes. This can only be accounted for by increased recharge to the aquifer below the mid slope. The magnitude of recharge to groundwater in November 2001 was estimated to be between 7 mm and 16 mm/month on the upper to middle slopes, compared with 18 mm to 46 mm/month in the middle to lower slope area. These values represent 8 to 55% of the total monthly rainfall of 83.3 mm.

It is unlikely that field data for K_h would improve these gross estimates, since K can be expected to vary over at least an order of magnitude in such an environment. However, fluxes based on K_h of 10^{-4} m/s would be unrealistically high, indicating that K_h of the weathered basalt is similar to K_v of the overlying clay.

It should be noted that fluxes during periods when the saturated zone thickness is relatively thin would be significantly less than this. Vertical fluxes of the order of several hundred mm per year are consistent with estimates of deep drainage derived from agronomic water balances.

Recharge to groundwater on the mid to lower slope is about 3 times greater than recharge in the upper to mid slope. Since the soil profile is likely to be relatively homogeneous, and cropping practices are uniform over this area, the difference could be attributed to direct recharge through the bed of the incised gully (Figure 2).

5.6 Groundwater hydrochemistry

Groundwater at the Hudson site is of good quality. Groundwater is fresh to moderately saline (TDS 674–3417 mg/L), contains measurable dissolved oxygen (DO 0.6–8.5 mg/L) and is characterised by alkaline pH (7.1–8.4). Major ion chemistry was dominated by Na, Mg, Cl and HCO_3 and total iron concentrations were low.

Considerable hydrochemical variability was evident, both spatially and temporally. Groundwater salinity

decreased downslope (Figure 5.18), particularly in the mid to lower slope area. Surface runoff, measured in Pump Station Creek and the adjacent piezometers (40832) was approximately 3 times more saline than groundwater below the hill slope.

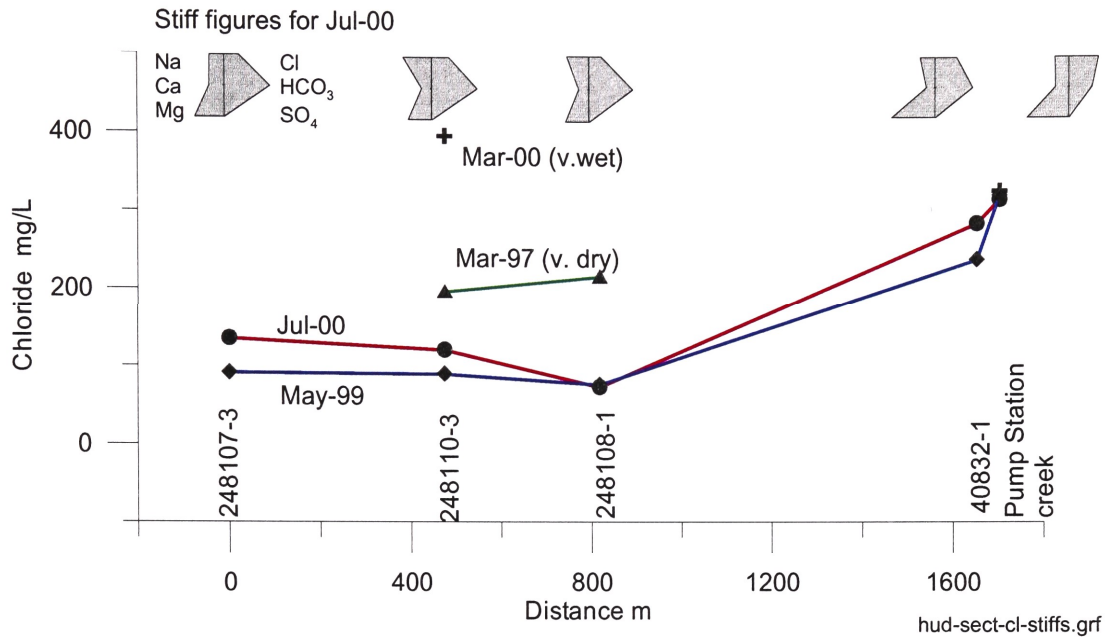

Figure 5.18: Hydrochemical variability across the Hudson slope, May-99 and Jul-00.

Groundwater salinity varied over time, but there was no apparent relationship with either rainfall or groundwater level for the relatively dry year of 1997, or for the wet years from 1998-2001 (Figure 5.19, Table 5.4). For example, between March and April, 1997, groundwater EC more than doubled, from 1210–2710 μS/cm, though no rainfall fell during this period. A second EC peak occurred in March 2000. There is no difference in rainfall preceeding this and other sampling events during the wet years, although it may be significant that sampling occurred at the end of a rising groundwater level trend. By comparison, groundwater salinity variability observed in the piezometers at the lower slope (248108) was relatively small, although sampling was not possible at the March 2000 peak of salinity.

The possibility that groundwater EC variation was related to turbidity of the sample was investigated by intensive EC monitoring and selected major ion analysis during purging of 248110-3. As this piezometer was purged by hand bailer, the sample varied from totally clear in the early stages, to a highly turbid muddy soup as the piezometer ran dry. Figure 5.21 shows that groundwater salinity was variable, but generally increased by about 2–3% with increasing turbidity. Such a small EC increase could not account for the temporal variability described above.

5.6.1 Major ion chemistry

Groundwater on the Hudson hill slope was characterised by $Mg - Na - HCO_3 - Cl$ type. The exceptions to this rule were the dominance of Cl at the windmill, and variable chemical composition at 248110-3. At this location, Cl dominated in March 2000, and the dominance of Na was at the expense of Ca in 248110-3 between 1998-2001 (Table 5.4).

The relative major ion composition of these ground waters has been plotted on a piper diagram (Figure 5.22). The relative proportion of Na increases downslope, though the proportion of HCO_3 is constant. These trends are distinct from waters within and adjacent to Pump Station Creek, which are marked by a variable proportion of Cl. The composition of most ground waters sampled during the dry conditions of 1997 are relatively enriched in Cl compared with samples from 1998 to 2001. The relatively constant proportion of Na over these two periods (except for an increase observed in 248108-3), suggests that ion exchange is an important process in the evolution of the waters.

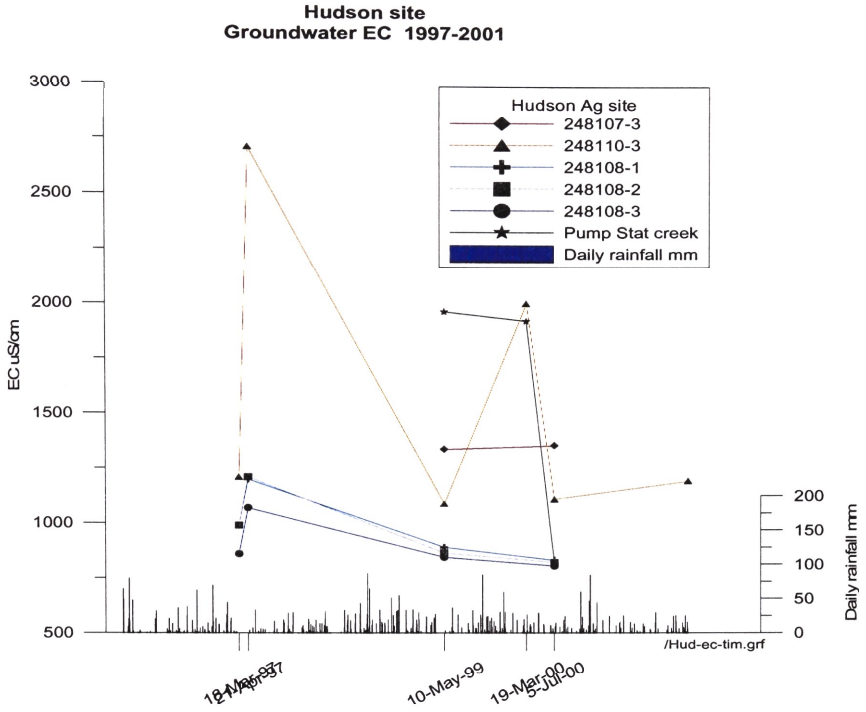

Figure 5.19: Groundwater salinity variability 1997-2000.

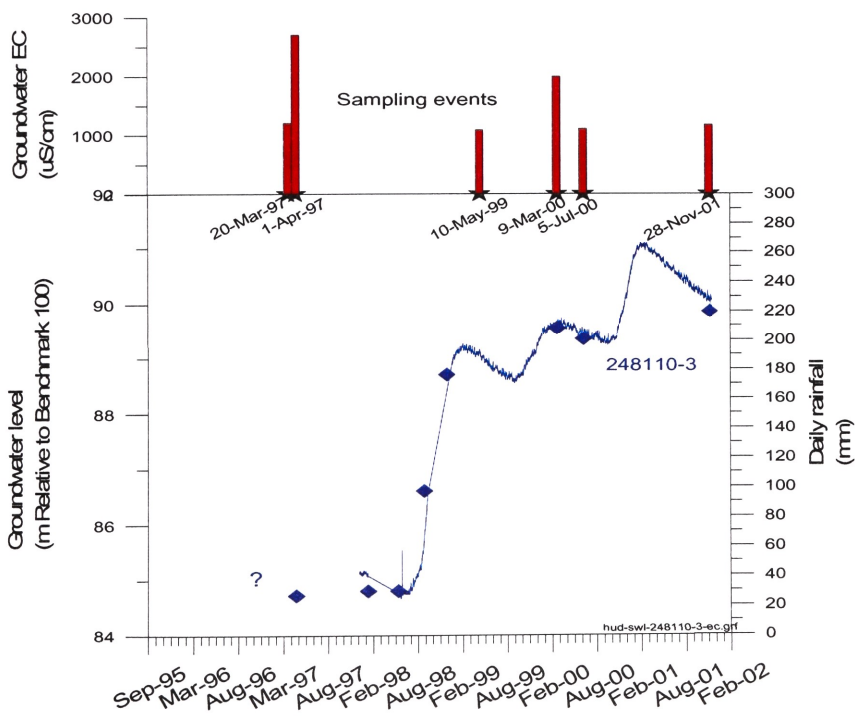

Figure 5.20: Groundwater EC compared with groundwater level.

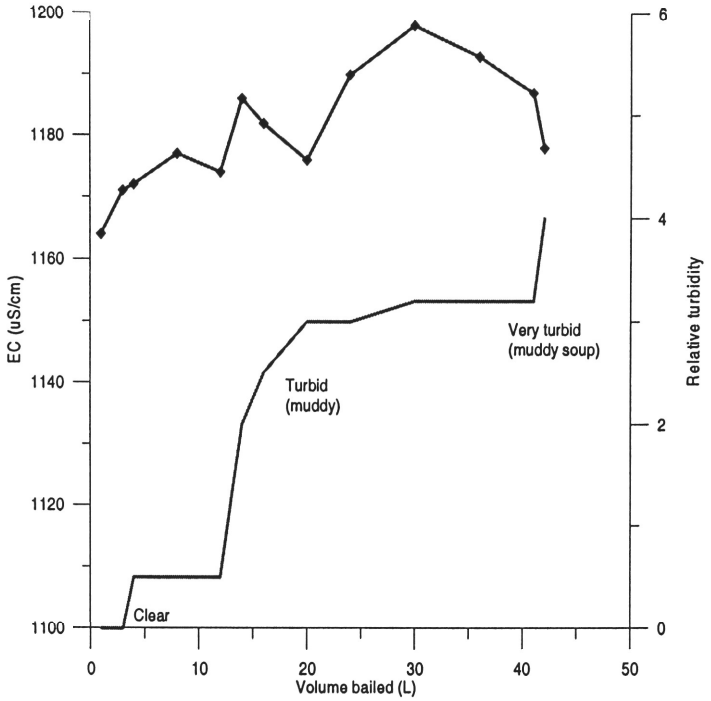

Figure 5.21: Groundwater EC variability with turbidity.

Table 5.4: Relationship between groundwater salinity, groundwater level and rainfall prior to sampling.

Sample date	EC (μS/cm)	Cl (mg/L)	Water Type	Groundwater level	Climatic condi-tions	Dry days[a]	Recent rainfall[b] (mm)
20-Mar-97	1210	197	Mg-Na-Ca-HCO3-Cl	low	dry	13	2.45
1-Apr-97	2710			low	very dry	45	0
10-May-99	1089	90	Na-Mg-HCO3-Cl	high, falling	dry	30	0
9-Mar-00	2000	396	Na-Mg-Cl-HCO3	high, rising	very wet	1	50.2
5-Jul-00	1110	121	Na-Mg-HCO3-Cl	high, falling	wet	5	22.6
28-Nov-01	1193			high, falling	very wet	0	59.4

[a]dry days prior to sampling
[b]Total rainfall in 2 weeks prior to sampling

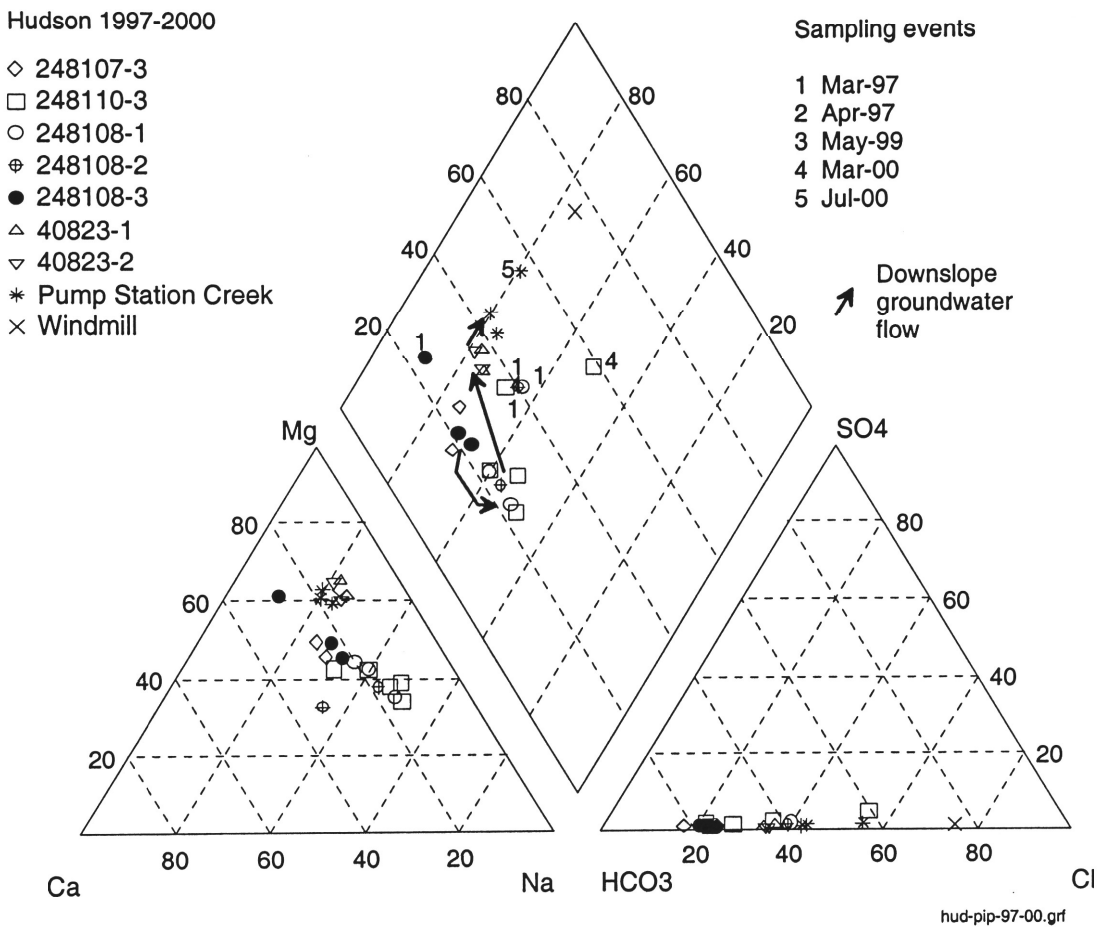

Figure 5.22: Piper diagram for Hudson groundwater 1997-2000.

5.6.2 Groundwater salinity variability over time

Significant groundwater salinity changes were observed over time which may be related to groundwater flux. Figure 5.19 and Table 5.4 summarises the relationship between groundwater salinity, groundwater level and rainfall prior to sampling. There was no simple association between groundwater salinity during dry conditions of 1997 and relatively wet conditions of 1999–2001 for piezometer 248110. Rather, groundwater salinity increased 4 fold (based on Cl concentration) in response to recharge. The recharge is indicated by the rising groundwater level.

This pattern suggests that episodic recharge events flush salt from the profile, but that groundwater levels are not sufficiently high to inundate saline clay. Geophysical borehole logs suggest that there is little salinity variation within the weathered basalt aquifer along the slope. High ECa peaks within the weathered zone, or near the surface, particularly at the lower slope (248108) may constitute a source of salts flushed into groundwater. A near surface source of salts is supported by data from the windmill which taps a hand-dug well, and is likely to be open to ingress of groundwater from the top of the saturated zone to the base of the well. Groundwater salinity near the top of the saturated zone is therefore likely to be considerably higher than the average EC ($5720\,\mu S/cm$) and major ion concentrations measured in this sample.

Relatively saline groundwater which was sampled in March, 2000 after major rainfall would thus have a larger proportion of groundwater sourced from the overlying profile. Although the data set is incomplete for other piezometers on the hill slope, Fig. 5.18 shows that groundwater salinity increases on the upper slope (248107) mirror those on the lower slope. This evidence, together with the relatively constant lateral distribution of saline clay, supports the interpretation that the saline groundwater is sourced from overlying clay, rather than being flushed laterally through the system.

In the absence of intensive groundwater level data for early 1997, it is difficult to explain why groundwater salinity doubled within 12 days from March to April (Table 5.4).

5.7 Hydrochemical processes

Hydrochemical mixing models for a flow path from the upper to lower slope, were assessed in detail by Chambers (1999). This work was based on data from May 99 and is considered to reflect typical processes along this flow path. Chambers (1999) concluded that significant dilution of groundwater was occurring in the mid to lower slope caused by direct infiltration of rainfall.

For this report, temporal changes at the mid-slope piezometer (248110) are assessed for 5 sampling periods between March, 1997 and July, 2000. Previous attempts by Chambers (1999) to quantify temporal changes require revision because of an error in SO_4 concentrations for Mar-97, and because the data set has since been extended by 3 additional sampling events.

5.7.1 Mixing and dilution

Hydrochemical mixing and dilution provide an estimate of the proportion of water that has mixed along a flow path. Ideally, the hydrochemical and isotopic signatures of waters which are mixing must be well defined and physically plausible from a hydraulic perspective. This means that the lateral and vertical variability of groundwater chemistry should be throughly understood. In this case, vertical differences in pore water composition are greater than lateral changes, and downwards flow is plausible, so it may be assumed that the changes observed over time are due to vertical recharge.

Hydrochemical mixing estimates of Chambers (1999) assumed that recharge water was rain water with very low TDS. Rainfall data for the Liverpool Plains (Table 4.2) suggest that NaCl is deposited both as wet and dry precipitation. However, it is also likely that pore water within the soil profile is relatively fresh, given the relatively low ECa of downhole geophysical logs. In fact, given the estimated time lag

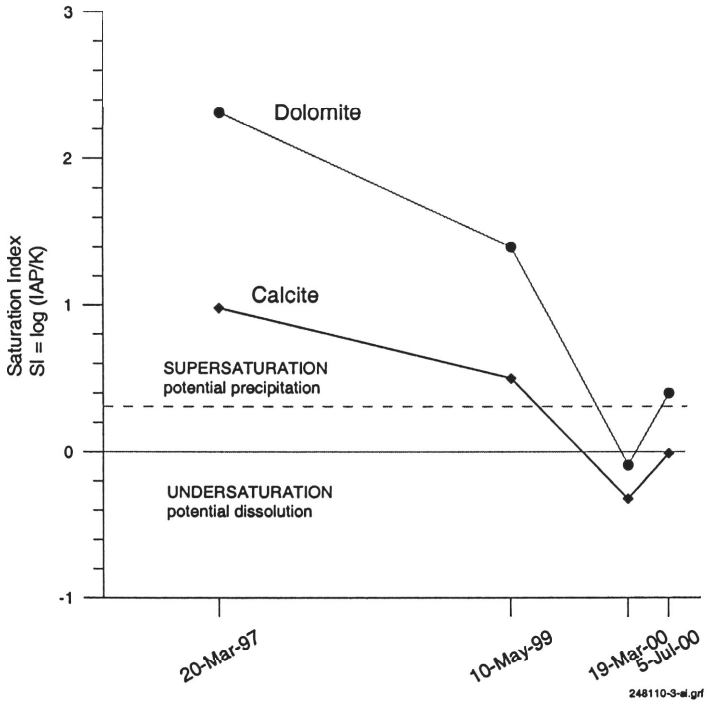

Figure 5.23: Variation in saturation indices over time for groundwater below the mid-slope (248110-3)

for a solute front to move through the matrix, mixing waters are more likely to be old waters which are displaced downwards in the profile.

Where rain water occasionally does penetrate to the saturated zone via fractures, some evaporated salt accumulated during long dry periods will also be flushed. However, without continuous logging of groundwater salinity to correlate with groundwater level data, it is not possible to assess the prevalence of this phenomena.

5.7.2 Precipitation and dissolution

Chambers (1999) noted that all ground waters on the slope were supersaturated with respect to calcite and dolomite. However, groundwater latter became undersaturated with calcite and dolomite, where dissolution would occur if the waters were in thermodynamic equilibrium (Figure 5.23). In natural environments, calcite is known to dissolve quickly enough to reach equilibrium, and if SI >0.3, to precipitate fast enough to establish equilibrium (Appelo & Postma 1994).

Based on this information, calcite and dolomite precipitation were important processes in March, 1997 and to a lesser extent in May, 1999 at the end of dry years with lowered groundwater levels. The influx of saline groundwater in March 2000 caused the groundwater to become undersaturated.

Ionic ratios for key major ions provide additional evidence that dissolution of calcite, and also halite sometimes occurs. The 1:1 ratio between $Ca+Mg/HCO_3+SO_4$ in the March, 2000 may be attributed to calcite dissolution (Figure 5.24C). Similarly, dissolution of halite can explain the chemical composition of groundwater in March, 1997 and March, 2000.

5.7.3 Ion exchange

Ion exchange involves the replacement of one ion for another at the solid surface. This process is particularly important in dynamic environments where the flow of groundwater of different composition triggers ion exchange, which acts as a temporary buffer in non-steady state situations such as a moving

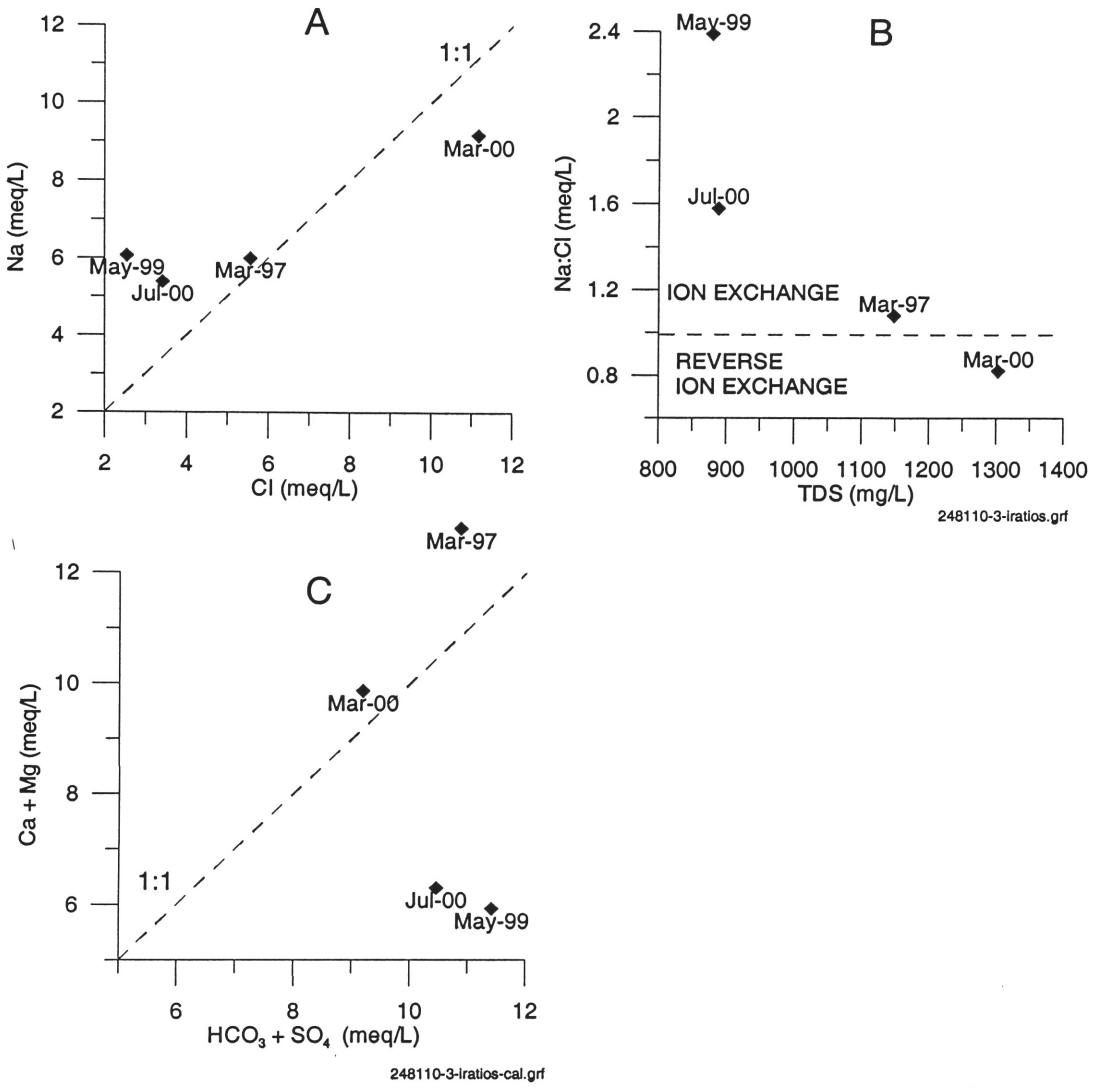

Figure 5.24: Ionic ratios over time for groundwater below the mid-slope (248110-3) A) Na vs. Cl, B) Na:Cl vs. TDS and C) Ca+Mg vs. $HCO_3 + SO_4$

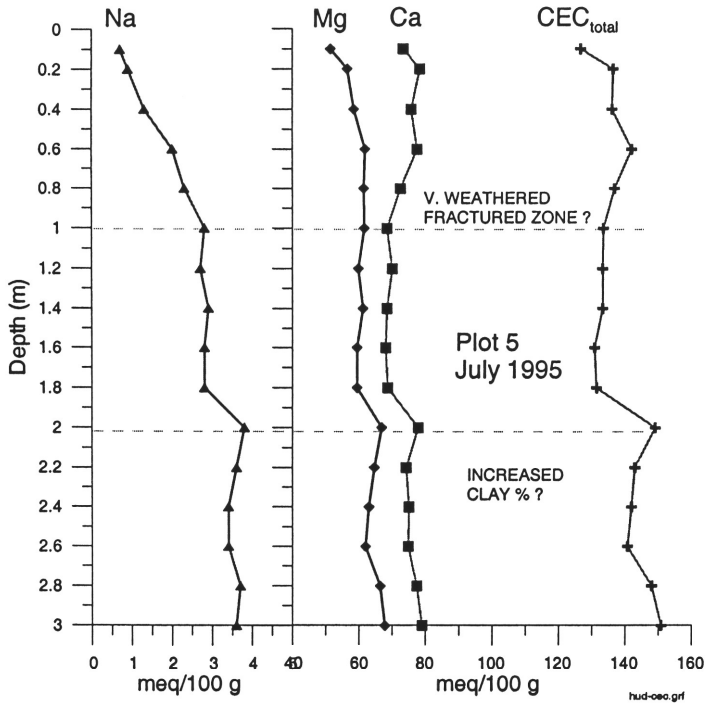

Figure 5.25: Cation exchange variability with depth for Plot 5, July 1995.

saline interface. Ion exchange reactions occur rapidly, and under natural groundwater flow conditions, equilibrium can be assumed (Appelo & Postma 1994).

For pH conditions typical of natural groundwater environments, cations are adsorbed by the negatively charged surface of clay minerals, while exchange of anions is possible on oxides and carbonate sediments (Appelo & Postma 1994). Divalent cations such as Ca^{2+} have a stronger adsorption affinity than monovalent cations such as Na^{+}. The normal preference of adsorbed cations for most clays is as follows:

$$H^{+} > Ca^{2+} > Mg^{2+} > K^{+} > Na^{+}$$

The clays at the Hudson site have very high CEC of 127–150 meq/100g, dominated by adsorbed Ca and Mg (Table 4.8). The very high CEC indicates that these clays are highly reactive, with a large buffering capacity. It is also possible that zeolites, which are known to be associated with the Liverpool Plains volcanics (Lavitt 1999), may contribute to CEC. Zeolite CEC are typically upto 400 meq/100g. Variable ion exchange ratios over time (Figure 5.24) confirm that ion exchange is active at Hudson.

An increasing proportion of Na^{+}, and decreasing proportion of Ca^{2+} was evident to a threshold depth of 1.0 to 1.4 m below Plot 5 (Figure 5.25) and Plot 14 respectively (Figure 5.26). The physical significance of this threshold depth is not known, but may be related to the depth of major fracture pathways. Below this depth, reverse ion exchange, with increased adsorption of Na onto clay in exchange for Ca and Mg may be related to relatively saline pore water in the matrix.

Reverse ion exchange

Reverse ion-exchange requires clay with exchangeable Ca or Mg (usually montmorillonite) and a flowing water to have a higher concentration of Na relative to the clay matrix to drive a reaction as the system equilibrates. Reverse ion-exchange is typically observed with seawater intrusion or brine contamination. At the saline intrusion front, Na is exchanged for Ca. However once calcium in the clay has been removed, the process cannot continue further - thus $CaCl_2$ type water occurs at the leading edge of contamination (Hounslow 1995).

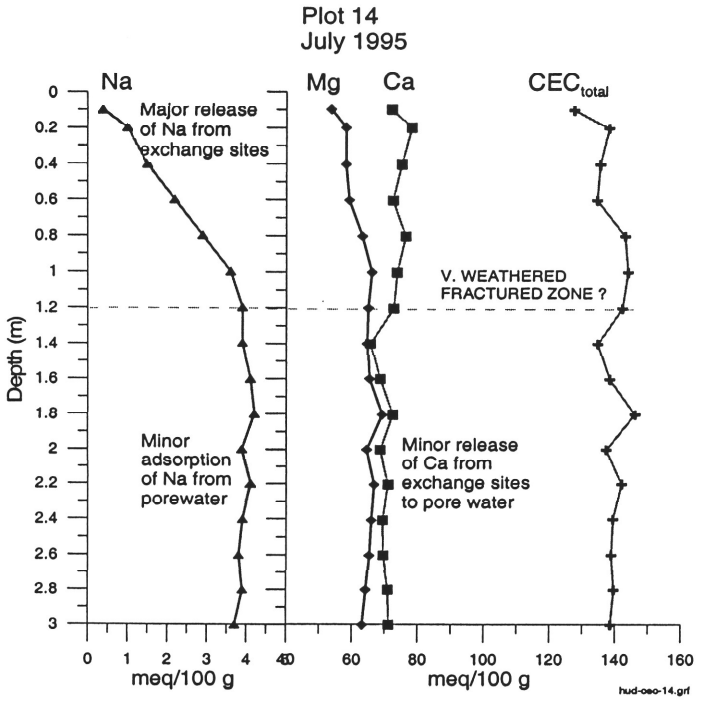

Figure 5.26: Cation exchange variability with depth for Plot 14, July 1995.

5.7.4 Formation of caliche

Caliche deposits of calcium and magnesium carbonates are common in the foot slope environment. On the Hudson site, caliche was observed as small nodules in the soil profile, as massive deposits in the gully (Figure 2), and may correlate with high gamma zones 0.5 m thick which were detected by downhole geophysics below the upper, mid and lower slope (Figure 4.2). Caliche also occurs on the lower slope below a remnant patch of woodland and is observed as massive sheet deposits exposed on the banks of nearby Blackville Creek.

The position of these features within the landscape, suggests that caliche deposits may act as preferential flow horizons. Once massive caliche deposits are formed, a relatively impermeable layer may direct groundwater to flow along the top of the deposit.

The mechanisms by which supersaturation of carbonate in groundwater are achieved are not fully understood, but appears to be related to episodic saturation of the profile. Chambers (1999) concluded that carbonate minerals precipitate while recharge rates are low after a major influx of meteoric water. However, further dilution by fresh water may cause under saturation and dissolution. In this way, carbonate gradually accumulates towards the end of flow paths.

Decreasing SI between March 1997 and May 1999 indicate that precipitation was occuring (Figure 5.23), but that in March 2000, groundwater became undersaturated. At this time, following another major rainfall event, groundwater EC had doubled and was dominated by Cl. However, the proportion of Na and Ca remained relatively constant (Figure 5.22) due to the buffering capacity of high CEC clay.

5.8 Isotopic data

Environmental isotopes, elements with varying atomic mass, provide a unique insight into recharge processes, groundwater quality, rock-water interaction, and the origin of salinity (Clarke & Fritz 1997). Stable isotopes such as carbon-13 ($\delta^{13}C$), deuterium ($\delta^{2}H$) and oxygen-18 ($\delta^{18}O$), provide a natural signature tracer for groundwater origin. Estimates of groundwater residence times are given by radio isotopes

such as tritium and carbon-14.

5.8.1 Local meteoric water line

The establishing a local meteoric water line (LMWL) is important to understanding the values of ^{18}O and ^{2}H observed in ground and surface waters. For instance, recent recharge may be detected by comparing the degree of enrichment in rain water and groundwater. Hydrogeochemical processes that have subsequently altered groundwater isotopic composition may also be identified if the slope and offset of the LMWL is defined.

A LMWL was established for Gunnedah using the measurements of rainfall isotopic concentrations derived from the Gunnedah Research Station site (Figure 5.27) and defined as follows:

$$\delta^2 H = 8.41\delta^{18}O + 15.99 \tag{5.2}$$

The LMWL was based on 17 samples collected from rainfall events between October 1999 and January 2001. Samples were collected by the method which has been outlined, and samples from events <6 mm magnitude were discarded as unimportant for groundwater recharge. This was to avoid the enriching effects of secondary evaporation during passage of raindrops through a warm, dry atmosphere typical of semi-arid areas - a process known as the amount effect (Dansgaard 1964).

The LMWL for Gunnedah is similar to the global meteoric water line (GMWL) that was first defined by Craig (1961) and later refined by Rozanski et al. (1993) (Equation 5.3).

$$\delta^2 H = 8.17\,\delta^{18}O + 11.3 \tag{5.3}$$

The slope of the Gunnedah LMWL is similar to the GMWL, since the amount effect is absent. The small slope difference could be related to the temperature at which fractionation occurred. The ^{2}H intercept of 15.99 is closer to that for Brisbane (13.1) than Alice Springs (4.5).

The deuterium excess ^{2}H, defined as d = δ^2H - 8δ^{18}O, is controlled by conditions during primary evaporation such as humidity. For the Gunnedah LMWL d is 12.2, which relates to a humidity of 80–85%.

Groundwater stable isotopes

The values of δ^2H and δ^{18}O for July, 2000 is given in Table 4.6. Groundwater at the Hudson site was depleted in both δ^2H and δ^{18} relative to average modern rainwater. This means that a large proportion of the groundwater store was recharged in cooler and/or wetter climatic conditions. Similarly depleted groundwater in confined aquifers further north have been attributed to recharge about 1 500 and 3 000 years ago by Coram (1999) and Lavitt (1999). As reviewed by these authors, there is abundant independent evidence of cooler and wetter climates in south-eastern Australia at this time.

The results at Hudson were similar to values for groundwater within clay at the Yarramanbah site and near the Pullaming site at the northern end of the Liverpool Plains. The similarity of values from a foot slope in the upper catchment with that observed for confined aquifers near the base of the catchment is surprising.

At Hudson, groundwater below the mid slope (248110-3) was slightly more enriched in these isotopes relative to groundwater on the lower slope. The three ground waters from Hudson were positioned on a line of slope 5 (Figure 5.28). This may be attributed to evaporation in a high humidity environment. However, since evaporation from these depths is not physically possible, this relationship must be interpreted as due to mixing between depleted groundwater and pore waters from the shallow profile which may have been enriched through evaporative processes.

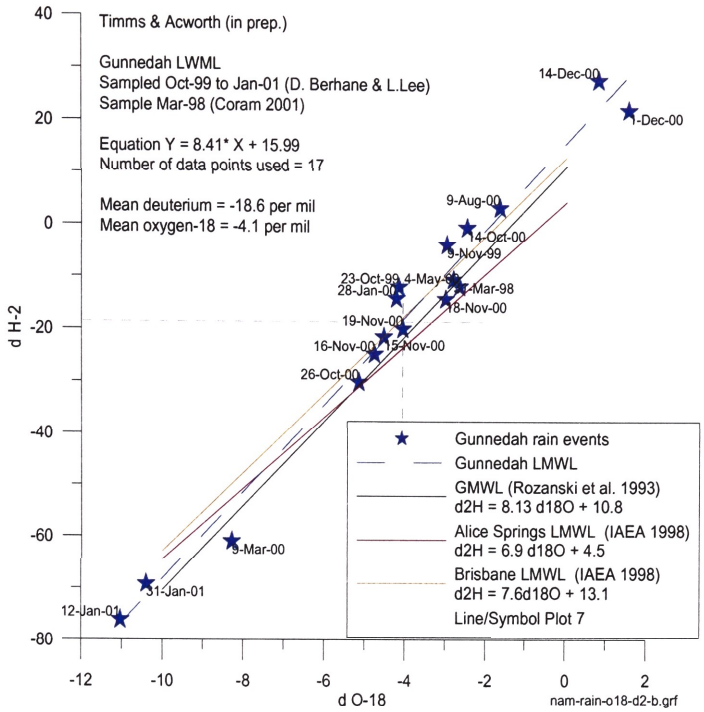

Figure 5.27: Oxygen-18 versus deuterium for rainfall events at Gunnedah between Oct-99 and Jan-01, showing the Gunnedah LMWL relative to the GMWL

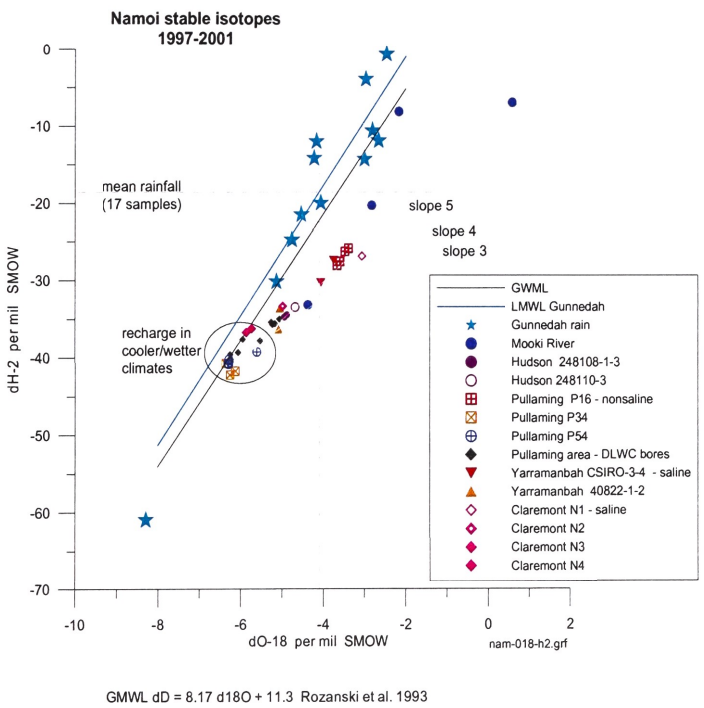

GMWL dD = 8.17 d18O + 11.3 Rozanski et al. 1993

Figure 5.28: Oxygen-18 versus deuterium for rainfall events at Gunnedah between Oct-99 and Jan-01, showing values for groundwater at Hudson relative to other sites on the Liverpool Plains.

5.8.2 Groundwater residence times

Residence times, based on tritium and carbon-14 indicate that groundwater is hundreds of years old below the mid slope and thousands of years at the base of the slope. Groundwater below the lower slope (248108), is characterised by an absence of significant tritium activity, and low percent modern carbon (pMC) of 45 to 58. Apparent groundwater ages, assuming no mixing and no matrix interaction are given in Table 5.5.

The stable isotope $\delta^{13}C$ provides an indication of the source of DIC in groundwater. Waters relatively enriched in $\delta^{13}C$ may be attributed to exchange with atmospheric CO_2 and dissolution of carbonate, which may increase apparent carbon-14 ages by dilution with 'dead' carbon. Values of $\delta^{13}C$ were highest at the mid slope (Table 4.7). Because there is a $\delta^{13}C$ difference of 4 ‰ between groundwater below the mid and lower slope, the apparent ages are not comparable. Dissolution of matrix carbonate appears to have been most significant for groundwater on the mid slope.

Assigning absolute ages, in calender years, to these ground waters is more problematic. The Pearson carbon-14 correction model was applied, assuming a matrix carbonate of $\delta^{13}C$ of 0 ‰. This model is a mixing model which accounts for observed groundwater $\delta^{13}C$ by mixing carbonate from soil CO_2 (with 100 pMC) and dissolved carbonate (with 0 pMC).

Apparent ages corrected by this technique vary greatly (Table 5.5), with both increased and decreased age depending on specific assumptions, highlighting the inadequacy of this method. However, the general conclusion can be made that groundwaters are generally several hundred to thousands of years old, except at the lower slope where groundwater may be relatively modern.

Tritium activity of these ground waters were very low, providing further evidence that groundwater at the site is older than recent land use changes at the site. The first samples analysed for tritium at ANSTO were inconclusive because of large detection errors of ±0.3 TU. Two additional samples were subsequently analysed at NZ INS in New Zealand where detection errors were an order of magnitude lower.

Very low, but significant tritium activity was detected in groundwater at the mid slope (248110-3). This result clearly indicates that groundwater at this site is a mix of modern water and old water, which may partly explain the inadequacy of the Pearson correction technique. The observed tritium activity may be explained by mixing <1% of rainwater (4.3 TU) with old, tritium free groundwater (Table 5.6). However, if displaced soil pore water, rather than rain water mixes with groundwater, the tritium input may be relatively small. The range of plausible mix values in Table 5.6 suggest a mix of <1 to 13% of displaced pore water with older groundwater.

5.9 Flux through the unsaturated zone

5.9.1 Matrix transit time

Residence time of water through the matrix of the unsaturated profile is expected to be decades to hundreds of years. An approximation of residence time is given by Oostindie & Bronswijk (1995).

$$t_u = T_u \Theta \, P_s \tag{5.4}$$

Where t_u is the residence time of water in the matrix (days), T_u is the thickness of the unsaturated zone (cm), Θ is the volumetric water content, and P_s is the precipitation surplus (cm/day). If it is assumed that the precipitation surplus is equivalent to deep drainage of 50 mm/year (0.014 cm/day), and $\Theta = 0.5$, then for an unsaturated zone thickness of 10 to 15 m, the residence time will be about 100 to 150 years. Similarly, if deep drainage were only a few mm/year, as would have been the case prior to cropping, then the residence time within the saturated zone would have been at least a thousand years.

Table 5.5: Residence times for groundwater at Hudson site, assuming matrix carbonate of zero per mil.

Piezo	Sampling date	TU	Apparent (years)	Pearson cor[a] (years)	Pearson cor2[b] (years)
248108-1	Jul-00	0.005	4435	1681	5752
248108-3	Mar-97		4897	2641	6712
248108-3	Jul-00		6511	3477	7548
248110-3	Jul-00	0.027	1836	-3967	104

[a]assumes soil $d^{13}C$ of -18 ‰
[b]assumes soil $d^{13}C$ of -11 ‰

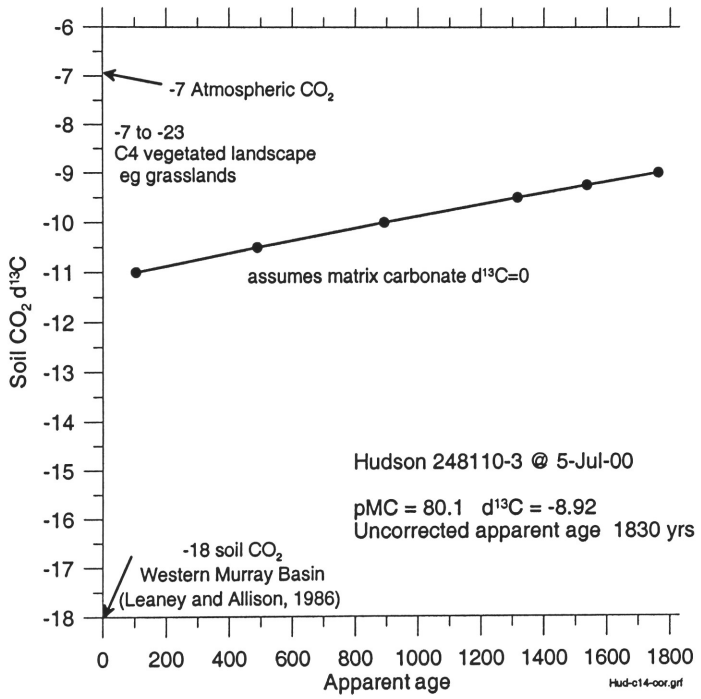

Figure 5.29: Correction of carbon-14 apparent age by Pearson method, Hudson 248110-3.

Table 5.6: Groundwater mixing at Hudson site.

Piezo	Sampling date	TU	Input TU	%mod in mix
248110-3	Jul-00	0.027	4.3	0.6
		0.027	1.0	2.7
		0.027	0.5	5.4
		0.027	0.2	13.2

Whilst this is a crude estimate, the estimate does illustrate that in the absence of fracture flow, individual water molecules that recharge aquifers at depth are unlikely to be direct infiltration of rain water, but have been displaced downward by invading water. This displaced pore water is old, with little tritium remaining. In addition, it would be expected that changes in solute concentration that may have occurred near the surface since cropping will not yet have reached the saturated zone, unless by fracture flow.

Chapter 6

DISCUSSION

6.1 General observations

The interpretations of diverse data sets in the preceding chapter provides sometimes conflicting indications and it is clear that much still remains to be understood concerning processes in these black soil systems. The soils derived from weathering of the underlying basalts are both chemically reactive and physically compressible and as such, present a complicated physiochemical system. The application of conventional techniques designed for non-reactive incompressible media are clearly inappropriate. The fact that the soils formed by weathering of the basalts, produce some of the best farming country means that the additional effort required to understand these systems is well justified.

In this chapter we synthesise a conceptual model for the system.

6.2 Evolution of the soil profile

The surface area of each basalt flow zone is very large - the result of degassing and inclusion of material at the base of the flow and then weathering of the flow top. Weathering of the flows therefore proceeds rapidly as long as water can circulate through the system (Acworth 1987). Groundwater is the weathering agent responsible for removing the initial unstable mineral elements with the result that the porosity of the weathered zone is between 5 and 10% (Hodnett & Bell 1981). Further chemical weathering then generates the smectite clay dominated yellow buff clays that underlie the surface soil. These clays appear to be generally massive and have been formed largely in situ by weathering. There have been no observations of lateral discontinuities, such as old soil horizons, within the massive clay overlying the basalt. The geochemical reactions involved in the transformation of solid basalt to smectite dominated clay are not well known but presumably depend upon a constant flush of groundwater through the top of the weathered basalt. Detailed studies of the mineralogy of the basalt and the clays would be of help here.

The surface soil layers are black due to staining by organic matter and grade into reddish brown through depths of 0.5 to 1.0 m. These layers demonstrate extensive swelling and shrinkage in response to soil moisture variation. The chemical makeup of the top soil is the same as the underlying more massive clay. There is distinct evidence of a loss of sodium due to cation exchange indicated in the profiles of soil cation exchange capacity (Figure 5.25). As the levels of calcium and magnesium remain constant, the reduction in sodium is possibly the result of exchange for protons provided by infiltration of slightly acidic rainwater.

It is possible that the massive clay formation occurs under different climatic conditions to those that currently occur at Hudson. Presumably warmer and wetter conditions would be more conducive to clay formation. However, the observation of similar materials from the Deccan Plateau in tropical India

suggests that some other physiochemical process is responsible.

Further to the north of the Hudson Site, the basalt derived weathered clays must have been deposited by alluvial action as there is no underlying unweathered basalt and the clays contain lenses of alluvial sand. It is possible that the weight of the overlying material causes some phase change to produce the more dense material that it characteristically found at depth (Acworth & Beasley 1998).

Deep cracking of clay is generally observed under natural vegetation and is considered to be the reason why trees seldom become established over deep clay profiles. In India, the clay is reported to crack to 6 m depth with a similar absence of trees. Similar depths have been suggested in Australia. Timms & Acworth (2002) have reported that fractures in the clay seem well established at Pullaming, close to Breeza, to 16 m depth. This is probably the result of deep drainage of the clay caused by lowering the hydraulic head in the underlying formations by over abstraction of groundwater. Cracks at Hudson are unlikely to be as deep. It seems clear however that cracking can occur to considerable depth.

At Betwa (Hodnett & Bell 1981) the soil profile was observed to wet up by forming a perched layer at 1.0 m depth with saturated conditions proceeding both upward and downward from this perched layer. Unfortunately there were no matric potential measurements made at Hudson to compare with the Indian observations however, other lines of evidence can be used to infer that a perched saturated zone frequently exists after heavy rain and that water can move through fractures at Hudson Site.

6.3 Evidence for fractures at Hudson

The mid-slope piezometer at Hudson has an intake zone between 16 and 17 m. The fact that this piezometer recorded rapid recharge on 23 June 1998 in response to heavy rainfall (Figure 5.11) means that bypass flow occurred on that occasion. It is possible that the ground cracked around the bore casing, but this seems unlikely to a depth of 16 m and the bore is located immediately down slope of a graded bank that would have protected it from run on. An alternative explanation in terms of a pressure response is possible but seems unlikely as the head dissipated more rapidly than the water could have been removed from the surface.

More general evidence for deep cracking is provided by the observation that the water levels in the bores respond to atmospheric pressure change. The discussion in Chapter 2 indicated that an unconfined and compressible aquifer should not develop a pressure differential between the formation and the water in the piezometer. Data has been presented (Figure 5.13 - Figure 5.15) to show that this has undoubtedly occurred. A probable mechanism to explain the high barometric efficiency is the isolation of air in cracks beneath the perched saturated zone. Air is far more compressible than the formation and will prevent the atmospheric pressure change from being transmitted through the formation to the top of the saturated zone.

Close examination of the barometric efficiency with season should reveal a significant change between dry conditions when cracks can propagate to the top of the tension saturated zone and a wet period when the perched saturated zone forms. Unfortunately, data loss from the loggers and a lack of local atmospheric data have prevented further investigation of this phenomena at the Hudson Site.

6.4 Relationship between water content and bulk electrical conductivity

The bulk electrical conductivity values derived from Figure 5.8 (measured on 31 July 2001) are plotted against the averaged soil moisture data from the 3 neutron access tubes for Plot 6 (measured on 5 June 2001) in Figure 6.1. There is clearly a good positive correlation between the two. While it would be easy to develop a simple linear correlation, further work is required to satisfactorily define the relationship.

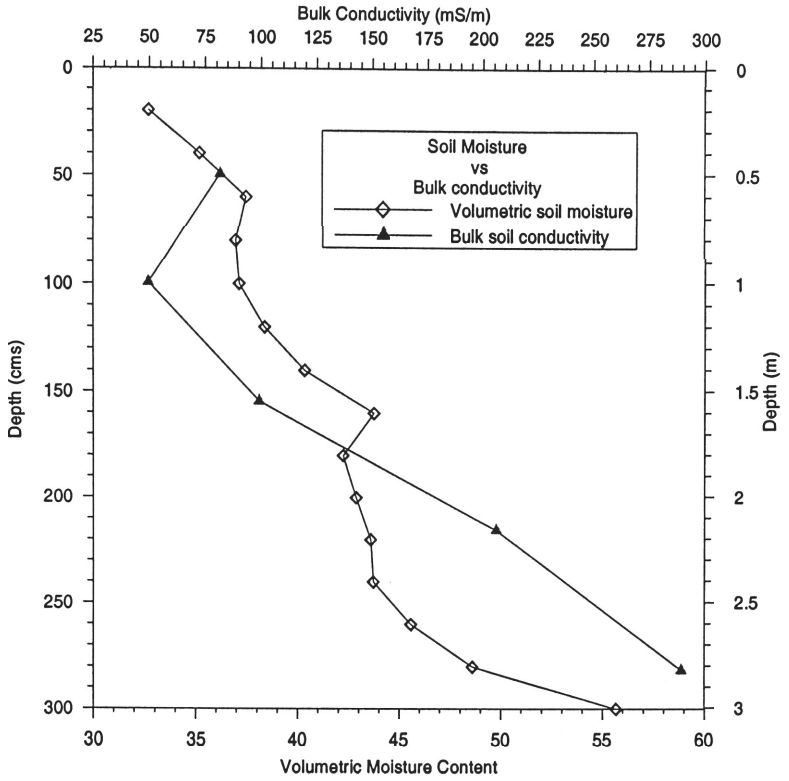

Figure 6.1: Relationship between volumetric soil moisture and bulk electrical conductivity

The volumetric soil moisture data shows change in moisture content between 30% and 55% beneath different profiles at Hudson. The sprayed out lucerne in Plot 20 (Figure 5.6) and the fallow in Plot 24 (Figure 5.7) demonstrate this range of moisture contents. Cracks in these soils occur as a result of 3 dimensional shrinkage in the top 2 to 3 m (Ringrose-Voase et al. 2002). Extensiometer studies carried out at Hudson (not reported here) indicate surface elevation changes of 200 mm between saturated and dry conditions (Ringrose-Voase et al. 2002). The change in elevation indicates movement in the vertical direction in response to moisture change. Cracks observed at the surface clearly indicate the contraction in the horizontal plain. Observation of slickenside faces in excavations suggest that plant roots preferentially follow these surfaces and may also be responsible for the same crack location forming in each drying cycle - dividing the massive clay into blocks of relatively unreactive material surrounded by water moving through the cracks and along slickenside faces. This would result in a dual porosity formation with water and solutes moving out of the peds by diffusion and being transported by advective flow of water in the surrounding matrix of cracks.

The electrical image data clearly show that the lucerne has changed the soil moisture status to depths of at least 6 m (Figure 6.1) with volumetric moisture contents of only 30 - 35% indicated. The reduced moisture content can presumably be taken as an indication of increased cracking at these depths - leading to increased hydraulic conductivity.

There is a clear association between the decreased soil moisture (Figures 5.3 and 5.4) and the increased resistivity (Figures 4.5 and 4.7). Figure 5.8 shows a moisture store between 3 m and 5 m that has not yet been impacted by the growth of the lucerne crop. The growth of lucerne in the buffer zones between the plots has clearly dried the soil profile to at least 6 m depth.

6.5 Hydrological evidence for deep drainage

There is clear evidence of short term deep drainage occurring down fractures. However, these events are not frequently observed in the available record. The water level data indicate considerably different

responses in different parts of the slope with very long responses to extended periods of higher rainfall. The response in the middle part of the slope (Piezometer 248110-3) occurs more slowly than the lower part of the slope (Piezometer 248108-3). Both responses must represent drainage of water (change in storage) as they occur long after the main periods of rainfall and can not therefore be the response to matrix compression caused by pressure change (Equation 2.17). The very slow response indicates many small delayed increments of water rather than single significant recharge events.

The more rapid response of the piezometer on the lower slopes is probably due to the reduced depth to the water table and therefore to the reduced thickness of the unsaturated zone. Further detailed water level measurements compared with a continuous record of on site rainfall and barometric pressure variation are required to better interpret the response.

6.6 Chemical evidence for deep drainage

The fact that there is a distinct variation in groundwater chemistry with time strongly indicates that a limited quantity of groundwater has penetrated to 16 m. The timing of the changes and the change that occurred indicates a complicated process not simply represented by freshening associated with deep drainage. The reduced salinity downslope, as compared to mid slope, could indicate a greater proportion of recharge occurring though the shallower unsaturated zone.

The fact that the clays are so chemically reactive indicates that saturation of various species is quickly achieved. Caliche ($CaCO_3$) deposition may be occurring in response to the release of calcium from the cation exchange complex of the clays. Magnesium carbonate deposits have also been noted. Further work on the weathering reactions would help explain these observations.

Stable isotope data suggests that the majority of the water is old, indicating slow release from soil peds rather than direct recharge through fracture networks.

6.7 Scale dependent flow pathways

No one conceptual recharge model is able to satisfactorily explain groundwater level and hydrochemical variability at the Hudson site. During drier periods the hydraulic head within the thin aquifer at the base of the weathered zone is depleted and lateral flow slows. Relatively high chloride concentrations and calcite saturation may reflect this lack of flushing. The system is believed to be dominantly unconfined during these periods.

Recharge to the upper parts of the soil profile is believed to form a perched aquifer. The underlying groundwater system then behaves as a confined system, effectively sealed from atmospheric pressure changes by a zone of saturated soil. With a very low storativity, small increases in groundwater storage that slowly infiltrate downwards through the profile, result in a very large groundwater level rise. The hydraulic response to major rainfall events, decreased over time from months to weeks. This indicates that the storage properties of the clay changed as the profile wetted up. Further work is required to detail this process.

6.7.1 Macroscale - gully flux

It is probable that most recharge on the mid-lower slope occurs via the eroded gully shown in Figure . The prevalence of gravel and cobble sized basalt in the base of this gully would enable fresh runoff water to infiltrate directly to groundwater. The orientation and depth of this gully crossing the mid-slope are consistent with the observed freshening of groundwater in this area. Figure 6.2 presents a conceptual model of the relationship between the gully and the soil profiles.

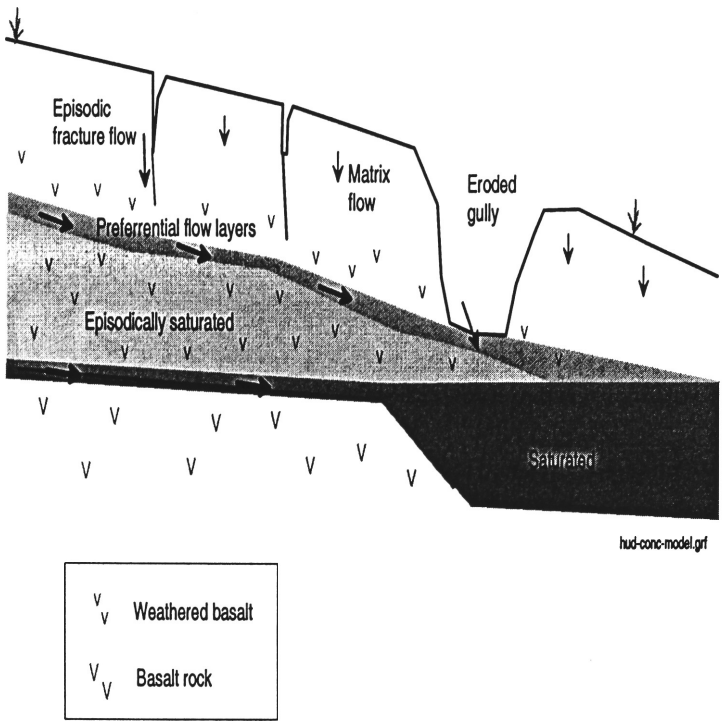

Figure 6.2: Flow pathways at the Hudson site.

6.7.2 Microscale - fracture and matrix flux

The likelihood of fracture flow below 3 m at the Hudson site has been shown by water balance estimates (Young 1998) and this report. However, quantifying the relative importance of this mechanism in relation to matrix flow is inherantly difficult. Ringrose-Voase et al. (2002) do not address fractures in their assessment of deep drainage, and soil water models such as APSIM do not consider fracture flow although both sources admit to the possible significance of fracture flow.

Fracture flow would not occur indefinitely due to the formation of a surface seal. Soil profiles have been observed in the field to wet from the top down rather than the bottom up (Young, discussion at Water Balance Forum 1998). Data from the deep neutron probe site at Plot 24 (Figure 5.7) also indicates the soil profile increasing in moisture content between 1.8 m and 3.5 m without change above and below this depth, similar to the observation at Betwa (Hodnett & Bell 1981). There are also indications of the change in moisture at depth in the electrical image line (B) that crosses Plot 24 (Figure 4.6).

If it is assumed that all the rainfall was taken into the storage, the specific yield of the weathered basalt aquifer would be 0.098. By comparison, a specific yield of 0.067 was determined for heavy clay within the Yarramanbah sub-catchment by Timms et al. (2001). These relatively high values for clay suggest that some storage must be available within fractures of a dry profile, particularly within the weathered basalt aquifer.

Figure 6.3 presents a conceptual model of the flow processes involved for a dual porosity medium. The matrix hydraulic conductivity is very low compared to the bulk (fractured) hydraulic conductivity. However, beyond the maximum fracture depth, the saturated matrix is not impermeable. The matrix structure of Ca-smectite imparts a relatively high hydraulic conductivity. The range of observed hydraulic conductivity values may thus be attributed to both physical and chemical factors.

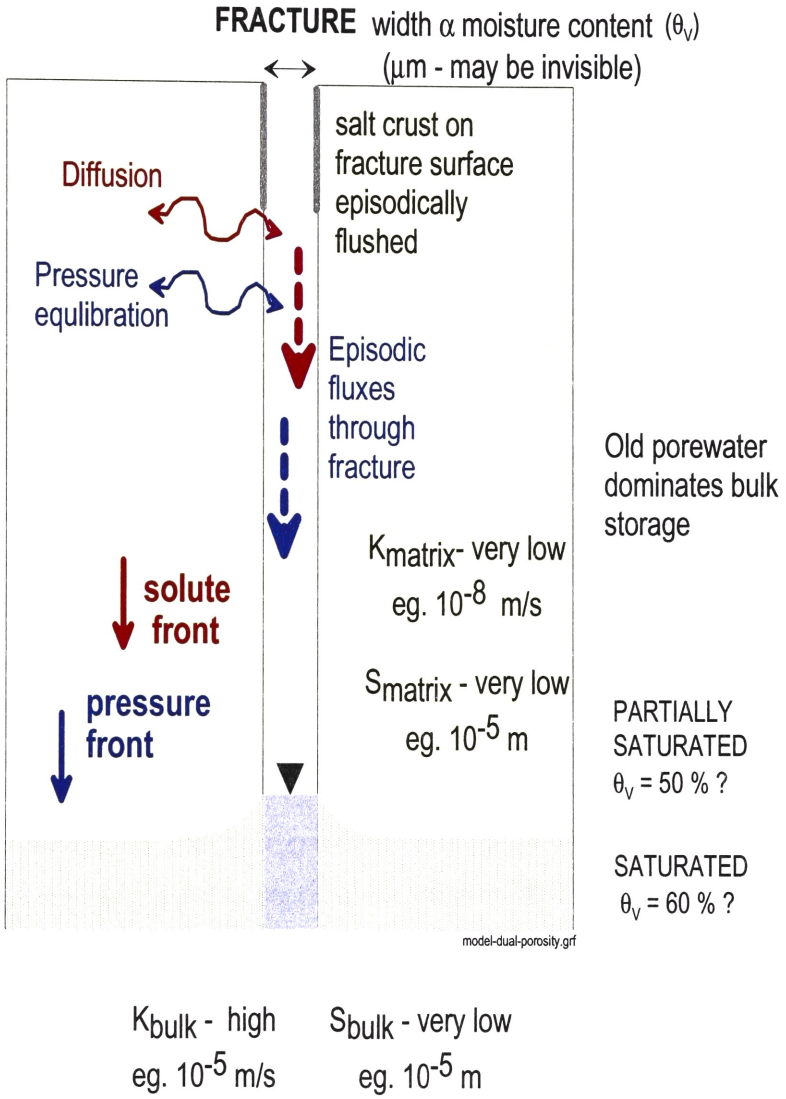

Figure 6.3: Conceptual model of dual porosity groundwater movement at the Hudson Site

Chapter 7

CONCLUSIONS AND RECOMMENDATIONS

7.1 Summary of main findings

The groundwater system that has developed in the weathered profile of Tertiary age basalt at the hudson Site responds in a complex manner to changes in the water balance at the surface. An extensive hydrogeological investigation involving geophysical, geochemical and hydrogeological methods indicates the following:

- After long dry periods small quantities of water can move rapidly to 15 m depth through fractures in the overlying clays.
- Groundwater on the mid-slope (beneath the trial plots) responds slowly to recharge with a time lag of several months.
- Groundwater salinity increase was observed during short periods (weeks), associated with rising groundwater level and other undetermined factors.
- Groundwater during dry periods is relatively enriched in chloride.
- The age of groundwater at 15 m depth indicated very little recent recharge.
- A good correlation exists between bulk electrical conductivity and volumetric soil moisture. A conductivity change from 50 mS/m to 250 mS/m represented a volumetric soil moisture change from 35% to 55%.
- Electrical resistivity image lines indicate that lucerne has dried the soil down to a volumetric moisture content of 35% at 8 m depth. This result requires further evaluation but there is a clear change in bulk resistivity between the plots that can only be due to moisture or salinity change. Of the two, moisture change is the most probable.
- Air trapped in fractures beneath a saturated zone high in the profile may be responsible for the 100% barometric efficiency of water levels in the deep piezometers.
- The age of groundwater at 15 m depth appears to be hundreds to thousands of years old. However, discordant results from various isotope techniques indicate that a very small proportion of recent water has mixed with old water within the clay matrix.

The deep drainage indicated by the initial water balance studies most probably represents water moving into storage above the water table rather than directly to the water table. This water appears to have

bypassed soil moisture deficits higher in the profile. Further work is required to monitor the moisture changes in clay above the weathered basalt but beneath the conventional soil zone depth. Deep rooted plants such as lucerne would appear to have the ability to develop soil moisture deficits to depths of as much as 8 m. Little is known of the ability of this material to recover from drying at this depth.

7.2 Implications for management

Recent crop water balance studies (Ringrose-Voase et al. 2002) using the APSIM package incorporating the water balance module (SoilWat2) assumes that a series of vertically linked soil moisture stores reach saturation before draining down to the next. Outward flux from each store is determined by evapotranspiration. The size of each soil moisture store is related to field determined or estimated soil properties. The approach has been used for many years and was first introduced by Penman (1949) and Lerner et al. (1990). Fundamental to this approach is the assumption that there can be no short circuit to the system - no possibility of water moving between the various stores, or out of the base, without extinguishing the various soil moisture deficits of the overlying layers.

The results of the hydrogeological work at the Hudson Site have shown that extensive fractures exist that are particularly well developed under lucerne and that these fractures do cause a short circuit. It is significant that the prediction of volumetric soil moisture for the P1 and P2 plots (lucerne) at Hudson that have been made using APSIM (Ringrose-Voase et al. 2002) also have the lowest accuracy.

The planting of lucerne appears to significantly increase the risk of cracking to depth and therefore, perhaps pardoxically, to increase the risk of deep drainage. The deep drainage that has occurred at Hudson seems to have been absorbed to a large degree in wetting soils at depths between 3 and 8 m. Whereas this is considered deep drainage from an agronomic perspective, it is not thought that large quantities of recharge have occurred to groundwater at 15 m depth. It is clear from the hydrochemical data that the additional water that has accessed deeper parts of the profile has resulted in significant hydrochemical change but it is not clear, based on the available data, exactly what reactions dominate. The lucerne appears to have activated hydrochemical change at depths in the profile not usually reached by native pasture. This may well be an unanticipated and unfortunate impact.

If the effect of lucerne is to reduce the initial rate of wetting of swelling clays, the immediate effect on paddock management is the length of time needed for fallowing after lucerne in preparation for annual cropping. This may not only be due to the extensive drying of the profile, but also the slower than expected rates of wetting of the clays. If deep drainage has occurred under lucerne, then vigorous, dense and well fertilised lucerne pastures as the P1 and P2 treatments were, may not provide the substantial buffer against drainage as is generally believed. Perennial grass based pastures may be more appropriate as a buffer against drainage.

7.3 Recommendations for future investigations

If the APSIM suite of models is to be widely used for water balance studies in soils of this type, then the significance of deep cracking and bypass flow needs to be clearly investigated and new modules developed to represent this flow, as also suggested by Bethune & Kirby (2001).

The electrical image data clearly shows change in volumetric moisture content at previously unsuspected depths. Routine measurement of these changes is strongly encouraged to better develop conceptual models linking the water balance in the shallow soil with that in the deeper soil. Processes in the deeper clays are not well understood at present. The observation of caliche formation, the development of enhanced hydraulic conductivity and the mobility of salts are each areas requiring detailed investigation before a simple water balance linking excess water in the top 3 m to groundwater recharge can be reasonably established. It may well be that most of the water thought to pass below the root depth does not get to the water table.

The small amount of deep drainage that does reach the saturated zone is difficult to quantify with available data. Direct measurement of hydraulic conductivity and specific storage within the deep silty-clay aquitard and the weathered basalt aquifer would improve upon current gross estimates. However, uncertainties remain regarding the stress dependency of specific storage over time and these will require further detailed investigation.

Bibliography

Abbs, K. & Littleboy, M. (1998). Recharge estimation for the Liverpool Plains. *Australian Journal of Soil Research 35*, 335–357.

Acworth, R. I. (1987). The development of crystalline basement aquifers in a tropical environment. *Quarterly Journal of Engineering Geology 20*, 265–272.

Acworth, R. I. (1999). Investigation of dryland salinity using the electrical image method. *Australian Journal of Soil Research 37*(4), 623–636.

Acworth, R. I. & Beasley, R. (1998). Investigation of EM-31 Anomalies at Yarramanbah/Pump Station Creek, on the Liverpool Plains of New South Wales. Research Report 195, Water Research Laboratory. ISBN 0 85824 0289.

Acworth, R. I. & Jankowski, J. (1997). The relationship between bulk electrical conductivity and dryland salinity in the Narrabri Formation at Breeza, Liverpool Plains, New South Wales, Australia. *Hydrogeology Journal 5*(3), 109–123.

Acworth, R. I. & Jankowski, J. (2001). Salt source for dryland salinity - evidence from an upland catchment on the Southern Tablelands of New South Wales. *Australian Journal of Soil Science 39*(1), 39–59.

Adams, J. & Hanks, R. (1964). Evaporation from soil shrinkage cracks. *Soil Science Society of America: Proceedings 28*, 281–284.

Appelo, C. & Postma, D. (1994). *Geochemistry, groundwater and pollution.* Rotterdam: A.A. Balkema.

Beck, P. (1999). *Transport of conservative and reactive inorganic elements in the saturated part of a heterogeneous sand aquifer, Botany Basin, Sydney, Australia.* Ph. D. thesis, Faculty of Applied Science, University of New South Wales.

Bethune, M. & Kirby, M. (2001). Modelling water movement in cracking soils - Workshop 16-17 May 2001. Technical report, Institute for Sustainable Irrigated Agriculture, ISAI, Agriculture Victoria (Tatura), Department of Natural Resources and Environment, Ferguson Road, Tatura, Victoria 3616.

Broughton, A. (1994). Mooki River Catchment Hydrogeological Investigation and Dryland Salinity Studies, The Liverpool Plains, New South Wales. Technical Services Report TS94.026, New South Wales Department of Conservation and Land Management. 2 Volumes.

Chambers, T. (1999). A hydrogeological appraisal of the Hudson Agricultural Trial Site. Master's thesis, School of Civil and Environmental Engineering, University of New South Wales.

Choi, J. W. & Oscarson, D. W. (1996). Diffusive transport through compacted na- and ca- bentonite. *Jounal of Contaminant Hydrogeology 22*, 189–202.

Clarke, I. & Fritz, P. (1997). *Environmental isotopes in hydrogeology.* Lewis Publishers.

Coram, J. (1999). Groundwater recharge in the Mooki River Catchment, Northern NSW. Technical report, Bureau of Rural Science. Draft.

Craig, H. (1961). Isotopic variation in meteroric waters. *Science 133*, 1702–1703.

Crawford, R. (1997). Hydraulic Conductivity and Mobility of Salt in Smectite Clays. Technical report, School of Civil and Environmental Engineering, The University of New South Wales. Final year - Project Report.

Daniells, I., Holland, J., Young, R., Alston, C., & Bernadi, A. (2001). Relationship between yield of grain sorghum (sorghum bicolor) and soil salinity under field conditions. *Australian Journal of Experimental Agriculture 41*, 211–217.

Dansgaard, W. (1964). Stable isotopes in precipitation. *Tellus 16*, 438–468.

DLWC (1995). Management Policy for the alluvial groundwater resources of the Upper Namoi Valley, Mooki Valley and Coxs Creek, New South Wales. Technical report, NSW Department of Land and Water Conservation, Barwon Region.

Domenico, P. & Schwartz, F. (1990). *Physical and Chemical Hydrogeology.* John Wiley and Sons.

Doser, L., Longstaffe, F., Ferrell, R., & Walthall, P. (1998). Fluid flow through clayey soils: stable isotope and mineralogical evidence. *Clay Minerals 33*, 43–49.

Drever, J. & Smith, C. (1978). Cyclic wetting and drying of the soil zone as an influence on the chemistry of groundwater in arid terrains. *American Journal of Science 278*, 1448–1454.

Fetter, C. (1994). *Applied Hydrogeology* (Third ed.). MacMillans.

Freeze, R. & Cherry, J. (1979). *Groundwater.* Prentice-Hall, Inc., Englewood Cliffs, NJ.

Gates, G. (1980). Liverpool plains drilling report. Unpublished project report, Department of Applied Geology, School of Mines, University of New South Wales.

Harrison, B., Sudicky, E., & Cherry, J. (1992). Numerical analysis of solute migration through fractured clayey deposits into underlying aquifers. *Water Resources Research 28*(2), 515–526.

Heideneich, S. (1999a). Groundwater level, 1998, Hudson, Connamara and Round Island trial sites. Technical report, DLWC Centre for Natural Resources. January, 1999.

Heideneich, S. (1999b). Groundwater level, 1st half 1999, Hudson, Connamara and Round Island trial sites. Technical report, DLWC Centre for Natural Resources. June, 1999.

Hodnett, M. G. & Bell, J. P. (1981). Soil physical processes of groundwater recharge through Indian black cotton soils. Report 77, Institute of Hydrology, Wallingford, UK.

Hounslow, A. (1995). *Water Quality Data: Analysis and Interpretation.* New York: CRC Lewis.

Isbell, R. F. (1996). *The Australian Soil Classification.* Melbourne: CSIRO Publishing.

Jacob, C. (1940). On the flow of water in an elastic artesian aquifer. *Transactions American Geophysics Union 21*, 574–586.

Johnston, C. (1987). Distributions of environmental chloride in relation to subsurface hydrology. *Journal of Hydrology 94*, 67–88. Special Issue - Hydrology and Salinity in the Collie River Basin, Western Australia.

Jones, N. T., Kavanagh, M. A., & Acworth, R. I. (1998). Hydrogeological investigation of a mound springs site in the Lake Goran Catchment, Liverpool Plains, NSW. In *Proceedings of the International Groundwater Conference 1998: Groundwater: Sustainable Solutions, Melbourne, 8 - 13 February, 1998.*

Kavanagh, M. A., Jones, N. T., & Acworth, R. I. (1998). Hydrogeological investigation of the soil and groundwater conditions at the Treloar Springs site in the Lake Goran Catchment, NSW. In *Proceedings of the International Groundwater Conference 1998: Groundwater: Sustainable Solutions, Melbourne, 8 - 13 February, 1998.*

Keller, C., van de Kamp, G., & Cherry, J. (1986). Fracture permeability and groundwater flow in a clayey till near Saskatoon, Saskatchewan. *Canadian Geotechnical Journal 23*, 229–240.

Lavitt, N. (1999). *Integrated approach to geology, hydrogeology and hydrogeochemistry in the Lower Mooki River Catchment.* Ph. D. thesis, School of Geology, The University of New South Wales.

Lavitt, N. & Jankowksi, J. (1998). Groundwater sustainability in the Lower Mooki River catchment: a resource at risk. In T. R. Weaver & C. Lawrence (Eds.), *Groundwater: Sustainable Solutions, Proceedings of the International Groundwater Conference 1998, Melbourne 11-13 February, 1998*, pp. ?–? University of Melbourne: Melbourne.

Lerner, D., Issar, A., & Simmers, I. (1990). *Groundwater Recharge - A Guide to Understanding and Estimating Natural Recharge.* Verlag Heinz Heise. Volume 8 of the International Contributions to Hydrogeology.

Loke, M. (2001). RES2DINV Ver 3.4 Manual - Rapid 2D and 3D Resistivity and IP inversion using the Least Squares Method. Published on the web site www.geoelectrical.com.

Love, A. & Herzceg, A. (2001). Exchange of solute between primary and secondary porosity in a fractured rock aquifer induced by a change in land-use. In R. Citu (Ed.), *Proceedings of the 10th International Symposium on Water-Rock Interaction*, Villasiumius, Italy, pp. 1149–1162.

McKay, L., Cherry, J., & Gillham, R. (1993). Field experiments in a fracture clay till 1. hydraulic conductivity and fracture aperture. *Water Resources Research 29*(4), 1149–1162.

McNeil, J. (1986). Geonics EM39 Borehole Conductivity Meter - Theory of Operation. Technical report, Geonics Limited. TN-20.

Minchin, W. (2001). An examination of the use of resistivity imaging as a tool for determining soil moisture changes in black clay soils. Master's thesis, School of Civil and Environmental Engineering, University of New South Wales.

Mitchell, J. K. (1993). *Fundamentals of Soil Behaviour* (Second ed.). New York: John Wiley and Sons.

Northcote, K. H. (1979). *A factual key for the recognition of Australian soils.* Melbourne: CSIRO Publishing.

Oostindie, K. & Bronswijk, J. (1995). Consequences of preferential flow in cracking clay soils for contamination-risk of shallow aquifers. *Journal of Environmental Management 43*, 359–373.

Penman, H. L. (1949). The dependence of transpiration on weather and soil conditions. *Journal of Soil Science 1*, 74–89.

Quirk, J. P. & Aylmore, L. A. G. (1971). Domains and quasi-crystalline regions in clay systems. *Soil Science Society of America Proceedings 35*, 652–654.

Ringrose-Voase, A. & Cresswell, H. (2000). Measurement and prediction of deep drainage under current and alternative farming practice. Technical report, CSIRO Land and Water. Final report to the LWRRDC - Project CDS16.

Ringrose-Voase, A. J., Young, R. R., Paydar, Z., Huth, N. I., Bernardi, A. L., Cresswell, H. P., Keating, B. A., Scott, J. F., Stauffacher, M., Banks, R. G., Holland, J. F., Johnston, R. M., Green, T. W., Gregory, L. J., Daniells, I., Farquharson, R., Drinkwater, R. J., Heidenreich, S., Donaldson, S., & Alston, C. L. (2002). Deep Drainage under Different Land Uses in the Liverpool Plains. Technical report, CSIRO Land and Water. To be issued as NSW Agriculture Technical Bulletin No. xx/CSIRO Land and Water Technical Report xx/02.

Rowe, R., Quicgley, R., & Booker, J. (1995). *Clayey barrier systems for waste disposal facilities.* London: E. and F.N. Spon.

Rozanski, K., Araguas-Araguas, L., & Gonfiantini, R. (1993). *Isotopic patterns in modern global precipitation.* American Geophysical Union Monograph.

Rudolph, D., Cherry, J., & Farvolden, R. (1991). Groundwater flow and solute transport in a fractured lacustrine clay near Mexico City. *Water Resources Research 27*(9), 2187–2201.

Schon, R. (1986). *The petrology and geochemistry of extrusive rocks from the Liverpool Range, a volcanic centre in eastern New South Wales.* Ph. D. thesis, University of Sydney.

Smiles, D. E. (2000). Hydrology of swelling soils: a review. *Australian Journal of Soil Research 38*, 501–521.

Snow, D. (1969). Anisotropic permeability of fractured media. *Water Resources Research 5*(6), 1273–1289.

Stace, H. C. T., Hubble, G. D., Brewer, R., Northcote, K. H., Sleeman, J. R., Mulcahy, M. J., & Hallsworth, E. G. (1968). *A handbook of Australian Soils.* Rellim Technical Publications.

Stauffacher, M., Walker, G., & Evans, R. (1997). Salt and water movement in the in the Liverpool Plains - Whats going on? National Dryland Salinity Program - Occasional Paper Series, Land and Water (LWRRDC).

Streltsova, T. (1976). Hydrodynamics of groundwater flow in a fractured formation. *Water Resources Research 12*(3), 405–414.

Sutherland, L. (1995). *The volcanic earth.* Sydney: The University of New South Wales Press.

Terzaghi, K. & Peck, R. (1948). *Soil Mechanics in Engineering Practice.* New York: John Wiley.

Timms, W. (1996). Salinity on the Liverpool Plains - a hydrogeologic investigation of Lower Yarramanbah Valley. Honours i thesis, Australian National University, School of Resource and Environmental Management.

Timms, W. (1997). Liverpool Plains Water Quality Project 1996/97: Report on Groundwater Quality. Cnr97.108, Department of Land and Water Conservation.

Timms, W. (1998a). Hudson and Connamara Agricultural Trial Sites: Report on piezometer installation and groundwater sampling. Technical report, Department of Land and Water Conservation. Gunnedah Research Centre.

Timms, W. (1998b). Hydraulic linkages between shallow saline groundwaters and pressurised alluvial aquifers. Research Project Report T2816, Department of Land and Water Conservation, Centre for Natural Resources.

Timms, W. & Acworth, R. I. (2002). Induced leakage due to groundwater pumping and flood irrigation at the Pullaming Agricultural Field Station, Liverpool Plains. Researh Report 208, Water Research Laboratory, 110 King Street, MANLY VALE 2093, NSW Australia. Available for download as a pdf file at www.wrl.unsw.edu.au/research.

Timms, W., Acworth, R. I., & Berhane, D. (2001). Shallow groundwater dynamics in smectite dominated clay on the Liverpool Plains of New South Wales. *Australian Journal of Soil Science 39*(2), 203–218.

Watson, K. K. (1966). An instantaneous profile method for determining the hydraulic conductivity of porous materials. *Water Resources Research 2*, 709–715.

Wood, W., Rainwater, K., & Thompson, D. (1997). Quantifying macropore recharge: examples from a semi-arid area. *Ground Water 35*(6), 1097–1106.

Wright, T. & Barker, J. (2001). Calibration of a double-porosity solute transport model using short and long term tracer tests. In K. Seiler & S. Wohnlich (Eds.), *Proceedings of the XXXI International Association of Hydrogeologists Congress "New Approaches to Characterising Groundwater Flow", 10-14 September, 2001*, Munich, Germany.

Young, R. (1998). Water use efficiency of cropping and pasture systems on the hudson site. In *Water balance and agriculture in the Liverpool Plains Catchment, Gunnedah, 22-23 September, 1998.*, pp. 69–79.

Young, R., Bernardi, A., Holland, J., Daniells, I., Paydar, Z., & Ringose-Voase, A. (1998). Water use efficiency of cropping and pasture systems on the Hudson Site. In *Proceedings of the Water Balance and Agriculture Research Forum. 22-23 September 1998.* Liverpool Plains Land Management Committee, Gunnedah.

Young, R., Broughton, A., Bradd, J., Holland, J., Rose, C., & Rose, H. (1996). Tritium content of shallow groundwaters in the Liverpool Plains catchment. In *Proceedings 8th Australian Agronomy Conference*, Number 103, Toowoomba.